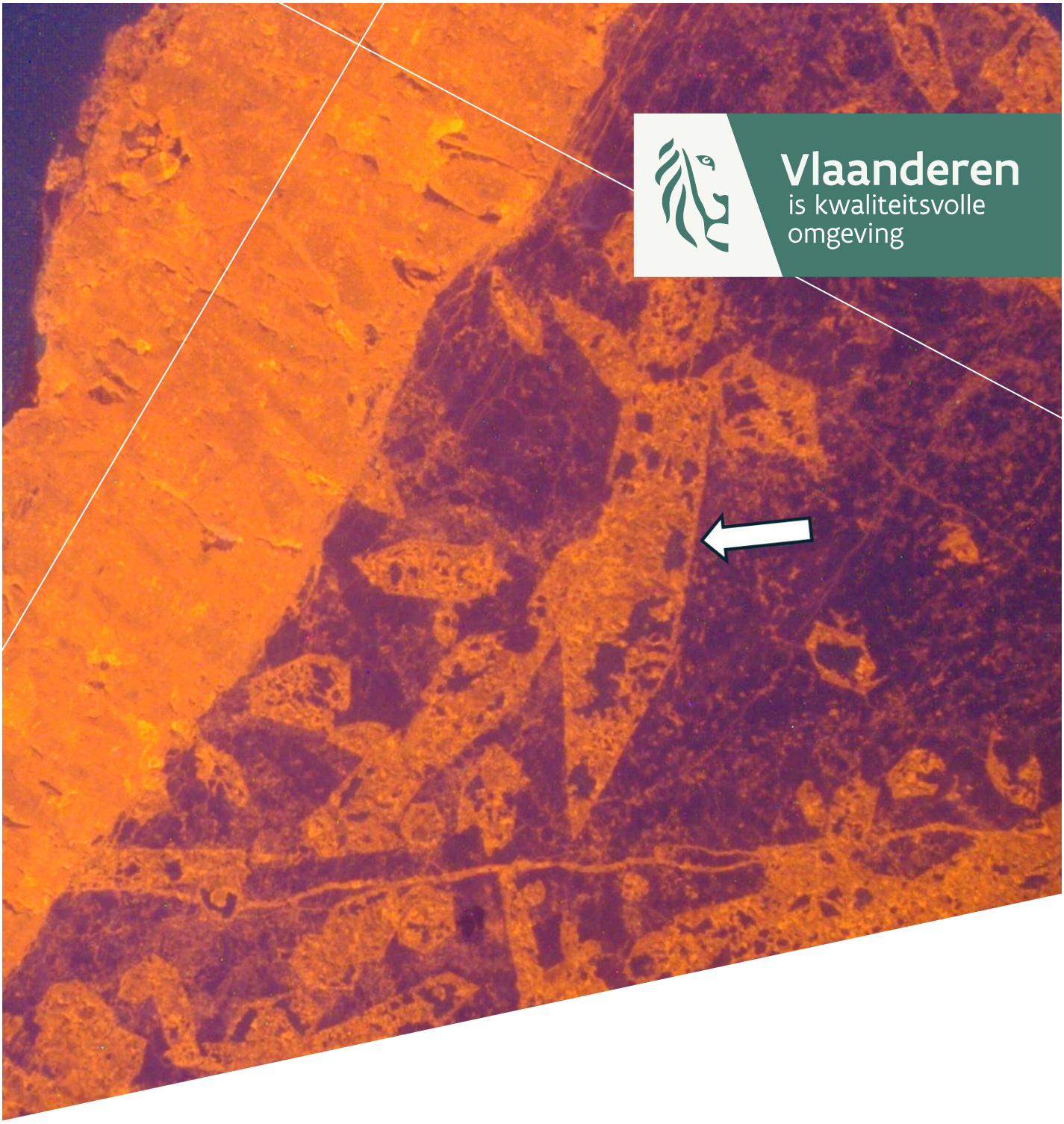

Vlaanderen
is kwaliteitsvolle
omgeving

DIAGENETIC RESEARCH ON SAMPLES FROM THE BEERSE GEOTHERMAL WELL GT 01 A

DEPARTEMENT
OMGEVING

vlaanderen.be/omgeving

DIAGENETISCHE STUDIE VAN BOORGRUIS VAN DE GEOTHERMIEBORING BEERSE GT 01 A

Dit rapport beschrijft de diagenetische evolutie en reservoirontwikkeling in de Dinantiaan Kolenkalk rond Beerse, aan de hand van gesteentegruis – cuttings - uit de geothermieboring Beerse GT 01 A. Na een eerste microscopische screening van representatieve cuttings met diagenetische kenmerken, werden slijpplaatjes gemaakt voor verdere petrografische studie, kathodoluminescentie en fluorescentiemicroscopie. Geochemische analyses vullen de petrografische interpretaties aan.

De resultaten tonen een sedimentologische setting van een overwegend ondiep mariene carbonaatshelf nabij de overgang naar het diepere bekken. Enkele opmerkelijke diagenetische waarnemingen zijn de ontwikkeling van vervangende authigene kwartsfasen tijdens de begraving, de afwezigheid van evaporietfasen en/of hun pseudomorfen (ondanks eerdere meldingen) en de aanwezigheid van ondermature steenkool en schalie in de belangrijkste breukzone. De reservoirontwikkeling kan worden verklaard als het resultaat van twee karstfasen die hebben geleid tot een uitgebreid ontwikkeld karstreservoir met Namuriaan opvullingen en verweerd gesteente. Ook oliemigratie, waarvan bitumenresten zijn gevonden, kan een rol hebben gespeeld.

In deze studie werd de mogelijkheid getest om computertomografie (CT) te gebruiken als snel eerste screeninginstrument voor onderzoek op natte stalen van cuttings uit diepe boorgaten. Hoewel het grofweg mogelijk is om verschillende lithologieën te onderscheiden, schiet de methode tekort voornamelijk door de aanwezigheid van boorvloeistof, het relatief groot monstervolume en de mate van vermenging.

COLOFON

Responsible editor
Toon Denys, Secretary General
Departement Omgeving
Koning Albert-II laan 15 bus 553, 1210 Brussel (mailing address)
vlaanderen.be/omgeving

An edition of the Department of Environment,
division: Flemish Planning Bureau for the Environment and Spatial Development

VPO.omgeving@vlaanderen.be

Author: Rudy Swennen

Publicatiedatum
November 17th 2025

Depotnummer
D/2025/3241/467

ACKNOWLEDGEMENTS

I like to thank Dr. Helga Ferket and her colleagues from the VPO Geotheek for their continuous help in finalizing this study. Herman Nijs (KU Leuven) is thanked for making the thin sections. Dr. Jeroen Soete (XCT – KU Leuven) helped to carry out the Computer Tomography research, while Prof. Dr. Ralf Littke provided the information on organic geochemistry. Both are gratefully thanked. For the isotope analysis we could rely on Yarrick Stroobandt (KU Leuven) as well as Prof. Dr. Michael Joachimski (U. Erlangen).

EXECUTIVE SUMMARY

A call for offers was sent out in July 2024 by the Flemish Department of Environment to better understand the reservoir-forming processes in the Dinantian carbonates, representing the most important deep reservoir in Flanders. The focus of the requested research was a diagenetic study of the drill cuttings of the recent Beerse geothermal wells.

Three series of drill cutting samples were available for the reservoir interval, most, however finely milled. There is one series from the original production well Beerse GT 01, a hole that was lost shortly after drilling, one (Beerse GT 01 A) from the side-track on this well and one from the injection well Beerse GT 02. The cuttings from Beerse GT 01 A show the best grain quality over the reservoir section due to more controlled drilling conditions and thus will be the focus of this study. The samples are preserved in the Flemish core store "Geotheek" at Vilvoorde and were put available for this assignment. The dominant limestone succession also contains shale intervals at several depths, which were, prior to this assignment, interpreted as Namurian infills along an extensively karstified fault zone.

The study included petrography on relevant samples and complementary analyses helping to unravel the reservoir evolution. Apart from new sampling done for this study, existing thin sections prepared for a previous sedimentological and biostratigraphic study (Vinci et al., 2023) were made available. Overall, there is limited useful material. Therefore, a small set of diagenetic samples (based on special mineralogy, crystallization or diagenetic relationships recognized through standard microscopy only) was put apart to save material for the geothermal license holder to answer future reservoir questions. This set was made available, but destructive analysis of those samples could only be performed after agreement with the Flemish government. Based on previous observations by the Department of Environment on this and other material from the Campine Basin, it was requested to pay attention to and apply techniques for distinguishing possible occurrence of hydrocarbons, anhydrite, fluorite, dolomite and authigenic quartz.

The study focused on 4 lithological intervals, namely (i) the interval 1800 –1840/1845m interpreted as Namurian shales and sandstones, which overly a (ii) dominantly Dinantian limestone succession (1840/1845m – 2400m), that is separated by (iii) a major fault zone occurring between about 2239m and 2300m, in which organic shales, bitumen and organic matter with a fibrous texture frequently occur next to limestone cuttings. In (iv) the lower limestone succession below 2400m calcareous marlstone, claystone and dolomite as well as clay interlayers occur. These cuttings were first studied based on a binocular inspection to select representative cuttings displaying diagenetic features (e.g. recrystallised limestones, dolomites, cements, veins, stylolites, …). If enough representative material was available, thin sections were prepared for a classical petrographic, cathodoluminescence (CL) and fluorescence microscopic inspection. Based on the latter, a paragenetic sequence was reconstructed and samples were selected for additional geochemical research (stable isotope and organic geochemistry on organic-rich cuttings).

In the Namurian succession (i) fine laminated organic-rich siltstones/shales, sometimes with flaser and/or laminated texture, occur next to non-porous intensively cemented coarse grained and well-sorted sandstones (often with authigenic quartz overgrowths) and siltstones. In the latter strata individual dull blue, blue purple (brown), and red luminescent quartz grains occur, sometimes floating in a clay-rich and/or micrite matrix. Diagenetic phases recognized consisted of authigenic quartz overgrowth, fracturing, dolomite cementation/veining, and stylolite development.

The Dinantian succession (ii) dominantly consists of recrystallised bioclastic wacke-/packstone containing open marine fauna, such as crinoids, shell fragments and foraminifera. Noteworthy is that pellets, intraclasts and oolites do not frequently occur. The lithological characteristics, however, apart from dolomite-rich intervals do not allow to differentiate particular intervals based on specific lithological features. Note also that organic-rich shales, siltstones and sandstone cuttings commonly occur in the limestone succession. The first diagenetic feature consists of thin dominantly non-luminescent syntaxial rim cements that developed around crinoid ossicles. Noteworthy is that isopacheous fibrous and radiaxial fibrous calcite cements, which according to Muchez et al. (1991) commonly occur in microbial buildups in the Campine Basin, have not been encountered. A common calcite cement consists of dull red purple (brown) luminescent sparite, that displays similarities with a dull luminescent coarse crystalline calcite reported by Muchez et al. (1991). According to the latter authors this cement, that originated from evolved marine or more likely meteoric water, precipitated after a period of fracturing and pre-dates the formation of burial stylolites. Few oversized dissolution cavities, cemented by dull blocky calcite, have also been encountered and likely reflect shallow burial conditions with buffered fluid redox conditions. They developed after a period of karstification that happened at relatively shallow burial depth, most likely during the Late Visean – Early Namurian Sudetic phase. However, a peculiar feature is that typical meteoric cements, i.e. the non-bright-dull luminescing cements, are very rare in the studied cuttings, possibly indicating that the limestones were not severely affected by the Late Visean – Early Namurian Sudetic emergence phase. However, as the limestones display features of recrystallization, the cement characteristics also may be altered. With respect to this recrystallisation, the $\delta^{13}C$ values of the limestone cuttings and most of the cements, reflect a host rock buffering. Only very few $\delta^{13}C$ values are slightly depleted and point to the involvement of a depleted C-source (such as soil derived CO_2).

In the interval 2020 – 2035m, sandstone cuttings with dull blue and purple luminescent quartz grains (some with authigenic quartz overgrowths), but devoid of feldspar grains, occur. Yellow to yellow orange luminescent veinlets and/or mono-crystalline cuttings, which locally also borders the authigenic quartz phases, and thus post-dating the latter, occur frequently below 2035m. Below 2070m transparent and/or impurity-rich non-ferroan monocrystalline calcite cuttings frequently occur. They display a wide spectrum of CL colors, ranging from (dull) orange to yellow, but due to the lack of systematic crosscutting relationships a detailed paragenetic succession could not be worked out. Also, the relationship with bed parallel stylolites is not straightforward. According to Muchez et al. (1991), similar cements developed during the early Westphalian from marine-derived waters at around 60°C. In the interval around 2000m till 2150m, authigenic quartz crystals replacing the limestone matrix are common. They sometimes are replaced by calcite. Their origin is interpreted to relate to clay mineral transformations (smectite to illite transformations) during burial, explaining the low smectite content in the clay fraction. In deeper parts of the borehole, bright yellow calcite cuttings are common which locally replace authigenic quartz phases. In the interval from 2140m till 2190m red luminescent xenotopic non-porous or hypiodiotopic porous dolomite occurs. The latter sometimes contains bitumen. The blotchy luminescence of these dolomites testifies of some recrystallisation. Also, some dedolomitization has been recognized.

Orange as well as yellow luminescent (cleavage twinned) monocrystalline calcite cuttings or veins continue to occur below 2220m, especially in the interval between 2239m – 2300m (iii), where also black shales, bitumen (containing floating quartz grains) and organic matter with a fibrous texture occur. The latter possess relatively low vitrinite reflectance values below 1.0 %, high TOC values (varying between 11,52 and 31,49 wt%) and rather low T_{max} values (varying around 433°C). The hypothesis of a Westphalian origin cannot be explained by some contamination during drilling, since

the Westphalian interval was cemented when the Dinantian succession was drilled. Therefore, a likely explanation is the development of a karst system that developed in the Dinantian limestones along a fault zone, along which also several extensional veins developed. However, such low maturity would point to involvement of Westphalian C & D strata, that do not occur in the Beerse area. Another hypothesis could be that the low maturity relates to weathered (oxidized) Namurian organic-rich shales, that were affected by the karstification. With regard to the coal particles, coal layers also occur in the Namurian. However, these coal particles are perfectly fresh, and thus not altered. This needs further investigations. The cleavage twins in the calcite cements testify from tectonic stresses that affected the coarse crystalline cements after its formation.

In the interval from 2380m till 2470m (iv) red luminescent dolomite locally seems to replace the yellow luminescent calcite or is filling up some space between the calcites, thus post-dating them. Here some bright yellow luminescent calcite veins or cements (zoned and/or forming skalenoeders) developed, testifying from open space infilling, either due to extensional fracturing and/or dissolution. Again, between 2415m – 2520m, sandstone and shale cuttings commonly appear, next to bitumen bearing cuttings as well as limestone cuttings. Coarse mono-crystalline cuttings, displaying a broad range of CL-colors, continue to be present, of which in some cases some crosscutting relationships could be worked out. Of interest is that locally some rare dissolution cavities, filled by a dull luminescent sparite occur next to recrystallisation features, i.e. microsparite. If the latter testifies meteoric diagenesis then a dissolution phase may have taken place. With regard to depleted $\delta^{18}O$ values of the limestone, dolomite and calcite cement cuttings, most of them likely reflect recrystallisation and/of cementation at elevated temperatures under burial conditions.

Final remark is that working with cuttings is not obvious, certainly if they are very fine grained as was the case in the Beerse GT 01 and GT 02 boreholes. Recognizing individual diagenetic phases is possible (as well as characterizing them for example by CL and/or isotopes), however, unraveling a detailed paragenesis is extremely difficult. Assessing the reservoir properties is another difficult issue, since the cuttings likely broke along open spaces. Thus, studying the porosity and inferring its related permeability is impossible. The frequent occurrence of mono-crystalline calcite cuttings allowed to constrain fractured zones and the organic geochemistry allowed to infer a fault zone containing cuttings resembling Westphalian or altered Namurian organic phases. Their presence is interpreted to relate to a major karst system that developed along a fault zone, a feature that has important reservoir implications, also with regard to the geothermal exploitation of the Beerse boreholes. We also hoped that Computer Tomography could help in selecting rapidly interesting samples (from wet vacuum bags containing cuttings), but this turned out to be virtually impossible. Another issue is that despite the fact that organic-rich phases have been encountered, no fluorescent fluid inclusions developed in the wide spectrum of diagenetic phases. Evaporites were reported in the log results, but could not be identified petrographically neither geochemically. Thus, it is worthwhile to investigate the existence of specific mineral phases using different approaches.

Summarizing, the main conclusions and results are:

- The limestones mainly consist of bioclastic wacke-/packstone containing open marine fauna, testifying of a dominantly shallow marine shelf setting occurring adjacent to some shelf slope facies with siliciclastics.
- From diagenetic point of view marine and meteoric phreatic cementation appears to be limited.
- Most of the limestones have been recrystallised, either within the meteoric realm but more likely in a shallow burial setting, likely also explaining the presence of the dull red purple (brown) luminescent sparite cement.

- The analysed $\delta^{13}C$ values of the limestone cuttings vary between +0,3 and +5,7 ‰ and likely reflect original (host-rock buffered) signatures, despite the recrystallised nature of many samples. There is a clear increase visible in $\delta^{13}C$ values with depth. In the limestone cuttings, no indication of soil derived CO_2 neither of hydrocarbons have been encountered.
- The analysed $\delta^{18}O$ values of the Dinantian limestones and dolomites are consistently more depleted than the original $\delta^{18}O$ marine signature and testify of recrystallisation at higher temperatures.
- Locally few oversized dissolution cavities have been noticed which are all filled by calcite cement. Whether they relate to one or possibly two emergence phases is difficult to infer. One may have developed during the Late Visean – Early Namurian Sudetic phase, and the second during the Cretaceous – Paleocene.
- Mono-crystalline calcite cuttings displaying well-developed cleavage twins are quite common below 2035m. They are vein infills thus testifying of some fracture development while the cleavage twins testify from subsequent tectonic stresses.
- $\delta^{13}C$ values of calcite cements are likely host rock buffered, with few exceptions. Their $\delta^{18}O$ values are depleted (with several of the micro-milled samples displaying the most depleted values), and to a major extend overlap with the depleted $\delta^{18}O$ signatures of the limestones, also testifying of relatively higher formation temperatures. No different populations in isotopic composition within the calcite phases could be differentiated.
- Xenotopic non-porous and/or hypiodiotopic porous dolomite intervals locally occur, but their origin is unclear also because their blotchy luminescence testifies of some recrystallisation. Noteworthy is that some porous dolomites contain bitumen.
- Stylolitisation has been encountered and dominantly testifies of burial pressure dissolution.
- Authigenic quartz crystals replacing the limestone matrix are common in the interval around 2000m till 2150m. They post-date a dull blocky calcite, interpreted to be meteoric in origin. They likely reflect burial authigenesis, related to clay mineral reactions (smectite to illite transformations) that occurred post-stylolitisation. This could relate to the burial of nearby siliciclastics along the slopes of the shallow marine limestones. They sometimes are replaced by calcite, likely relating to the alkaline nature of the limestones and their related fluid flow.
- The organic-rich shale cuttings from the interval 1800 –1840/1845m possess a high thermal maturity with reflectance values, varying between 3.0 and 4.0 %, which are in line with time equivalent strata in the study area.
- Organic-rich cuttings also were encountered in the interval between 2275m till 2310m, between a succession of Dinantian carbonates. Most of these cuttings possess high TOC values (from 11,52 and 31,49 wt%), rather low T_{max} values (varying around 433°C) and vitrinite reflectance values below 1.0 %. The values are in line with values encountered in Westphalian C & D coal measures in the Campine Basin, which, however, do not occur in the Beerse area. Another hypothesis could be that they relate to weathered (oxidized) and thus altered Namurian organic-rich shales that also contain thin coal layers, however, also high maturity organic cuttings as well as fresh (non-altered) coal particles but with low maturity have been encountered. The presence of these organic-rich cuttings is interpreted to relate to infiltration of possibly Westphalian or more likely Namurian material in a karst system that developed in the Dinantian fault zone.
- Also, bitumen-rich samples containing floating quartz grains have been encountered in the 2275m till 2310m interval. They testify of some oil migration, while the floating nature of the quartz grains best can be explained by karst infill that became impregnated by bitumen.
- No fluorescent hydrocarbon phases have been noticed in none of the diagenetic phases.
- No evaporite and/or relicts of evaporites were encountered.

- Sulphide phases, especially minute dominantly framboidal pyrite crystals, were especially encountered in the organic-rich cuttings, while larger crystals, likely of recrystallisation origin, occur in some of the sandstone cuttings. Locally, chalcopyrite as well as hematite was recognized.
- Due to the severe recrystallization as well as the tectonic stresses that affected the strata, planned microthermometric analysis were not carried out.

SAMENVATTING

In juli 2024 lanceerde het Vlaams Departement Omgeving een oproep tot het indienen van voorstellen om de reservoirvormende processen in de Dinantiaan Kolenkalk, het belangrijkste diepe reservoir in Vlaanderen, beter te begrijpen. De focus van het gevraagde onderzoek lag op een diagenetische studie van het boorgruis van de recente geothermische putten in Beerse.

Er waren drie reeksen boormonsters beschikbaar van het reservoirinterval, de meeste echter bestaande uit fijn vermalen materiaal. Eén serie is afkomstig van de oorspronkelijke productieput Beerse GT 01, een boorgat dat kort na het boren verloren ging, één (Beerse GT 01 A) van de nieuwe zijboring van deze put en één van de injectieput Beerse GT 02. Het boorgruis uit Beerse GT 01 A vertoont de beste korrelkwaliteit over het reservoirgedeelte dankzij beter gecontroleerde booromstandigheden en vormt daarom het onderwerp van deze studie. De monsters worden bewaard in de Vlaamse "Geotheek" te Vilvoorde en werden voor deze opdracht beschikbaar gesteld. De dominante kalksteenopeenvolging bevat ook schalie-intervallen op verschillende diepten, waarvan de voornaamste vóór deze opdracht geïnterpreteerd werd als Namuriaan opvullingen langs een sterk gekarstifieerde breukzone.

De studie omvatte petrografie van relevante monsters en aanvullende analyses om de reservoirontwikkeling verder te ontrafelen. Naast nieuwe bemonstering die voor deze studie werd uitgevoerd, werden bestaande slijpplaatjes, gemaakt voor een eerdere sedimentologische en biostratigrafische studie, beschikbaar gesteld. Over het algemeen is er zeer beperkt bruikbaar materiaal. Daarom werd een kleine set van diagenetische monsters (gebaseerd op speciale mineralogie, kristallisatie of diagenetische relaties die louter op basis van standaardmicroscopie werden voorgeselecteerd) apart gezet om materiaal te bewaren voor de aardwarmte-vergunninghouder om toekomstige vragen over het reservoir te kunnen beantwoorden. Deze set werd weliswaar beschikbaar gesteld, maar destructieve analyse van deze monsters kon enkel worden uitgevoerd na overleg met de Vlaamse overheid. Op basis van eerdere observaties door het Departement Omgeving op dit en ander materiaal uit het Kempens Bekken, werd gevraagd specifiek aandacht te besteden aan en technieken toe te passen om de mogelijke aanwezigheid van koolwaterstoffen, anhydriet, fluoriet, dolomiet en authigene kwarts te onderscheiden.

De studie focuste op 4 lithologische intervallen, namelijk (i) het interval 1800–1840/1845 m, geïnterpreteerd als Namuriaan schalie en zandsteen, die bovenop een (ii) dominant Dinantiaan kalksteenpakket (1840/1845 m – 2400 m) ligt, dat gescheiden wordt door (iii) een grote breukzone tussen ongeveer 2239 m en 2300 m, waarin organisch-rijke schalie, bitumen en organisch materiaal met een vezelachtige textuur vaak naast kalksteenfragmenten voorkomen. In (iv) de diepere carbonaatlagen onder 2400 m komen kalkhoudende mergel, kleisteen en dolomiet voor, evenals klei-tussenlagen. De cuttings werden eerst gescreend op basis van een binoculaire inspectie om representatieve fragmenten te selecteren die diagenetische kenmerken vertoonden (bijvoorbeeld gerekristalliseerde kalksteen, dolomieten, cementen, aders, stylolieten, ...). Wanneer voldoende representatief materiaal beschikbaar was, werden slijpplaatjes geprepareerd voor klassieke petrografie, kathodoluminescentie (CL) en fluorescentiemicroscopie. Op basis daarvan werd een paragenese gereconstrueerd en werden monsters geselecteerd voor aanvullend geochemisch onderzoek (stabiele isotopen en organische geochemie op organisch-rijke cuttings).

In het Namuriaan pakket (i) komen fijn gelaagde, organisch-rijke siltstenen/schalies voor, soms met een flaser- en/of gelaagde textuur, naast niet-poreuze, intensief gecementeerde, grofkorrelige en goed gesorteerde zandstenen (vaak met authigene kwartsovergroeiingen) en siltstenen. In deze

laatste lagen komen individuele dofblauwe, blauwpaarse (bruine) en rood luminescerende kwartskorrels voor, soms zwevend in een kleirijke en/of micrietmatrix. De herkende diagenetische fasen bestonden uit authigene kwartsovergroeiingen, breukvorming, dolomietcementatie/ adervorming en stylolietontwikkeling.

Het Dinantiaan-pakket (ii) bestaat voornamelijk uit gerekristalliseerde bioklastische wacke-/packstone met open mariene fauna, zoals crinoïden, schelpfragmenten en foraminiferen. Opmerkelijk is dat pellets, intraclasten en oölieten niet frequent voorkomen. De lithologische kenmerken, afgezien van dolomietrijke intervallen, laten echter niet toe om specifieke intervallen te differentiëren op basis van specifieke lithologische kenmerken. Merk ook op dat partikels van organisch-rijke schalie, siltsteen en zandsteen veelvuldig voorkomen in de kalksteenlagen. Het eerste diagenetische product bestaat uit dunne, overwegend niet-luminescerende syntaxiale randcementen die zich rond crinoïdfragmenten ontwikkelden. Opmerkelijk is dat isopache vezelige en radiaxiale vezelige calcietcementen, die volgens Muchez et al. (1991) vaak voorkomen in microbiële afzettingen in het Kempens Bekken, hier niet zijn aangetroffen. Een veelvoorkomend calcietcement bestaat uit dof roodpaars (bruin) luminescerend spariet, dat overeenkomsten vertoont met een dof luminescerend grof kristallijn calcietcement zoals beschreven door Muchez et al. (1991). Volgens laatstgenoemde auteurs is dit cement, dat afkomstig is uit geëvolueerd zeewater of, waarschijnlijker, meteorisch water, neergeslagen na een periode van breukvorming en dateert het van vóór de vorming van begravingsstylolieten. Enkele overmaatse oplossingsholtes, gecementeerd door dof blokvormig calcietcement, zijn ook aangetroffen en weerspiegelen waarschijnlijk ondiepe begravingsomstandigheden met gebufferde vloeistofredoxomstandigheden. Ze ontwikkelden zich na een periode van karstificatie die plaatsvond op relatief geringe begravingsdiepte, hoogstwaarschijnlijk tijdens de Laat-Viseaan - Vroeg-Namuriaan Sudetische fase. Een merkwaardig kenmerk is echter dat typisch meteorische cementen, d.w.z. de opeenvolging van “niet // helder // dof” luminescerende cementen, zeer zeldzaam zijn in de bestudeerde fragmenten, wat mogelijk aangeeft dat de kalksteen niet sterk werd aangetast tijdens de Laat-Viseaan - Vroeg-Namuriaan Sudetische fase van opheffing. Omdat de kalksteen echter kenmerken van rekristallisatie vertoont, kunnen echter ook de cementeigenschappen veranderd zijn. Wat deze rekristallisatie betreft, weerspiegelen de $\delta^{13}C$-waarden van de kalksteenfragmenten en de meeste cementen een bufferende werking van het nevengesteente. Slechts enkele $\delta^{13}C$-waarden zijn licht verlaagd en wijzen op de betrokkenheid van een negatieve koolstofbron (zoals CO_2 afkomstig uit bodemprocessen).

In het interval 2020 – 2035 m komen zandsteenfragmentjes voor met doffe blauwe en paarse luminescerende kwartskorrels (sommige met authigene kwartsovergroeiingen), maar zonder veldspaatkorrels. Gele tot geeloranje luminescerende adertjes en/of monokristallijne calcietfragmenten, die plaatselijk ook grenzen aan de authigene kwartsfasen en dus na die fasen gevormd werden, komen vaak voor onder 2035 m. Onder 2070 m komen vaak transparante en/of inclusierijke, niet-ijzerrijke monokristallijne calcietfragmentjes voor. Ze vertonen een breed spectrum aan CL-kleuren, variërend van (dof) oranje tot geel, maar door het ontbreken van systematische doorsnijdingsrelaties kon een gedetailleerde paragenese niet worden uitgewerkt. Ook de relatie met laagparallelle stylolieten is niet eenvoudig. Volgens Muchez et al. (1991) ontwikkelden gelijkaardige cementen zich tijdens het vroege Westfaliaan uit marien water bij ongeveer 60 °C. In het interval tussen 2000 en 2150 meter diepte komen authigene kwartskristallen vaak voor ter vervanging van de kalksteenmatrix. Soms worden ze zelf vervangen door calciet. Hun oorsprong wordt geïnterpreteerd als gerelateerd aan kleimineraaltransformaties (van smectiet naar illiet) tijdens de begraving, wat het lage smectietgehalte in de kleifractie verklaart. In diepere delen van het boorgat komen heldergele calcietfragmenten veel voor die plaatselijk authigene kwartsfasen

vervangen. In het interval van 2140 tot 2190 meter diepte komt rood luminescerend xenotopisch niet-poreus of hypiodiotopisch poreuze dolomiet voor. Deze dolomiet bevat soms bitumen. De vlekkerige luminescentie van deze dolomieten getuigt van enige rekristallisatie. Ook werd soms dedolomitisatie waargenomen.

Oranje en gele luminescerende (met splijtingstweelingen) monokristallijne calcietfragmentjes of -aders blijven voorkomen onder 2220 m, vooral in het interval tussen 2239 m - 2300 m (iii), waar ook zwarte schalies, bitumen (waarin kwartskorrels “drijven”) en organisch materiaal met een vezelachtige textuur voorkomen. Deze laatste bezitten relatief lage vitrinietreflectiewaarden onder 1,0%, hoge TOC-waarden (variërend tussen 11,52 en 31,49 wt%) en vrij lage T_{max}-waarden (variërend rond 433 °C). De hypothese van een Westfaliaan oorsprong voor dit materiaal kan niet worden verklaard door contaminatie tijdens het boren, aangezien het Westfaliaan interval al gecementeerd was toen het Dinantiaan werd aangeboord. Daarom moet een verklaring wellicht eerder gezocht worden in de ontwikkeling van een karstsysteem langs een breukzone, waarlangs ook verschillende extensionele aders zich ontwikkelden. De lage maturiteit van het organisch materiaal in deze breukzone suggereert betrokkenheid van Westfaliaan C- en D-lagen, die echter niet voorkomen in het gebied rond Beerse. Een andere hypothese zou kunnen zijn dat de lage maturiteit verband houdt met verweerde (geoxideerde) organische schalie uit het Namuriaan, die door de karstificatie werd aangetast. Wat de steenkoolfragmenten betreft, steenkoollagen komen ook voor in het Namuriaan. De gevonden steenkoolfragmenten zien er echter volledig vers en onveranderd uit. Dit vereist nader onderzoek. De splijttweelingen in de calcietcementen getuigen van tektonische spanningen die de grof kristallijne cementen hebben vervormd.

In het interval van 2380 m tot 2470 m (iv) lijkt rood luminescerende dolomiet lokaal de geel luminescerende calciet te vervangen of vult een deel van de ruimte tussen de calcieten op, waardoor ze jonger moeten zijn. Hier ontwikkelden zich enkele heldergeel luminescerende calcietaders of cementen (gezoneerd en/of skalenoeders), wat getuigt van opvulling van open ruimten, hetzij door extensionele breukwerking en/of oplossing. Ook tussen 2415 m en 2520 m verschijnt vaak zandsteen- en schaliegruis, naast bitumenhoudend gruis en kalksteengruis. Grof monokristallijne fragmenten, met een breed scala aan CL-kleuren, blijft aanwezig, waarvan in sommige gevallen enkele doorsnijdingsrelaties konden worden uitgewerkt. Interessant is dat lokaal enkele zeldzame oplossingsholten, gevuld met een dof luminescerend spariet, voorkomen naast rekristallisatiekenmerken, d.w.z. microspariet. Als dit laatste wijst op meteorische diagenese, kan er een oplossingsfase hebben plaatsgevonden. Wat betreft de verlaagde $\delta^{18}O$-waarden van de kalksteen-, dolomiet- en calcietframenten, weerspiegelen de meeste waarschijnlijk rekristallisatie en/of cementatie bij verhoogde temperaturen onder begravingsomstandigheden.

Tot slot is het werken met cuttings niet vanzelfsprekend, zeker niet als ze zeer fijnkorrelig zijn, zoals het geval was in de boringen Beerse GT 01 en GT 02. Het herkennen van individuele diagenetische fasen is mogelijk (en het karakteriseren ervan, bijvoorbeeld met behulp van CL en/of isotopen), maar het ontrafelen van een gedetailleerde paragenese is uiterst moeilijk. Het beoordelen van de reservoireigenschappen is een andere lastige kwestie, aangezien de fragmenten waarschijnlijk langs open ruimtes zijn gebroken. Het bestuderen van de porositeit en het afleiden van de bijbehorende permeabiliteit is daarom onmogelijk. De frequente aanwezigheid van monokristallijne calcietfragmenten maakte het mogelijk om gecementeerde spleetzones af te lijnen en de organische geochemie maakte het mogelijk om een breukzone af te leiden met cuttings die leken op organische fasen uit het Westfaliaan of het Namuriaan. Hun aanwezigheid wordt geïnterpreteerd in relatie tot een groot karstsysteem dat zich langs een breukzone heeft ontwikkeld. Dat heeft belangrijke gevolgen voor de reservoirontwikkeling en de geothermische exploitatie van de boringen in Beerse.

We hoopten ook dat computertomografie zou kunnen helpen bij het snel selecteren van interessante monsters (uit natte vacuümzakken met cuttings), maar dit bleek vrijwel onmogelijk. Een ander probleem is dat, ondanks het feit dat er organisch-rijke fasen zijn aangetroffen, er zich geen fluorescerende vloeistofinsluitsels ontwikkelden in het brede spectrum van diagenetische fasen. Evaporieten werden gerapporteerd in de logresultaten, maar konden noch petrografisch noch geochemisch worden geïdentificeerd. Het is dus de moeite waard om het bestaan van specifieke minerale fasen met verschillende benaderingen te onderzoeken.

Samenvattend zijn de belangrijkste conclusies en resultaten:

- De kalksteen bestaat hoofdzakelijk uit bioklastische wacke-/packstone met een open mariene fauna, wat getuigt van een overwegend ondiep mariene shelf die grenst aan een shelf helling met siliciklasten.
- Vanuit diagenetisch oogpunt lijkt mariene en meteorische freatische cementatie beperkt te zijn.
- De meeste kalksteen is gerekristalliseerd, hetzij in een meteorische, hetzij (waarschijnlijker) in een ondiepe begravingsomgeving, wat waarschijnlijk ook de aanwezigheid van het doffe roodpaarse (bruine) luminescerende sparietcement verklaart.
- De geanalyseerde $\delta^{13}C$-waarden van de kalksteencuttings variëren tussen +0,3 en +5,7 ‰ en weerspiegelen waarschijnlijk de oorspronkelijke (door het nevengesteente gebufferde) signatuur, ondanks rekristallisatie van veel monsters. Er is een duidelijke verhoging zichtbaar in $\delta^{13}C$-waarden met de diepte. In de kalksteencuttings zijn geen aanwijzingen gevonden voor bodem-CO_2, noch voor koolwaterstof gerelateerde koolstof.
- De geanalyseerde $\delta^{18}O$-waarden van de Dinantiaan kalksteen- en dolomietmatrix fragmenten zijn consequent verlaagd ten opzichte van de oorspronkelijke $\delta^{18}O$-mariene signatuur en getuigen van rekristallisatie bij hogere temperaturen.
- Lokaal zijn enkele grote oplossingsholtes waargenomen, die allemaal gevuld zijn met calcietcement. Of deze betrekking hebben op één of mogelijk twee emersiefasen is moeilijk te achterhalen. Eén ervan kan zich hebben ontwikkeld tijdens de Laat-Viseaan-Vroeg-Namuriaan Sudetische fase, en de tweede tijdens het Krijt-Paleoceen.
- Monokristallijne calcietfragmenten met sterk ontwikkelde splijttweelingen komen veel voor onder de 2035 m. Het zijn aderopvullingen die wijzen op spleetvorming, terwijl de splijtingstweelingen wijzen op latere tektonische spanningen.
- De $\delta^{13}C$-waarden van calcietcementen worden waarschijnlijk gebufferd door het nevengesteente, op enkele uitzonderingen na. De $\delta^{18}O$-waarden zijn verlaagd (waarbij verschillende van de microgeboorde monsters de sterkst verlaagde waarden vertonen) en overlappen grotendeels met de verlaagde $\delta^{18}O$-signaturen van de kalksteenmatrix, wat opnieuw wijst op relatief hogere vormingstemperaturen. Er konden geen verschillende populaties in isotopensamenstelling binnen de calcietfcementfasen worden onderscheiden.
- Xenotope, niet-poreuze en/of hypiodiotope poreuze dolomiet komt lokaal voor, maar de oorsprong is onduidelijk, mede omdat de vlekkerige luminescentie getuigt van enige rekristallisatie. Opmerkelijk is dat sommige poreuze dolomieten bitumen bevatten.
- Er is stylolitisatie aangetroffen en dit getuigt vooral van drukoplossing tijdens het begravingsproces.
- Authigene kwartskristallen die de kalksteenmatrix vervangen, komen veel voor in het interval tussen 2000 en 2150 meter. Ze dateren van na een dof luminescerend blokvormig calcietcement, waarvan wordt aangenomen dat het van meteorische oorsprong is. De authigene kwartskristallen weerspiegelen waarschijnlijk begravingsauthigenese, gerelateerd aan reacties van kleimineralen (transformaties van smectiet naar illiet) die plaatsvonden na

de stylolitisatie. Dit zou verband kunnen houden met de begraving van nabijgelegen siliciclasten op de helling aan de rand van de ondiep mariene kalksteenshelf. Soms wordt de authigene kwarts vervangen door calciet, waarschijnlijk gerelateerd aan de alkalische aard van de kalksteen en de lokale fluïdamigratie.

- De organisch-rijke schalie-cuttings uit het interval 1800 – 1840/1845 m vertonen een hoge thermische maturiteit met vitrinietreflectiewaarden die variëren tussen 3,0 en 4,0 %, wat in lijn is met tijdsequivalente lagen in het studiegebied.
- Organisch rijke schaliefragmenten werden ook aangetroffen in het interval tussen 2275 m en 2310 m, tussen een opeenvolging van carbonaten uit het Dinantiaan. De meeste van deze schaliefragmenten bezitten hoge TOC-waarden (van 11,52 en 31,49 wt%), vrij lage T_{max}-waarden (variërend rond 433 °C) en vitrinietreflectiewaarden onder 1,0 %. Deze waarden komen overeen met waarden die worden aangetroffen in Westfaliaan C & D-steenkoollagen in het Bekken van de Kempen, maar die echter niet voorkomen in het gebied rond Beerse. Een andere hypothese zou kunnen zijn dat het gaat om verweerde (geoxideerde) en dus veranderde Namuriaan organisch rijke schalies die ook dunne steenkoollagen kunnen bevatten. Er zijn echter ook hoogmature organische cuttings en verse (niet gealtereerde) steenkoolfragmenten met een lage maturiteit aangetroffen. De aanwezigheid van deze organisch rijke cuttings wordt geïnterpreteerd als verband houdend met infiltratie van mogelijk Westfaliaan of waarschijnlijker Namuriaan materiaal in een karstsysteem dat zich ontwikkelde langsheen de Dinantiaan-breukzone
- In het interval van 2275 tot 2310 meter zijn ook bitumenrijke monsters aangetroffen waarin kwartskorrels drijven. Deze getuigen van oliemigratie, terwijl het “drijven” van de kwartskorrels het best kan worden verklaard door een karstvulling die geïmpregneerd werd met bitumen.
- In geen enkele van de diagenetische fasen zijn fluorescerende koolwaterstoffasen waargenomen.
- Er werden geen evaporiet en/of relicten van evaporieten aangetroffen.
- Sulfidefasen, met name minuscule, overwegend framboïdale pyrietkristallen, werden vooral aangetroffen in de organisch-rijke cuttings, terwijl grotere kristallen, waarschijnlijk afkomstig van rekristallisatie, voorkomen in sommige zandsteenfragmenten. Lokaal werden zowel chalcopyriet als hematiet aangetroffen.
- Vanwege de sterke rekristallisatie en tektonische spanningen die de lagen beïnvloed hebben, werden de geplande microthermometrische analyses niet uitgevoerd.

TABLE OF CONTENTS

1 INTRODUCTION

1.1 CONTEXT AND SCOPE

A call for offers was sent out in July 2024 by the Flemish Department of Environment to better understand the reservoir formation processes in the Dinantian carbonates, representing the most important deep reservoir in Flanders. The focus of the requested research was a diagenetic study of the drill cuttings of the recent Beerse geothermal wells.

Janssen Pharmaceutica nv is fully engaged in a heat transition to lower temperatures and sustainable energy sources at its Beerse site. The main heat source for a new intelligent heat network is a deep geothermal installation with two boreholes at depths of over 2 km. The exploration phase, including extensive testing, was successful, allowing the project to move on to the long-term production phase. During the drilling phase, the project encountered unforeseen geological conditions due to the presence of shales intercalated between the limestones at various depths. Prior to this assignment, these shale intercalations were interpreted as Namurian infills along an extensively karstified fault zone. Initial petrographic descriptions during the drilling project mentioned the presence of anhydrite, although this could not be confirmed by later examining cuttings under the microscope.

Three series of drill cutting samples were available, most, however, finely milled. There is one series from the original production well Beerse GT 01, a hole that was lost shortly after drilling, one (Beerse GT 01 A) from the side-track on this well and one from the injection well Beerse GT 02. The cuttings from Beerse GT 01 A show the best grain quality over the reservoir section due to more controlled drilling conditions and thus will be the focus of this study. All samples are preserved in the Flemish core store “Geotheek” at Vilvoorde and were made available for this assignment.

The study included petrography on relevant samples and complementary analyses helping to unravel the reservoir evolution. Apart from new sampling performed for this study, existing thin sections prepared for a previous sedimentological (Vinci et al., 2023) and biostratigraphic study (Hance, 2023) were made available. Overall, there is limited useful material. Therefore, a small set of “diagenesis reference samples” was put apart to save material for the geothermal license holder to answer future reservoir questions. These are cuttings that might correspond to special mineralogy, crystallization or diagenetic relationships that were recognized through standard microscopy of whole cuttings only. They represent fragments of euhedral crystals, bitumen, tentatively interpreted quartz crystals to check for fluid inclusions and possible anhydrite fragments. The reference set was made available for this study, but destructive analysis of those samples could only be performed after agreement with the Flemish government. Based on previous observations by the Department of Environment on this and other material from the Campine Basin, it was requested to pay specific attention to and apply techniques for distinguishing possible occurrence of hydrocarbons, anhydrite, fluorite, dolomite and authigenic quartz.

The Department of Environment asked to establish a paragenetic history as far as the challenging material would allow and to give insights into reservoir development in the Dinantian carbonates in the Campine Basin. For the geological setting of the Campine Basin and specifically during the Dinantian, we refer to Vinci et al. (2023) and Rombaut et al. (2024).

1.2 APPROACH AND METHODOLOGY

On request of VPO a detailed petrographic and geochemical investigation was carried out on the Beerse cuttings of well GT 01 A (including also the selected "diagenesis reference samples"). Notice that all sample depths refer to the measured "Along Hole Depth" (AHD)). The borehole was drilled deviated with a total length of 2555m, corresponding to a true vertical depth of 2234m. For comparison purposes also few cutting samples from GT 01 were inspected, but are not reported in this study, since they only provided complementary data. This study is the extension of a previous study carried out on 12 samples originating from the Beerse GT 01 (covering an interval of 2455 till 2830m AHD), and 23 samples originating from Beerse GT 01 A (covering an interval of 1865 till 2520m) (see Swennen, 2023; i.e. the "enclosure 8.6 TS description Beerse" in Vinci et al., 2023). The latter study focused on the sedimentary characteristics of the cuttings, as starting point for a detailed biostratigraphical study (Hance, 2023, unpublished). In this report we sometimes will refer to the former report as well as to some of the provided pictures in that report (by stating: "S23 – X - plate Y" with X being the depth position).

As the cuttings of the Beerse GT 01 were very small it was soon decided to focus on the coarser cuttings of the Beerse GT 01 A, since enough material for geochemical investigations was needed. In annex I, microphotographs of these Beerse GT 01 A cuttings are shown, as well as a brief report on the lithology of the cuttings shown in the pictures.

Making thin sections of cuttings is not easy. It may happen that the cuttings are irregular in shape and thus are not fully in contact with the underlying glass slide. In that case often an artefact can be seen in the pictures of the thin section. Furthermore, it can happen that the different cuttings consist of different lithologies, in our case for example limestone, dolomite, sandstone, shale and/or bitumen. Due to their difference in hardness this can also lead to some problems when polishing the thin section. In the latter case the different lithologies might have different thicknesses as well as differences in quality of the polishing.

Notice also that some pictures originate from thicker "thin sections" (up to 250µm thick), so called "thick sections". This was on the one hand done to be able to study them under cathodoluminescence and on the other hand to be able to micro-sample specific phases for stable C- and O- isotope analyses (see micro-sampling, Figure 1 & 2). Sample selection took place after CL-characterization of the cuttings. In annex III the depth position of these thick sections is given (in bold). In most cases the thick sections consisted of transparent monocrystalline calcite, occurring next to less transparent to sometimes grey-brown colored calcite cuttings, as well as inclusion or impurity rich calcite cuttings, often displaying lattice defects. These calcite cuttings in the thick sections will be described as "classical calcite cuttings" abbreviated as "CCC" below, to avoid too much repetition. The latter calcites dominantly display a (dull) yellow orange luminescence and sometimes display cleavage twinning. Only if other features were observed are they mentioned separately.

In some thick sections some artefacts occur due to thick section preparation. In several cases this is because the cuttings do not occur at the surface that was polished. In that case with transparent light one can see the cutting, but it does not appear in cathodoluminescence since its surface is not hit by the electron-beam since it occurs below the resin.

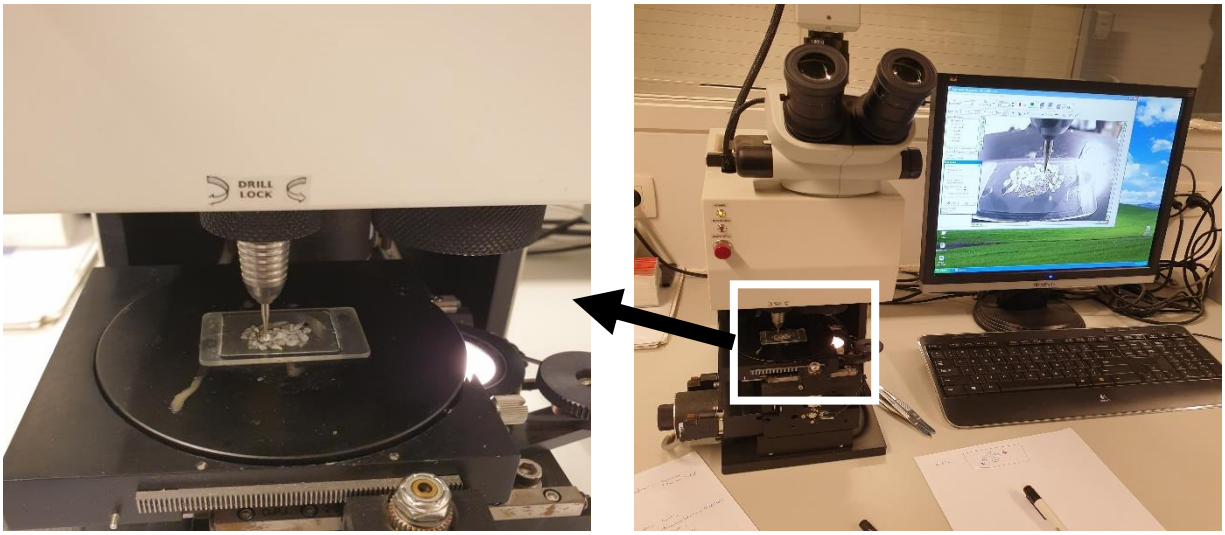

Figure 1: Micro-sampling devise with thick section of Beerse cuttings.

Notice that the cathodoluminescence images were all taken at maximum exposure time (10.000 ms), clearly indicating that the luminescence is indeed rather weak. It is important to know that the cathodoluminescence (CL) pictures are often corrected either to increase the contrast between components and/or to enhance the color differences. In several samples it was not even possible to take decent pictures.

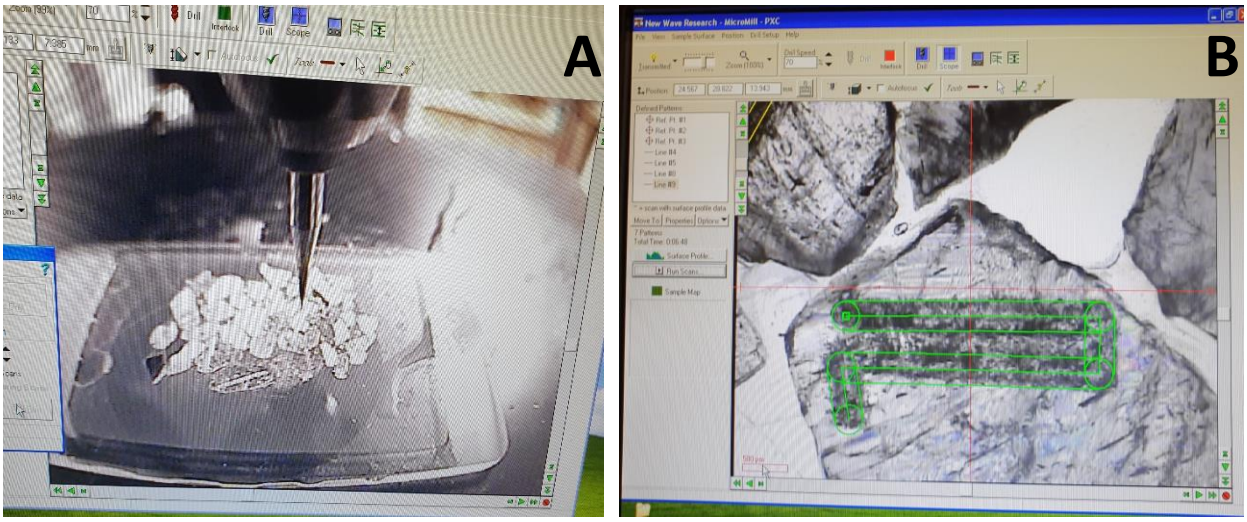

Figure 2: Thick section with drill bit (A) and drilled trajectory in cutting in the thick section (B).

In the photo-collection of the thin sections studied under cathodoluminescence in annex III we sometimes copied some interesting pictures out of the former report (Swennen, 2023). Their description below is indicated in italic.

Organic-rich cuttings were studied on the one hand by incident light microscopy to identify the maceral content and by Rock-Eval to assess the amount of existing hydrocarbons as well as the remaining hydrocarbon generation potential. Based on the amount of TOC, 50 to 100 mg powdered samples were analyzed following the method described in Behar et al. (2001). During the isothermal

heating step at 300 °C for 3 min, free and adsorbed hydrocarbons were vaporized and detected by an IR detector as S1 peak (mVs), while the S2 peak (mVs) was detected during linear heating at 25 °C/min up to 650 °C representing the amount of hydrocarbons generated from kerogen cracking. T_{max} represents the corrected temperature of the maximum pyrolysis yield of the S2 peak. Further parameters were derived using the following equations, including hydrogen index (HI) as remaining hydrocarbon generation potential, bitumen index (BI) as existing hydrocarbons remaining in the rock and production index (PI) indicating both maturity and impregnation or migration loss of source rocks.

HI = S2/TOC × 100 (mg HC/g TOC)
BI = S1/TOC × 100 (mg HC/g TOC)
PI = S1/(S1+S2)

2 NAMURIAN PETROGRAPHY

Cuttings from the Namurian succession were encountered in the interval 1800 – 1820/1825m (Chokier equivalent) and 1820/1825 – 1840/1845m (Souvré equivalent). Three characteristic lithologies were encountered in the cuttings, i.e.:

- Sandstones of which two types could be differentiated, namely (i) non-porous intensively cemented coarse grained and well-sorted sandstones (often with authigenic quartz overgrowths) and (ii) sandstones in which less well-sorted individual quartz grains could be differentiated, sometimes floating in a clay-rich and/or micrite matrix. The quartz grains were dominantly dull blue luminescent (with different shades) as well as blue purple (brown) luminescent (Figure 3). The two dominant CL colors support two provenance origins of the detrital quartz grains, however, based on their colors it cannot be differentiated whether they have a plutonic, volcanic and/or metamorphic origin (Götte and Richter, 2006). Sometimes the sandstones were crosscut by dull blue luminescent quartz veins (crack & seal type), as well as non-luminescent or dull purple red (brown) sometimes zoned dolomite veins. The latter postdate the quartz overgrowths.
- Siltstone, with small dull blue, blue purple (brown), and red luminescent quartz grains (e.g. 1870-2 & 3 in Swennen, 2023) floating in a very fine grained, often organic-rich matrix.
- Fine laminated organic-rich siltstone/shale sometimes with flaser and/or laminated texture (e.g. 1885-1 & 2 in Swennen 2023). In sample 1970m the siltstone was crosscut by a stylolite oriented perpendicular to the bedding). Whether this corresponds to a tectonic stylolite is unclear since in small cuttings it is not so obvious whether this is not an offshoot of a bed parallel (compactional) stylolite, especially since tectonic stylolites have not been reported yet from the Campine Basin. Notice that some of these organic-rich cuttings have been studied with respect to the organic components.

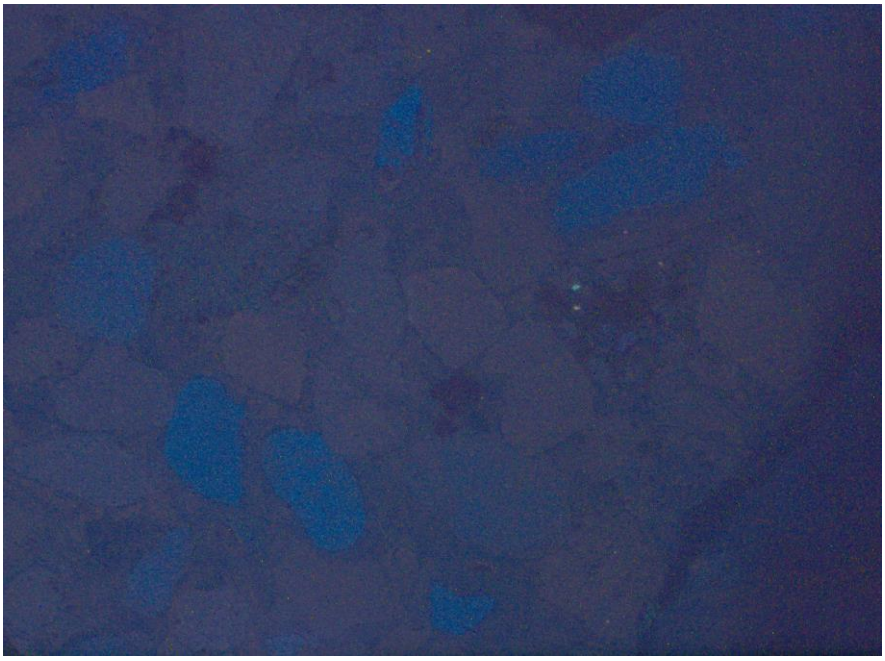

Figure 3: Sandstone with dominantly dull blue luminescent (with different shades) as well as blue purple (brown) luminescent quartz grains (Sample 1800m).

The Namurian paragenesis based on the studied cuttings is: detrital sedimentation (with marked variations in depositional setting based on sorting and grain size), authigenic quartz overgrowth, fracturing, dolomite cementation/veining, bed parallel (compactional; S23 - 13 plate 2 in Swennen, 2023) and subsequent tectonic stylolite (1870 - 1) development.

Noteworthy is that in the Dinantian succession, especially below 2310m, organic rich cuttings frequently have been encountered, that will be addressed in the section below, entitled “organic-rich cuttings”.

3 DINANTIAN PETROGRAPHY

3.1 INTRODUCTION

According to the core logging of well GT 01 A, the Dinantian succession starts at a depth of about 1836m. In the logging report it is reported that in the limestone succession the following special features occur:

- Dolomitic limestone and dolomite (common from 1960m – about 2000m)
- Anhydrite was mentioned to be present in the interval from 2020 – 2070m.
- A major fault zone was reported between about 2239m and 2300m. It is in this interval that black shales dominate. Some of these black shale cuttings have been investigated for organic geochemistry.
- Below 2400m calcareous marlstone, claystone and dolomite as well as clay interlayers are reported to occur between the limestones.

3.2 GENERAL DESCRIPTION: LITHOLOGY AND DIAGENETIC PRODUCTS

The dominant limestone cuttings in well GT 01 A consist of bioclastic wacke-/packstone containing open marine fauna, such as crinoids, shell fragments and foraminifera. Curiously, pellets, intraclasts and oolites do not frequently occur and thus the overall lithology does not change much, i.e. based on the lithological characteristics no particular intervals could be differentiated (except where dolomite occurs). Apart from these limestone cuttings, organic-rich shales, siltstones and sandstone cuttings commonly occur. They often display similar features as described for the Namurian shales above.

Most of the wacke-/packstones display either (dull) yellow orange or dull red purple luminescence. Several of the limestones show recrystallisation features (such as spotted CL textures). Recrystallisation is also supported by the oxygen isotope signature of the limestone cuttings (see below). Muchez et al. (1991) also mentioned that the Late Visean limestones in the Poederlee, Heibaart and Turnhout boreholes also testify of neomorphism. Most of the crystalline bioclasts, however, are non-luminescent and thus seem less affected by recrystallisation. Upon the crinoids often thin non-luminescent syntaxial rim cements developed (sometimes with minute CL-zonations), a feature also reported by Muchez et al. (1991). They are likely marine phreatic in origin. In contrast with Muchez et al. (1991) no isopacheous fibrous and radiaxial fibrous calcites, which are omnipresent in the microbial buildups, encountered in the western part of the Campine Basin have been encountered. This is in line with the absence of microbial boundstones. In addition, often the intergranular pores are filled by a dull red purple (brown) luminescent sparite. Based on their luminescence, the latter might be equivalent to the dull luminescent stage D calcite cement reported by Muchez et al. (1991), that according to these authors precipitated after a period of fracturing and pre-dating the formation of burial stylolites. However, in the Beerse cuttings the relationship with regard to stylolites is unclear. In line with the latter authors, these sparites likely are of shallow burial origin in relation to the circulation of either evolved marine or more likely meteoric water. Another feature that could relate to meteoric phreatic diagenesis are some few oversized dissolution cavities (e.g. 1920m and 2185m) that have been cemented by dull blocky

calcite, that also locally cover the syntaxial cements. Based on their luminescence they could be marine in origin, however, they more likely reflect shallow burial conditions with buffered redox conditions. According to Muchez et al. (1991), who also reported the development of secondary pores and cavities, these cements are relatively shallow burial in origin (a few hundred meters). They developed during the Late Visean – Early Namurian Sudetic phase, and the fluids originated according to the latter authors from near the Brabant – Wales Massif. Noteworthy is that in the Beerse GT 01 A, the typical meteoric cements, i.e. the non-bright-dull cements (reflecting changes in redox-potential during burial and typical for meteoric phreatic diagenesis) rarely have been observed. They might have been recrystallised as is the case for their host rocks. Only in the interval from 2105m till 2190m some bright yellow (sector) zoned calcite crystals occur, sometimes with well-developed crystal habitus that could reflect a meteoric cementation in some open spaces.

In the **interval 1855m – 2030m** not many fractures occur. The very few veinlets that were encountered are two dull luminescent calcite infillings that precede a bright yellow orange veinlet generation. The dull luminescent veinlets could have formed at the same time as the dull sparite cements, i.e. corresponding to stage D of Muchez et al. (1991). Indeed, the latter authors report that the most important fracturing was before and during the development of the stage D cements. No anhydrite was recognized, also not in the interval from 2020m – 2070m where it was formerly reported. Based on CL-petrography and short time etching with HCl 2N, no anhydrite was present in reference samples 1855m, 1910m and 1950m (despite the resemblance with anhydrite; see section 4.6 and Figure 4 & 5). The first limestones with authigenic quartz crystals (Figure 6) in this study were encountered at 1980m (see “Microphotographs of thin sections Beerse_GT_01a”, 1980 – 1 & 2 and 3 & 4. Note that in Swennen (2023) this was already recognized in sample 1965m (S23 -17- plate 2). They remain common till 2165m. These authigenic quartz crystals that often display an inclusion rich core will be addressed in section 4.5. They post-date the dull red purple (brown) luminescent blocky calcite.

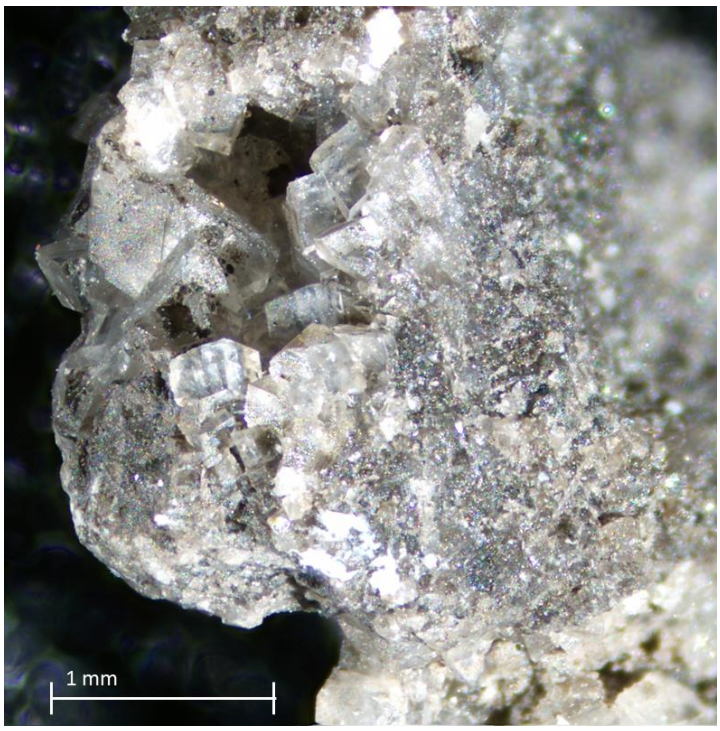

Figure 4: Euhedral calcite crystals developing around a cavity. Notice also the recrystallized nature of the grey colored limestone (“diagenesis reference sample” 1855m).

Figure 5: Calcite cement with well-developed skalenoeder with minute pyrite crystals (right picture).-From the "diagenesis reference sample" set, 1950m.

In the **interval 2020 – 2035m**, sandstone cuttings with dull blue and purple luminescent quartz grains (some with authigenic quartz overgrowths) occur of which their abundance decreases from 2040m. Feldspar grains are uncommon. A rare non-luminescent quartz vein is cut by a stylolite (See photoplates in "Microphotographs of thin sections Beerse_GT_01a", 2035-7 & 8). Several of the sandstones are cemented by yellow to yellow orange luminescent (sometimes zoned) calcite, which also exists as yellow orange luminescent mono-crystalline calcite cuttings which become common in cuttings from below 2035m. They clearly testify from some intense fracturing. This calcite cement postdates the quartz vein. This is the zone where anhydrite was reported in the well logging, but no anhydrite was identified. At the interval 2030m (see "Microphotographs of thin sections Beerse_GT_01a", 2030 - 5 & 6) and at 2045m (2045 - 5 & 6) some yellow to yellow orange luminescent veinlets, similar to the one described above, locally border an authigenic quartz crystal, and thus seem to post-date the latter.

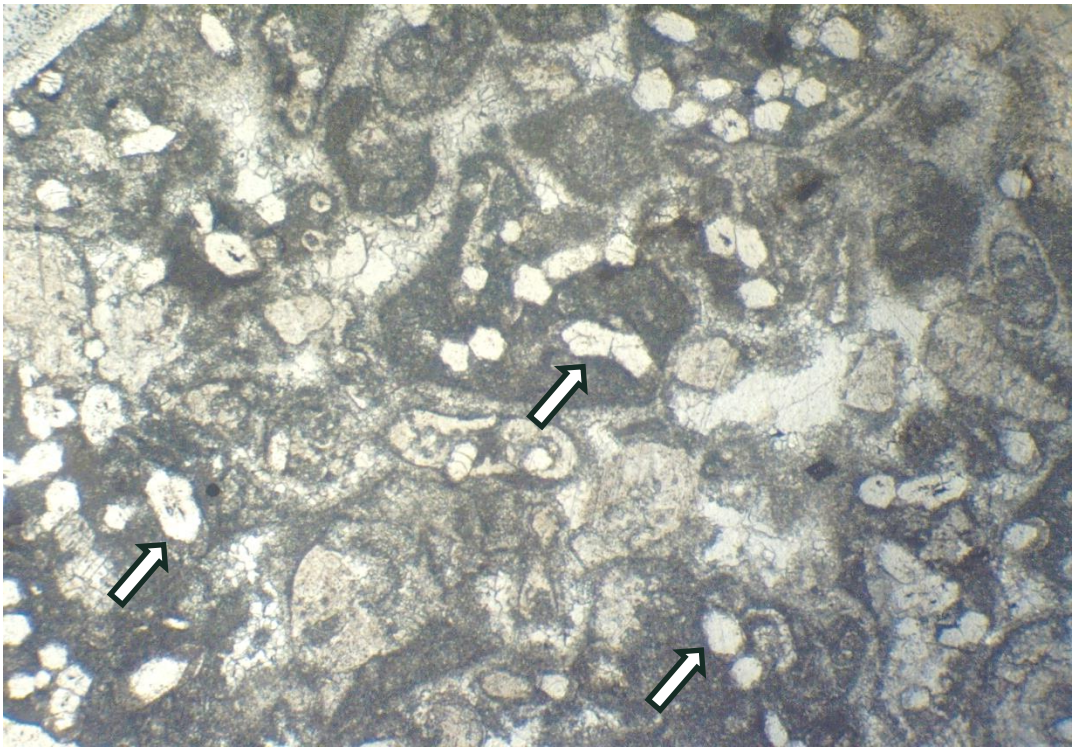

Figure 6: Bioclastic packstone with several authigenic quartz crystals (Sample 1980m)

From 2070m and below monocrystalline calcite cuttings that are either transparent or contain many impurities as well as fluid inclusions, frequently occur (and explains why here thick sections were made). They have a wide spectrum of CL colors, ranging from (dull) orange till yellow. The (dull) orange cements might be equivalent to the volumetrically most important cement in fractures which according to Muchez et al. (1991) is a non-ferroan, dull luminescent calcite, which occurs throughout the Campine Basin. They were interpreted to have formed during the early Westphalian from marine-derived waters at around 60°C. Crosscutting relationships in the cuttings are seldom. In sample 2060m, a yellow luminescent calcite veinlet is crosscut by an orange brown luminescent calcite veinlet (Figure 7). Another rare example occurs in sample 2105m, where a uniform orange luminescent calcite is surrounded by (sector) zoned orange to yellow orange sparite (possibly of meteoric origin) which are then covered by a brown luminescent calcite. The zoned calcite has been observed till 2190m. In one case it is cut by a stylolite. In samples 2105m, 2125m, 2130m, 2140m and 2200m also red orange luminescent calcite is replacing authigenic quartz (Figure 9). Notice that in none of the "diagenesis reference samples" individual quartz crystals were identified (again also based on CL petrography and HCl 2N etching). At 2120m but also in deeper settings (e.g. 2215m) a dull luminescent calcite veinlet or cement, is crosscut or covered by a bright yellow orange calcite veinlet (which is the reverse order then before). In "diagenesis reference sample" 2120m euhedral calcite crystals testify of the crystallization in open space (Figure 8). The latter is a characteristic feature from now onwards in deeper parts of the well. In samples 2140m till 2150m some quite large purple blue luminescent quartz crystals with an impurity rich (dark) core occur which are cemented by a bright yellow calcite that also locally seem to occur within the authigenic quartz crystals.

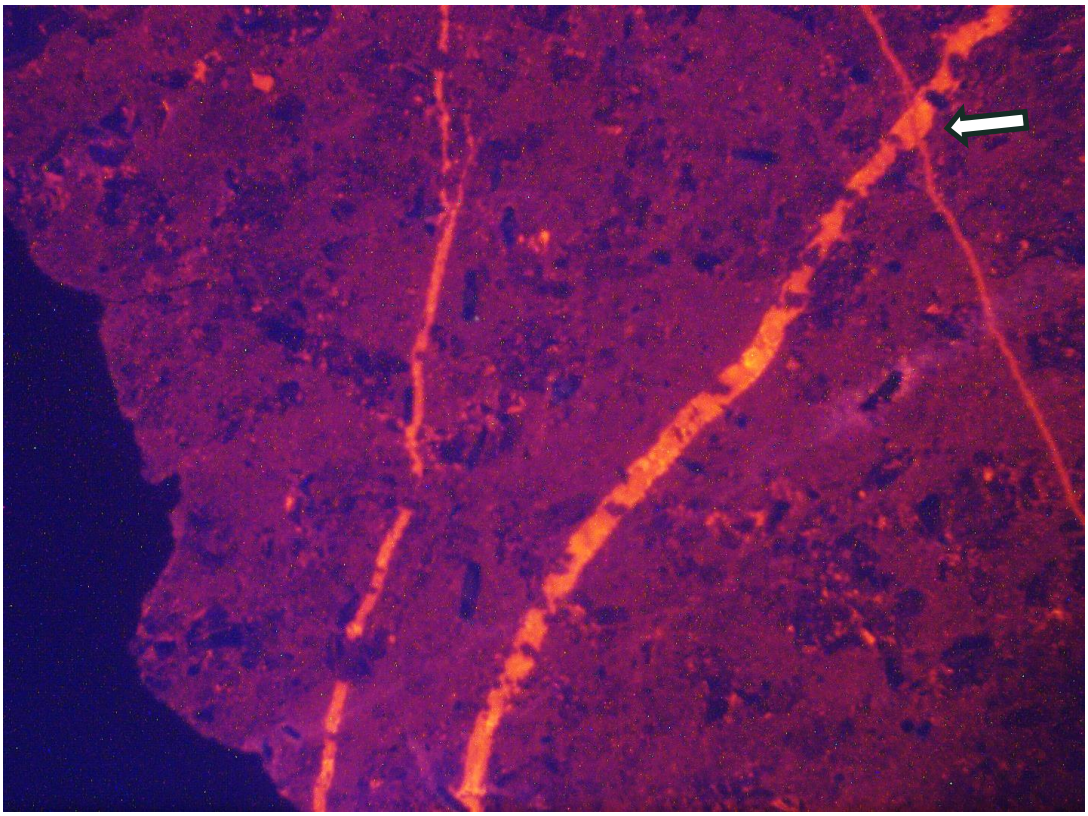

Figure 7: Red luminescent bioclastic packstone, crosscut by yellow luminescent calcite veinlets, of which one is crosscut by an orange brown luminescent calcite veinlet (arrow) (Sample 2060m).

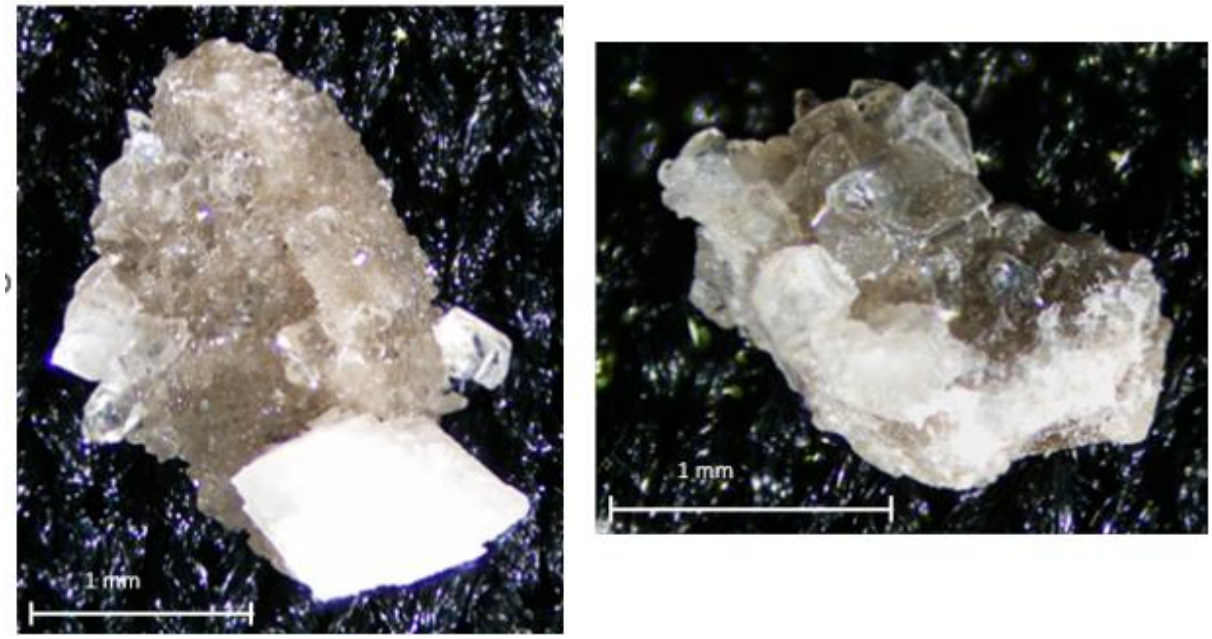

Figure 8: Calcite cement with well-developed crystals testifying of crystallization in open space ("diagenesis reference sample" 2120m).

From 2140m till 2190m red luminescent dolomite occurs. It makes up either xenotopic non-porous textures or hypidiotopic porous dolomites, that sometimes contain bitumen in intercrystalline pores.

Floating dolomite rhombs in a limestone matrix also were encountered. Also, locally some blotchy coarse crystalline dull purple luminescent dolomite occurs, whereby the blotchy nature testifies of recrystallisation. There likely are more than one generation of dolomitization. Some dedolomite phases were encountered in sample 2190m. They display the characteristic yellow orange luminescent calcite phases surrounding dull luminescent remnant phases. In this interval also some transmitted mono-crystalline calcite crystals occur (Figure 9).

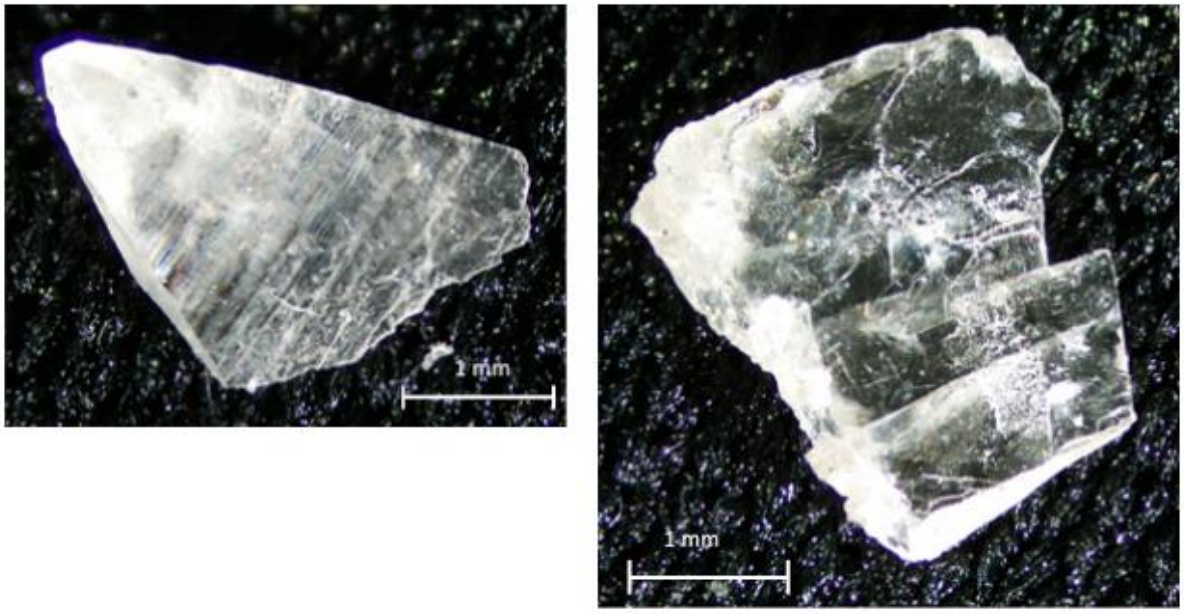

Figure 9: (Semi)transparent calcite cement. Notice that the right one displays features that could lead to the misinterpretation that it is anhydrite ("diagenesis reference sample" 2140m).

From 2220m onwards the limestones are again often non to dull luminescent (Figure 10). Orange as well as yellow luminescent (zoned) monocrystalline calcite cuttings or veins still occur (Figure 10 & 11) and testify of some fracturing related to a fault zone. One vein with crack & seal characteristics has been encountered. Additional fracture fillings are dull luminescent (sometimes zoned) (blocky) calcite which predates a dull orange luminescent vein type. The fault development also explains the dominance from 2275m – 2310m of black shales, which continues to be present till 2325m. Here they commonly occur next to bitumen containing floating quartz grains. Many of the limestones show clear features of intense recrystallisation, with microspar development yielding several shades of orange brown to orange luminescence. The bioclastic wacke-/packstone are dominantly dull to orange red luminescent. They become again common below 2305m. Since in the **interval from 2335m till 2350m** many coarse crystalline calcite cuttings commonly occur, thick sections were studied. Again, the latter testify from a nearby fault zone. In "diagenesis reference sample" 2325m one porous calcite cutting containing bitumen was identified, while the other 6 coarse calcite cuttings do not contain bitumen (Figure 12). In line with Muchez et al. (1991) the coarse calcites are extensional in origin and according to the latter authors crosscut stylolites. Their colors vary from yellow orange to dull orange, to zoned red orange. In the study by Muchez et al. (1994) the non-ferroan veins are filled by moderate to dull brown-orange homogeneous luminescent cements, which in the Heibaart borehole contain numerous cleavage planes.

Unfortunately, crosscutting relationships are uncommon in the studied cuttings.

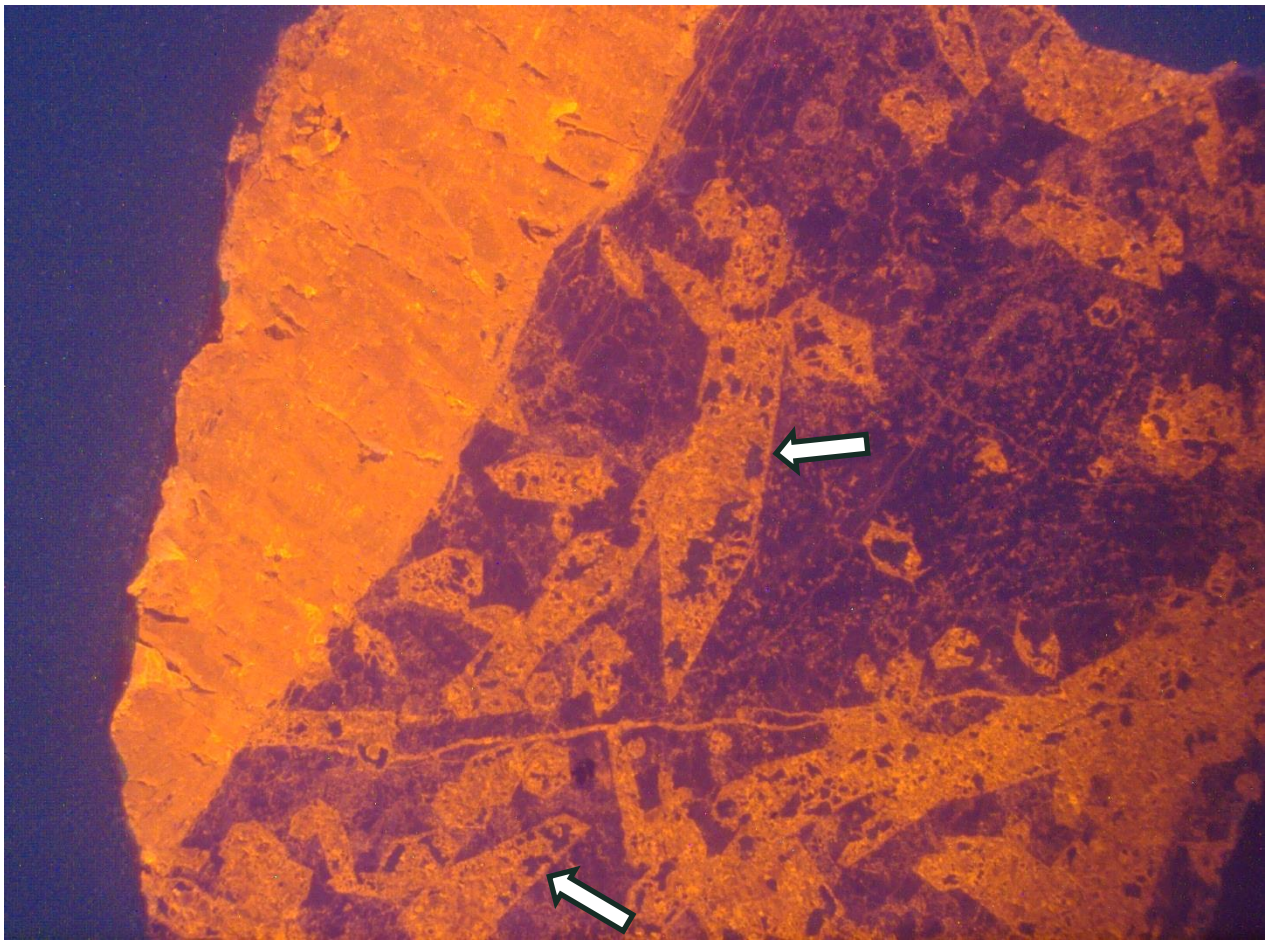

Figure 10: Dull brown luminescent recrystallized bioclastic packstone, bordered in its left part by an orange luminescent calcite vein. Notice the orange luminescent calcite which is replacing authigenic quartz crystals (Sample 2125m)

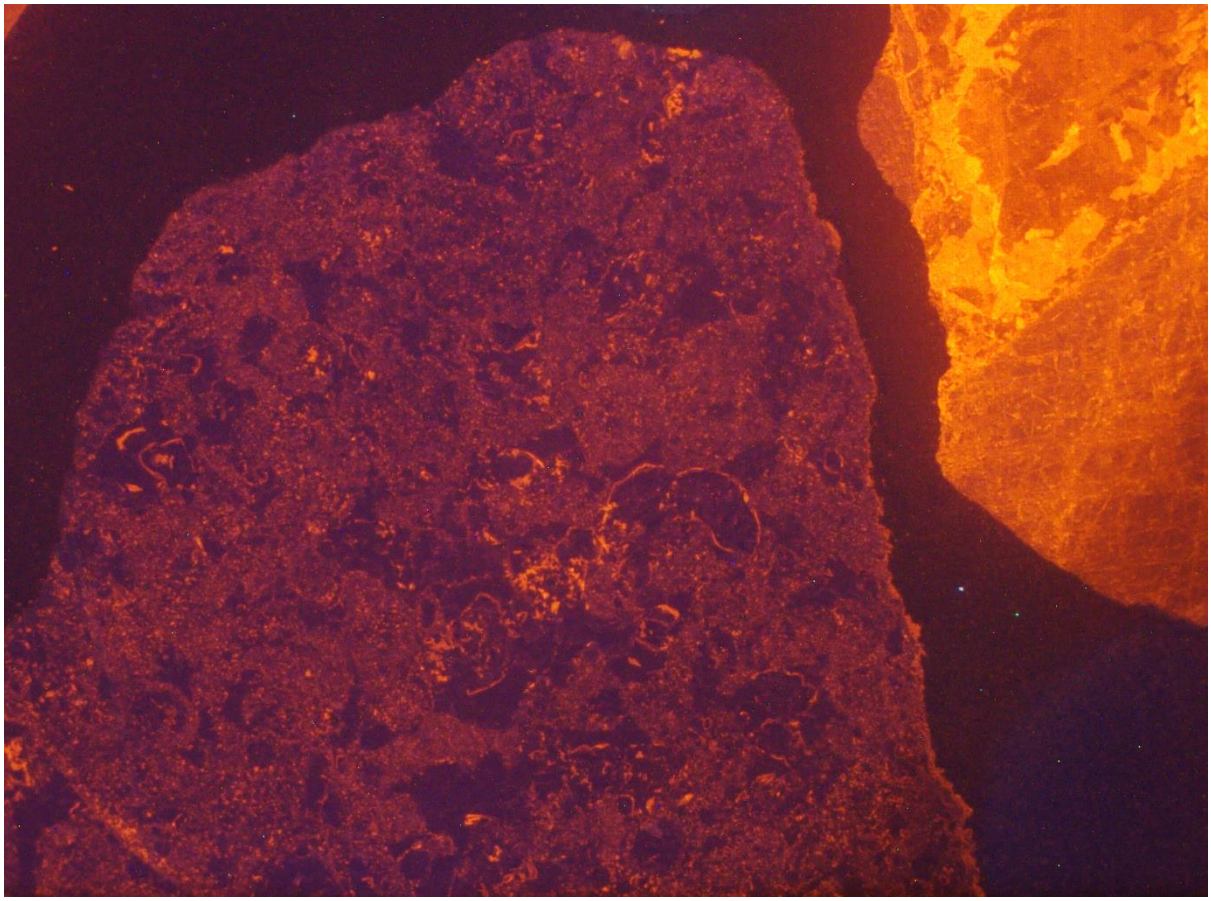

Figure 11: Dull luminescent bioclastic wackestone with in the upper part a yellow luminescent (zoned) monocrystalline calcite cutting (Sample 2215m)

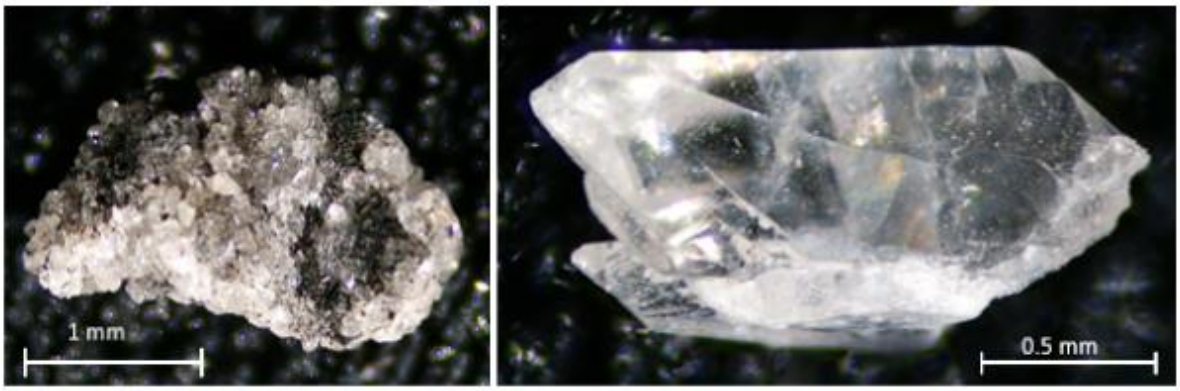

Figure 12: Calcite cement with well-developed crystals. Notice that the left one is covered with bitumen and the right one displays features that could lead to the misinterpretation that it is euhedral quartz ("diagenesis reference sample" 2140m).

Within the **interval from 2380m till 2470m**, dolomite samples similar as the ones described above (zoned dolomite rhombs floating in a limestone matrix and/or hypidiotopic dolomite with dull red luminescence) commonly occur (Figure 13) next to mainly bioclastic wacke-/packstone. Bitumen regularly occurs as intercrystalline infill. Bright yellow luminescent calcite veins or cements (zoned and/or forming skalenoeders) are also common in this dolomite-rich interval. These calcite cements testify from some open pore space, thus likely reflecting meteoric cementation after a phase of dissolution. Locally the red luminescent dolomite seems to replace the yellow luminescent calcite or

is filling up some space between the calcites. Thus, this dolomite post-dates the yellow luminescent calcite. In the **interval 2415m – 2520m** sandstone and shale cuttings commonly appear, next to bitumen bearing cuttings. Bitumen bearing calcite (and sometimes dolomite) also has been recognized in several of the "diagenesis reference samples" 2345m, 2420m, 2445m and 2520m.

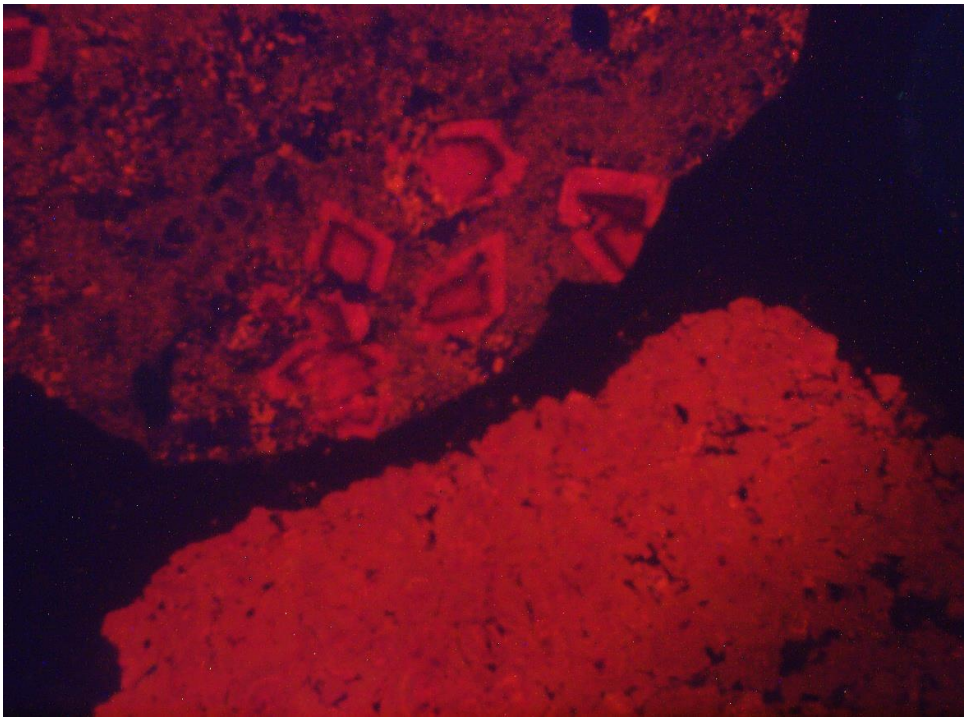

Figure 13: Zoned red luminescent dolomite rhombs floating in a dull brown orange luminescent mudstone (upper cutting) and red luminescent hypidiotopic dolomite with dull red luminescence (lower cutting) (Sample 2380m)

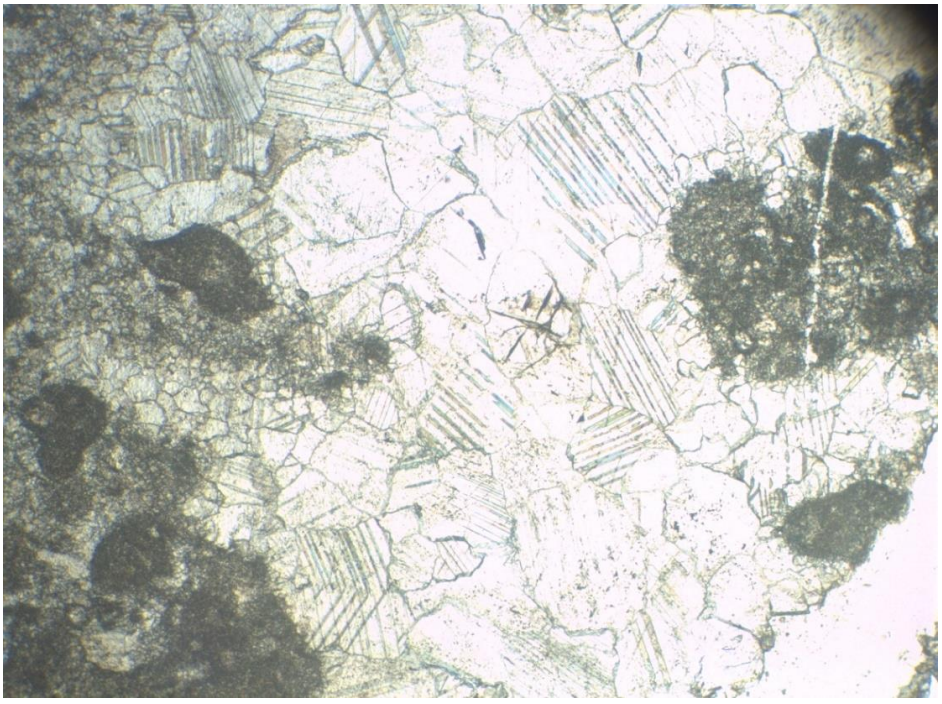

Figure 14: Dissolution cavity filled by (a dull luminescent) sparite (displaying cleavage twins) occurring next to recrystallisation features, i.e. microsparite (Sample 2520m).

Coarse mono-crystalline cuttings, displaying a broad range of CL-colors regularly occur again **from 2465m till 2545m**. Based on few crosscutting relationships non luminescent veinlets are crosscut by monocrystalline bright yellow luminescent calcite veins. Finally in sample 2520m, a rare dissolution cavity which is filled by a dull luminescent sparite occurs next to recrystallisation features, i.e. microsparite (Figure 14). Both features support a meteoric dissolution stage. The dull luminescent cement infill likely developed during shallow burial reflecting rather rock buffered redox conditions.

3.3 PARAGENESIS AND INTERPRETATION OF THE DIAGENETIC PHASES

As expected, it was not easy to infer a paragenesis based on cuttings. Furthermore, one should be aware that the paragenesis may (to some extent) be lithology dependent and may change through time (thus in function of the depth position). In section 5.2 a figure illustrating the paragenesis is given (Figure 29).

After sedimentation, the sediments underwent limited marine phreatic cementation (incl. non-luminescent syntaxial rim cements). Subsequently a dull red purple (brown) luminescent sparite developed, likely reflecting shallow burial meteoric diagenesis. In the interval from 2105m till 2190m the bright yellow (sector) zoned calcite crystals, sometimes with well-developed crystal habitus occur that could reflect a meteoric cementation. In many of the samples recrystallisation features have been noticed, of the bio- and allochems and of the marine cements. Locally oversized dissolution cavities have been noticed which are filled by dull blocky calcite. The dissolution likely is meteoric in origin, and the dull uniform luminescence of the infilling cement points towards cementation in a shallow burial setting. Likely one of the two dull luminescent calcite veinlets relates to this shallow burial cementation. These dull luminescent veinlets precede a bright yellow orange veinlet generation.

Stylolitisation has been encountered in several of the cuttings, but it was not possible to infer with certainty its orientation. It seems likely that bed parallel stylolites exist, testifying of burial related pressure dissolution. Whether tectonic stylolites also exist, as was potentially noticed in a Namurian shale sample, is unclear. But since these stylolites develop perpendicular to stratification, they likely do not frequently occur in a vertical well. However, the fact that many of the mono-crystalline calcite cuttings display well-developed cleavage twins, which testifies of some tectonic stresses, tectonic stylolites might exist. In one sample a non-luminescent quartz vein is cut by a stylolite.

The subsequent diagenetic phases testify of some burial diagenesis with several fracturing and fracture infilling events. One of the typical cements is yellow to yellow orange luminescent (sometimes zoned), which seems also to occur as a calcite cement in some of the sandstones. Crosscutting relationships are rare, and thus it is not possible to work out a complete paragenesis of the fracture infills. The yellow luminescent calcite veinlet is locally crosscut by an orange brown luminescent calcite veinlet. Furthermore, a uniform orange luminescent calcite is in some of the cuttings surrounded by (sector) zoned orange to yellow orange sparite. Elsewhere a yellow orange luminescent mono-crystalline calcite (vein-type) is covered by a brown luminescent calcite. Also, a bright yellow luminescent calcite vein type also occurs as cements bordering open space. The latter might indicate a new phase of meteoric cementation that followed a dissolution phase. With respect

to the different generations of mono-crystalline calcite cuttings, it is noteworthy to mention that they do not occur together with bitumen (see below). Furthermore, several of these mono-crystalline calcite cuttings possess cleavage twins, thus indicating that they developed before they were affected by some tectonic constraints. According to the classification by Burkhard (1993), the cleavage twins belong to his type I & 2, and thus respectively reflect alteration temperatures of respectively <200°C and 150-300°C.

Host rock dolomitization has been observed, but its timing is unclear. Dolomitization was indeed noticed in some of the boreholes studied by Muchez (1988). An early diagenetic origin cannot fully be excluded. The coarse crystalline dull purple luminescent dolomite likely is burial in origin, as is the recrystallisation of dolomite. The locally observed dedolomitization is also likely burial in origin (see comments on "Dedolomite").

Another peculiar feature is the occurrence of replacive authigenic quartz crystals (interval 1965m - 2165m). Notice that in several samples the authigenic quartz crystals have been replaced by red orange luminescent calcite, that also occurs as vein infill (Figure 10).

Of major interest is the presence of different types of organic-rich cuttings, of which one impregnates rather well-sorted sandstone or incorporates floating quartz grains. Thus, oil migration took place, and likely source rocks are the black organic-rich Lower Namurian shales. Organic-rich cuttings are locally an important component in the studied cuttings. Noteworthy is that the quartz grains in the with bitumen impregnated sandstones have the same luminescence as the quartz grains in the Namurian strata, namely they are faint blue or red purple (brown) luminescent. They occur from below 2330m. If they are possibly Namurian or Westphalian sandstones (see discussion below), then they very likely testify of either contamination or influx of sand or sandstones (and black shales) within large karst cavities, of which a first phase of karstification took place at the end of the Dinantian (Poty, 2016). It, however, cannot fully be excluded that a second episode of karstification took place at the end of the Cretaceous – Paleogene time, explaining some of the open veins encountered in the study by Swennen et al. (2021). However, as discussed in the section below addressing the organic constituents, a Westphalian origin of some sandstone cuttings and organic phases is also a very likely scenario.

More information on lithology and diagenetic products are given in annex II, while in annex III the different cathodoluminescence and transmitted light micrographs are given.

3.4 DISCUSSION OF SPECIFIC DIAGENETIC FEATURES

3.4.1 Search for hydrocarbon inclusions by Fluorescence petrography

A screening of the cuttings based on hand-held fluorescence, i.e. a Long Wave 365nm pocket lamp did not show any limestone/dolomite nor calcite cuttings that were fluorescing.
We subsequently studied all thin section by fluorescence microscopy with a focus on detecting hydrocarbon bearing phases linked to fluid inclusions. We also studied the samples from the VPO reference collection in the hope of finding suitable samples for eventual additional microthermometric research of these fluid inclusions.

Unfortunately, it turned out that the limestones all were non-fluorescent. They locally displayed a green shade, however, this shade is caused by the refraction of the incident fluorescent light on rock

heterogeneities, such as grain boundaries, cleavage twins, micrite, etc. … (Figure 15A & B). Also, none of the dolomite cuttings was fluorescent, neither the authigenic quartz crystals (Figure 10C), nor the bitumen. We especially studied the mono-crystalline calcite cuttings, which as mentioned above were either transparent or inclusion-rich (but not necessarily related to fluid inclusions) or impure and thus non-transparent. All were non-fluorescent (Figure 15D & 16), but with increasing impurities and heterogeneities a green color appeared. A typical example are the cleavage twins that become apparent, as well as the inclusions. The non-transparent calcite cuttings displayed a homogeneous shade, due to the refraction of the incident fluorescent light (Figure 15D & 16). Also, the study of the few fluid inclusions did not identified fluorescent hydrocarbon inclusions.

In conclusion the study based on fluorescent light did not result in additional information of the cuttings. In annex IV some additional pictures are shown.

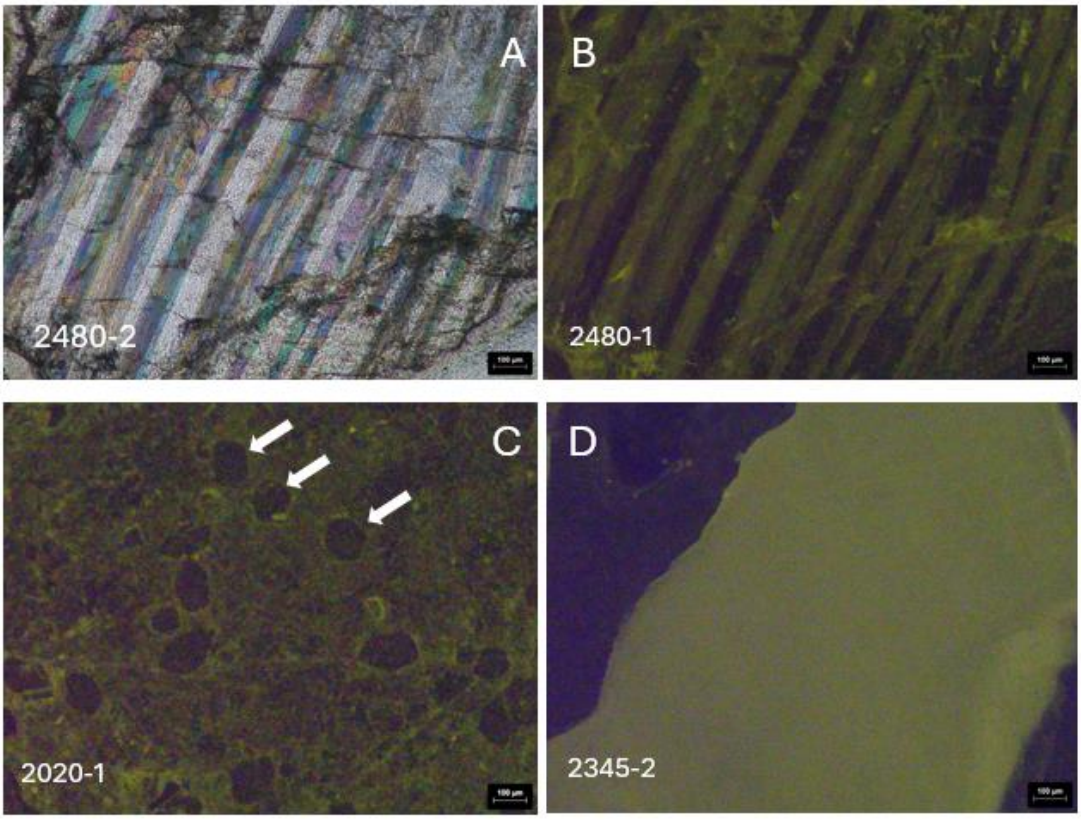

Figure 15: A. & B. Photomicrographs of transmitted and fluorescent light of monocrystalline calcite with clear cleavage twins. C. Fluorescent light photomicrograph of bioclastic limestone with several non-fluorescent authigenic quartz crystals (of which three are indicated with an arrow). D. Fluorescent light photomicrograph of non-transparent calcite cutting (sample numbers are indicated).

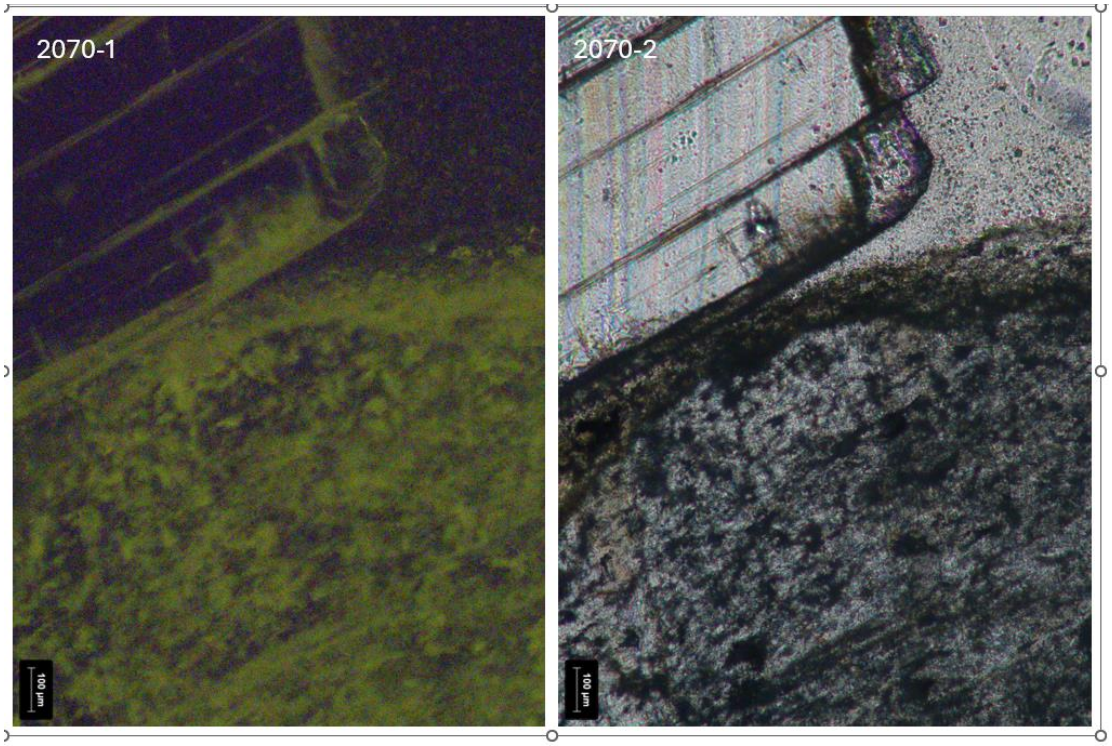

Figure 16 A. & B. Photomicrographs of transmitted and fluorescent light of two monocrystalline calcite cuttings, of which the lower contains many inclusions, while the upper one is transparent displaying some cleavage features (sample number is indicated).

3.4.2 Sulphides (incident light microscopy)

In the file "Description incident light and fluorescence microscopy" (annex IV) an overview is given of the most important observed features. Notice that the color shades in the incident light microphotographs may vary due to the bright reflection of the light.

In the cuttings from the organic-rich Namurian shales and sandstones, minute pyrite crystals were regularly encountered. In the shales they often have a framboid outline, while in the sandstones they are larger (up to 300µm), likely due to some recrystallisation (crystal enlargement). Here, chalcopyrite has also been identified. However, a common opaque mineral is hematite, regularly forming lath-shaped or elongated streaks. In one case a stylolite was cemented by hematite. Some of the opaque minute phases seem to follow some bioturbations in the shales.

Since the pyrite framboid diameter can be used as redox proxy, i.e. the difference in crystallization conditions between dysoxic to oxic, euxinic to anoxic conditions can be inferred (Wilkin et al., 1996), its diameter was measured in a limited number of organic-rich Namurian cuttings. Its mean diameter of Beerse framboids varies between 4,1 and 7,2 µm with standard deviation (SD) from 0.8 to 2.5. This plots in the euxinic to anoxic domain, and is in line with the results of the Namurian A organic-rich mudstones in the Turnhout well where values ranges between 4.2 and 7.7 µm with standard deviation (SD) from 0.9 to 2.7 (Wei, 2023) They are lower than the measured values in the Geverick GVK-01 with mean diameters of 4.0 to 8.4 µm and SD of 0.9 to 4.9.

In the Dinantian cuttings only locally some sulphides like pyrite and chalcopyrite were identified (Figure 17A & B). Pyrite displays different habitus, like cubic, pentagon dodekaeders as well as framboïds. In one case a honeycomb type of pyrite texture was encountered. Pyrite was also

identified on top of some of the “diagenesis reference samples” and thus formed also in open space. Pyrite was never encountered in the dolomite samples, and only seldom in the mono-crystalline calcite phases. No other sulphides, such as galena or sphalerite were encountered.

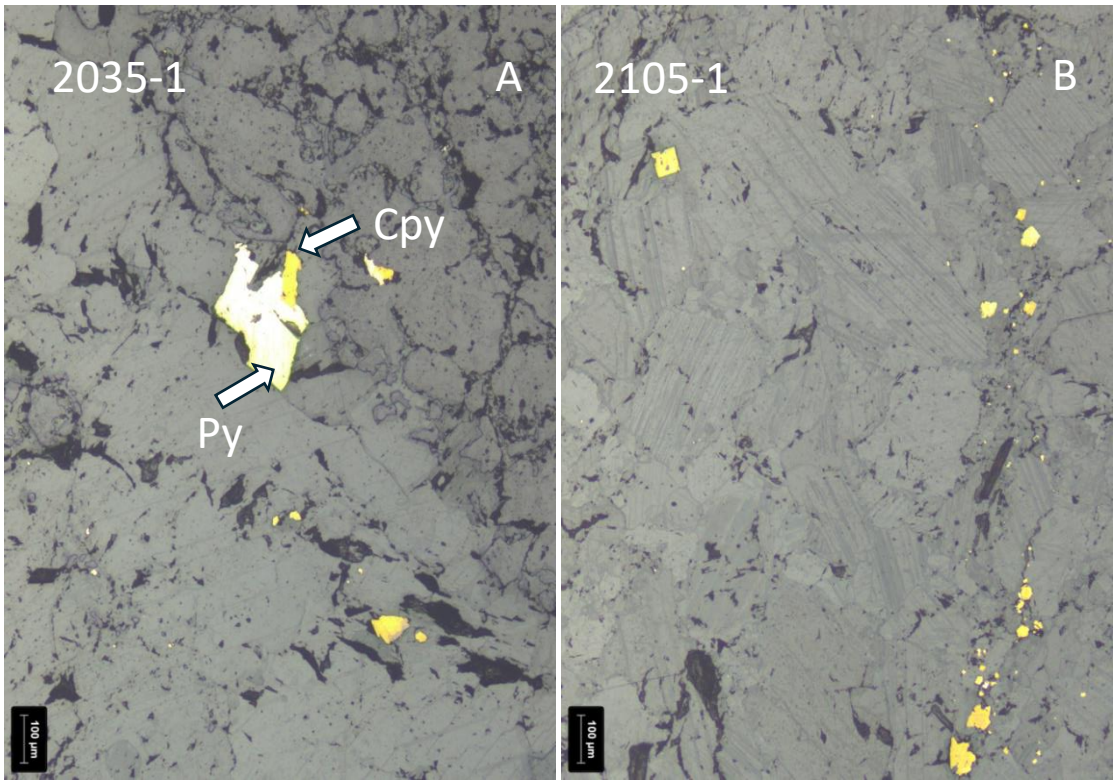

Figure 17: A & B. Incident light microscopy of polycrystalline calcite with in A the presence of pyrite (Py) and chalcopyrite (Cpy), while in B only chalcopyrite occurs. Notice in B the cleavage twins in the calcite crystals (sample numbers are indicated).

4 COMPLEMENTARY ANALYSES

4.1 MICROTHERMOMETRY

Microthermometric investigations of fluid inclusions of, for example the mono-crystalline calcite cuttings were not carried out because:

- A clear paragenetic succession could not be worked out due to the nearly complete absence of crosscutting relationships.
- The existence of many cleavage twins which testify that the calcite cements have undergone some tectonic stresses likely causing leakage and resetting of the fluid inclusion parameters.
- The fact that Muchez et al. (1994) mentions that based on the absence of any apparent relationship between T_m and T_h, it was suggested that any or all of the processes such as mixing of fluids, stretching, leakage and refilling may have taken place. The authors also mentioned that it was also not evident to differentiate primary from secondary inclusions.

Only in a few exceptional cases, e.g. euhedral crystals bordering open spaces (which were rare) possibly some few minute primary inclusions could be differentiated. Their number, however, was too low to infer a statistical relevant T_h value.

4.2 STABLE ISOTOPES

The analytical protocol used for stable isotope analysis is given in annex V. Stable C and O-isotope analysis were performed on 72 samples and are given in Figure 18 and in annex VI. Samples R1 to R21 correspond to samples collected by micro milling and thus correspond to calcite cement. In total 39 dominantly mono-crystalline calcite samples were analyzed, as well as 5 dolostone samples and 28 possibly recrystallized limestone samples. Notice that it was not always clear whether the limestones were recrystallized, e.g. on the blotchy spotted CL texture or presence of microspar or neomorphosis.

When interpreting stable isotopes of carbonates, first always reference should be made to the original isotopic composition of limestones of the same age that formed in equilibrium with marine water. This value can sometimes be acquired from sampling not-diagenetically altered brachiopods, but this was not possible with the cuttings of the Beerse well. We therefore have to rely on the reported isotopic limestone composition in literature. The assumed original marine isotopic signature of the Lower Carboniferous was retrieved from Swennen & Muchez (2016), indicating $\delta^{18}O$ values between -1 ‰ and +2 ‰, and $\delta^{13}C$ values between 0 ‰ and +4.5 ‰ for the Dinantian strata.

The analysed $\delta^{13}C$ values of the limestone cuttings vary between +0,3 and +5,7 ‰ (Figure 18). There is a clear increase visible in $\delta^{13}C$ values with depth with values varying between +0,3 to +1,8 ‰ for limestones of the depth interval 1845m till 1980m (with one exception of +2,4 ‰ of a limestone sample from 1945m) (Annex V). In the depth interval from 1995m till 2520m the values mainly plot between +2,3 to +5,7 ‰ (with 2 exceptions), and with the highest values for the two deepest samples (Annex V). Muchez et al. (1994) reported host rock $\delta^{13}C$ values that varied between +0,6 and +2,4 ‰. Overall, the measured values plot into the range of Dinantian limestones (except the two deepest samples) and thus likely correspond to the original signatures. Indeed, it is well known that

$\delta^{13}C$ values are less susceptible to fractionation effects (Meyers and Lohmann, 1985). No negative $\delta^{13}C$ values were encountered in these limestones, thus recrystallisation in a setting with depleted C can be excluded (such as the effect of C derived from hydrocarbons).

The analysed $\delta^{18}O$ values consistently are more depleted than the original $\delta^{18}O$ signature of Dinantian marine limestones. Their values vary between -8,5 to -14,5 ‰ (Figure 18) and thus testify of resetting of the marine signature. This resetting cannot simply be explained by interaction of meteoric waters, which would lead to a depletion of 4 to 5 ‰, thus the resetting took certainly place at relatively high temperatures. Regarding $\delta^{18}O$ values no obvious depth trend can be observed. Muchez et al. (1994) reported $\delta^{18}O$ values for host rock values from the Turnhout and Heibaart boreholes that varied between -8,8 to -13,4 ‰, which overlap quiet well with the Beerse limestone cutting values.

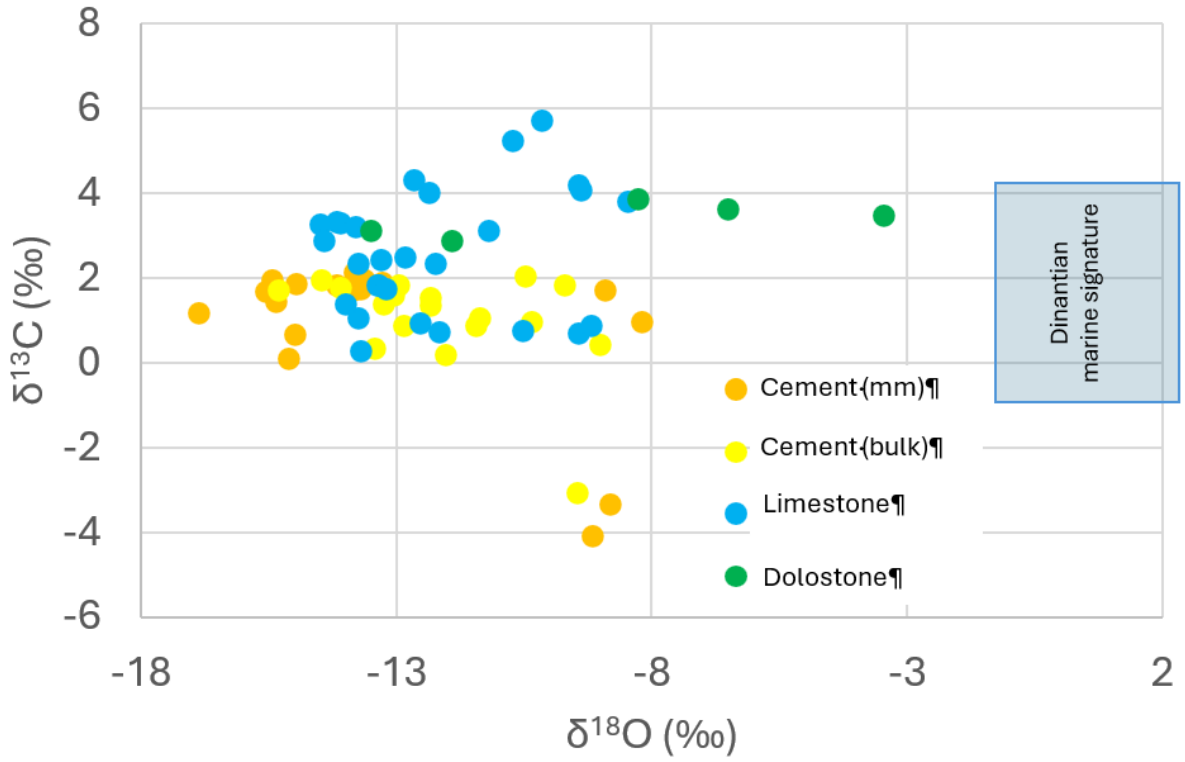

Figure 18: Stable isotope plot with indication of the Dinantian marine calcite signature. Abbreviation mm = micro milling.

With regard of the dolostone samples, their $\delta^{13}C$ values vary between +2,9 to +3,9 ‰ (Figure 18) with highest values again for the deepest samples of depth interval 2440 – 2470m (Annex V). The $\delta^{18}O$ signature of the two (assumed) dolostone samples of 2220 – 2230m vary between -11,9 and -13,5 ‰ and thus overlap with the depleted limestones signatures. However, $\delta^{18}O$ values of the dolostone samples from the depth interval 2440 – 2470m are clearly less depleted and plot between -3,5 to -8,3 ‰ (annex V). While interpreting these $\delta^{18}O$ values one needs to take the fractionation of +3-4 ‰ between calcite and dolomite into account (Matthews and Katz, 1977), which means that the signatures, even the less depleted testify of dolomitization and/or dolostone recrystallisation again at higher temperature, but less high temperatures for the deepest samples.

With regard to the pure calcite cements, the micro milled samples correspond to monophase samples originating from one type of calcite, while for the bulk samples it cannot be excluded that different calcite generations were mixed together and thus that the isotope signature reflects a mixed signature of these calcites.

In the micro milled samples, most of the $\delta^{13}C$ values vary between +0,1 to +2,1 ‰, also for the deepest samples taken from below 2500m (annex V & Figure 18). Their isotopic signatures therefore are likely host rock buffered. There are only two samples from a depth of 2345m with depleted $\delta^{13}C$ values varying between -3,3 and -4,1 ‰. Here we can assume the involvement of a depleted C-source, such as derived from hydrocarbons or organic material. Notice that in the thick section of the latter sample from 2345m, one calcite did not possess this depleted signature (annex V). The $\delta^{13}C$ values reported by Muchez et al. (1994b) for non-ferroan extensional calcite veins that cross-cut stylolites vary for the Poederlee samples between +1,3 and 2,4 ‰, and between -3,1 and -1,3 ‰ for the Heibaart and Turnhout calcites.

The $\delta^{18}O$ values of the micro milled calcites, with the exception of the two $\delta^{13}C$-depleted calcites which have respective values of -9,2 and -8,8 ‰, and with the exception of the calcites from 2545m with values of -8,9 and -8,2 ‰, all possess very depleted signatures with values varying between –13,3 to -16,9 ‰ (annex V). They thus possess $\delta^{18}O$ signatures that plot at the most depleted end of the limestones (Figure 18), however, there is no clear trend visible if the calcites are compared with the limestones taken at the same depth position (annex V, A & B samples). Muchez et al. (1994b) reported $\delta^{18}O$ values of blocky calcites varying around -9,3 ‰ in the Poederlee borehole, and around an average value of -13,5 ‰ for the Heibaart and Turnhout calcites, but values as low as -17 ‰ have been recorded in the Heibaart borehole.

If the bulk calcite samples are taken into account, then again, the sample at a depth of 2345m is most depleted in $\delta^{13}C$ (-3,1 ‰) and $\delta^{18}O$ (-9,5 ‰) (annex V). The other bulk samples possess $\delta^{13}C$ values varying between +0,2 to +2,0 ‰, quite similar to the micro milled samples (Figure 18 and annex V). For $\delta^{18}O$ the values range between -9,0 to -15,3 ‰, again with the most depleted values of -13 to -15,3 ‰ derived from the deepest samples, however, there exists some variation in this with less depleted values at 2420m with -9,0 ‰ (annex V). Overall, it is not so obvious to differentiate different populations in isotopic composition within the calcite phases (Figure 18). However, what is clear is that the $\delta^{18}O$-signatures, which are depleted likely point to involvement of hot basinal brines, that also can explain the resetting of the limestone signatures.

If crystallization temperatures of 45 to 93°C are considered, as proposed by Muchez et al. (1994b) for blocky calcites from the Northern Campine basin, then $\delta^{18}O$ calcite signatures between -9,0 to -15,3 ‰ result in $\delta^{18}O_{SMOW}$ values of -3 to -3,5‰ (Figure 19), which according to the former authors reflect involvement of marine derived fluids that mixed with meteoric water. To get an independent additional argument to support this interpretation additional Sr-isotope and/or clumped isotope analysis are recommended. Similarly, Muchez et al. (1994b) based on fluid inclusion micrometry data, calculated that the Poederlee calcites (temperatures of 45 – 75 °C) precipitated from a fluid with $\delta^{18}O_{SMOW}$ values of +4 to -2 ‰, while the blocky calcites from Turnhout and Heibaart (temperatures 70 – 93°C) crystallized from fluids with $\delta^{18}O_{SMOW}$ values of -4 to -1,1‰. The latter authors argued that these ranges suggest that precipitation occurred from “marine derived” fluids which mixed with meteoric fluids (Muchez et al., 1994). Their interpretation is also based on the inferred composition of Carboniferous meteoric water of -7 ‰ $\delta^{18}O_{SMOW}$ from Derbyshire as reported by Walkden and Williams (1991).

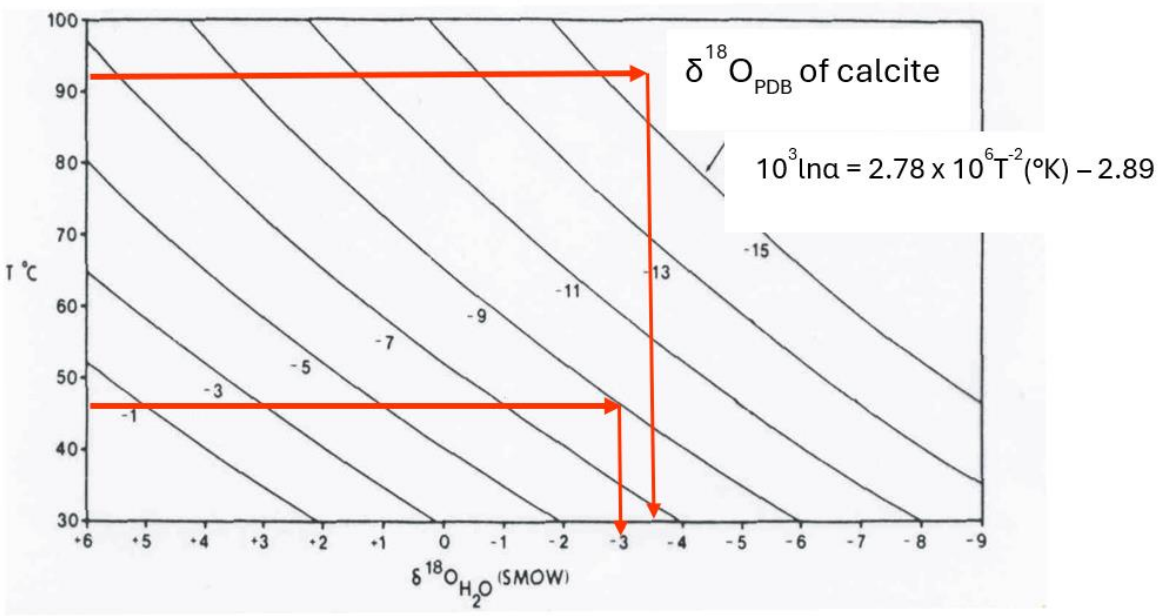

Figure 19: Inferred $\delta^{18}O_{SMOW}$ composition of the blocky calcites based on the fractionation equation given in the figure.

4.3 ANALYSIS OF ORGANIC-RICH CUTTINGS AND MINERALOGY OF NAMURIAN BLACK SHALES

As mentioned above Namurian black shales were encountered in the interval 1800 –1840/1845m. Their presence also explains the frequent occurrence of organic-rich shale cuttings in the underlying Dinantian strata. Seven samples from this interval have been studied regarding their organic components. They all gave quite consistent results. Solid bitumen is present and has high reflectance values, roughly between 3.0 and 4.0 % indicating high thermal maturity (Table 1). This is comparable to the high vitrinite reflectance measured in the Namurian A strata of the Turnhout well with values varying around 3,5%. It was decided not to carry out Rock-Eval analysis on these samples since on the one hand most material was used for making polished sections and on the other hand it was not expected to generate a valid Rock-Eval S2 signal (as was also noticed in the Namurian A strata of the Turnhout well; Wei and Swennen, 2022) due to very high thermal maturity. Regarding the depositional setting of these Namurian black shales the reader is referred to the recent paper by Wei and Swennen (2022).

Table 1: Vitrinite reflection data of Namurian samples

depth	VR/%	Std. Dev.	points
1800	2.94	0.29	50
1810	3.37	0.36	54
1815	2.98	0.24	50
1820	3.05	0.26	50
1830	3.34	0.26	53
1840	3.8	0.23	50
1845	3.56	0.31	40

Table 2: Mineralogy of Namurian black shales of different boreholes studied in the Campine basin (Wei and Swennen, 2022) compared with mineralogy data from the Beerse borehole (interval 1800 – 1850m). Abbreviations: BHG = Browerhavense Gat; GVK = Geverik. Clay content in Beerse is the sum of Chlorite + Kaolinite + Muscovite + Smectite.

Mineral (%)		BHG-01	GVK-1	Halen	Turnhout	Beerse
Quartz	Mean	22	35	48	44	22
	Min	20	19	10	2	18
	Max	25	62	96	79	26
Alkali Fsp.	Mean	2	4	0	2	0,8
	Min	1	0	0	0	0,5
	Max	3	11	0	10	1,3
Plagioclase	Mean	1	4	2	2	4,6
	Min	0	0	0	0	2,7
	Max	3	7	8	10	5,2
Clay	Mean	66	41	8	26	16,7
	Min	54	12	0	14	11,4
	Max	71	65	37	79	18,1
Calcite	Mean	1	3	40	3	3,9
	Min	0	0	4	0	2,3
	Max	4	20	89	64	9,8
Dolomite	Mean	2	8	1	0	3,6
	Min	0	0	0	0	1,6
	Max	6	52	4	0	4,6
Siderite	Mean	2	2	0	0	1,1
	Min	1	0	0	0	0,7
	Max	3	33	1	1	1,5
Pyrite	Mean	2	3	1	4	1,2
	Min	1	0	0	0	0,4
	Max	5	7	2	19	2,6
Apatite	Mean	0	0	0	0	0,4
	Min	0	0	0	0	0
	Max	0	0	0	0	0,7

In Table 2 data on the mineralogy of Namurian shales are summarized. It can be seen that overall, the Beerse cuttings have lower quartz as well as clay content than neighboring wells from the Campine Basin. In the Beerse samples chlorite and muscovite are the most common clay minerals, and kaolinite is nearly absent, a feature also encountered in the Geverik and Turnhout Namurian black shales (Wei and Swennen, 2022). The mineralogy content in the Beerse samples is also much more homogeneous, which could relate to the limited depth interval studied in this borehole. The plagioclase content is relatively high, compared to K-feldspar, which is rather unusual since plagioclase weathers more easily than K-feldspar. Overall, the carbonate content is rather low but comparable to the other boreholes if the extreme values are left out. Of interest is that the barite content in the Namurian interval in Beerse varies between 1,1 and 2,7% (not shown in Table 2). No information is available on the barite content in the other boreholes. Finally, the siderite content in the Beerse interval is low. This is of importance since siderite would point to more brackish

depositional and early diagenetic conditions but knowing the position of the Beerse borehole with respect to the Brabant Massif coastline, euxinic to anoxic marine conditions prevailed as also inferred from the study of the pyrite framboids.

4.4 ORGANIC-RICH CUTTINGS FROM THE INTERVAL 2275M TILL 2575M

Black shales and sandstones have also been reported from the fault zone within the interval between 2275m till 2310m. From several of these samples vitrinite reflectance has been studied at RWTH Aachen (Table 3). Samples also originated from deeper intervals (Table 3). Furthermore, a selection of these samples was studied based on organic geochemical techniques at RWTH Aachen (Prof. R. Littke) (Table 4). As could be expected siliciclastic cuttings locally were also encountered in the underlying carbonates. However, what is of major importance is that from 2330m and below bitumen cuttings regularly were encountered and locally become a dominant component of the cuttings (e.g. interval 2435m – 2440m).

Table 3: Vitrinite reflectance of organic-rich cuttings in the interval 2275m - 2575m. Notice that most samples have a low maturity, however, there are a few exceptions.

depth	VR/%	Std. Dev.	points
2275 m	0,59	0,075	50
2280 m	0,69	0,026	45
2285 m	0,7	0,055	50
2290 m	0,72	0,06	50
2295 m	1,82	0,149	13
2310 m	0,63	0,077	50
2335 m	0,86	0,095	59
2335 m	3,2	0,31	19
2350 m	0,73	0,028	43
2390 m	0,8	0,54	46
2430 m	0,95	0,067	50
2435 m	0,74	0,094	50
2435m	0,71	0,13	50
2435m	2,8	0,9	14
2440m	0,67	0,14	17
2440m	3,34	0,37	33
2445m	0,64	0,07	15
2445m	0,96	0,085	12
2445m	2,2	0,067	23
2445 m	0,78	0,057	50
2490 m	0,85	0,087	47
2500 m	0,89	0,057	57
2550 m	0,82	0,028	50
2575 m	0,72	0,063	50

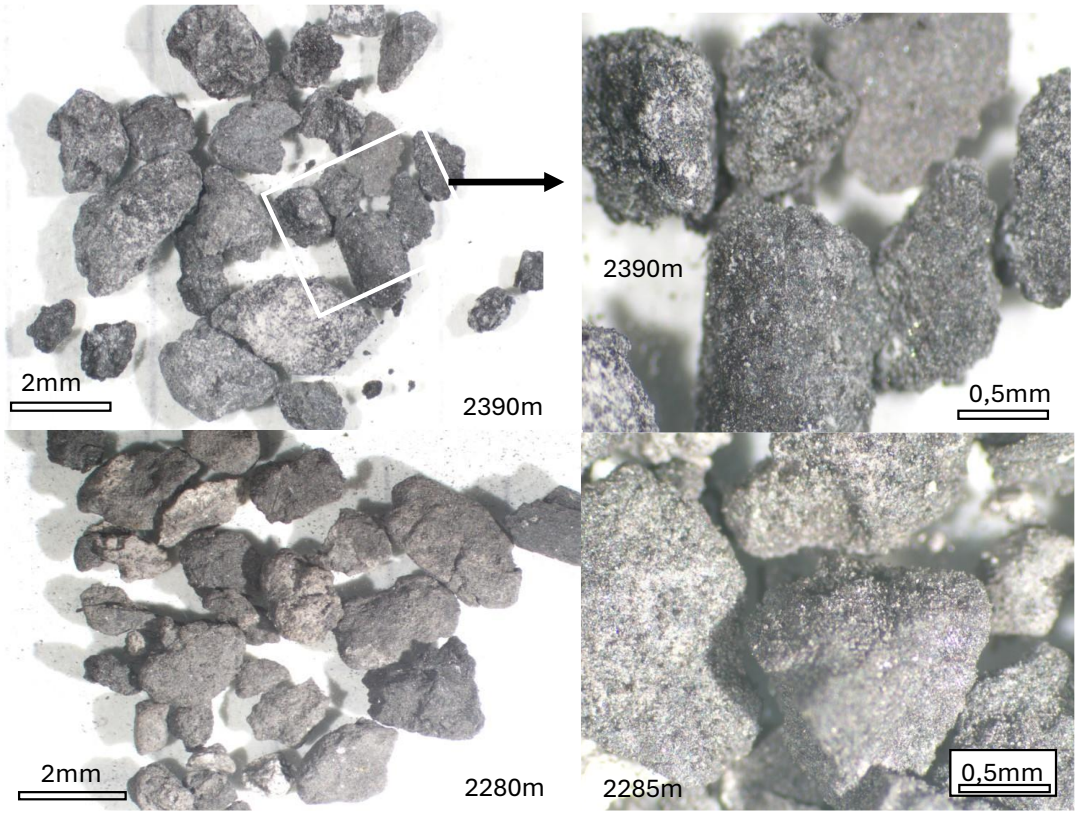

Figure 20: Fine grained aggregates with bitumen.

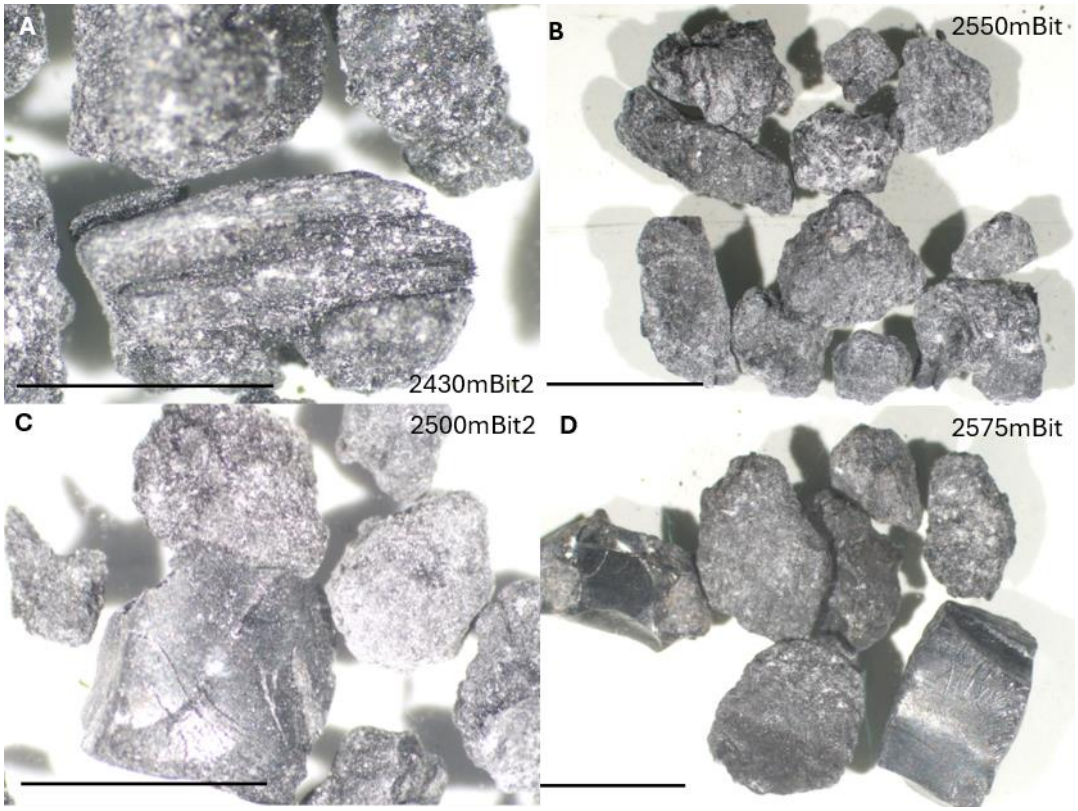

Figure 21 A) Fibrous organic-rich cutting; B) Fine-grained organic aggregates; C & D) Fine-grained organic aggregate cuttings next to cuttings displaying some curved shiny outlines (solid bitumen). Scale bar = 2mm.

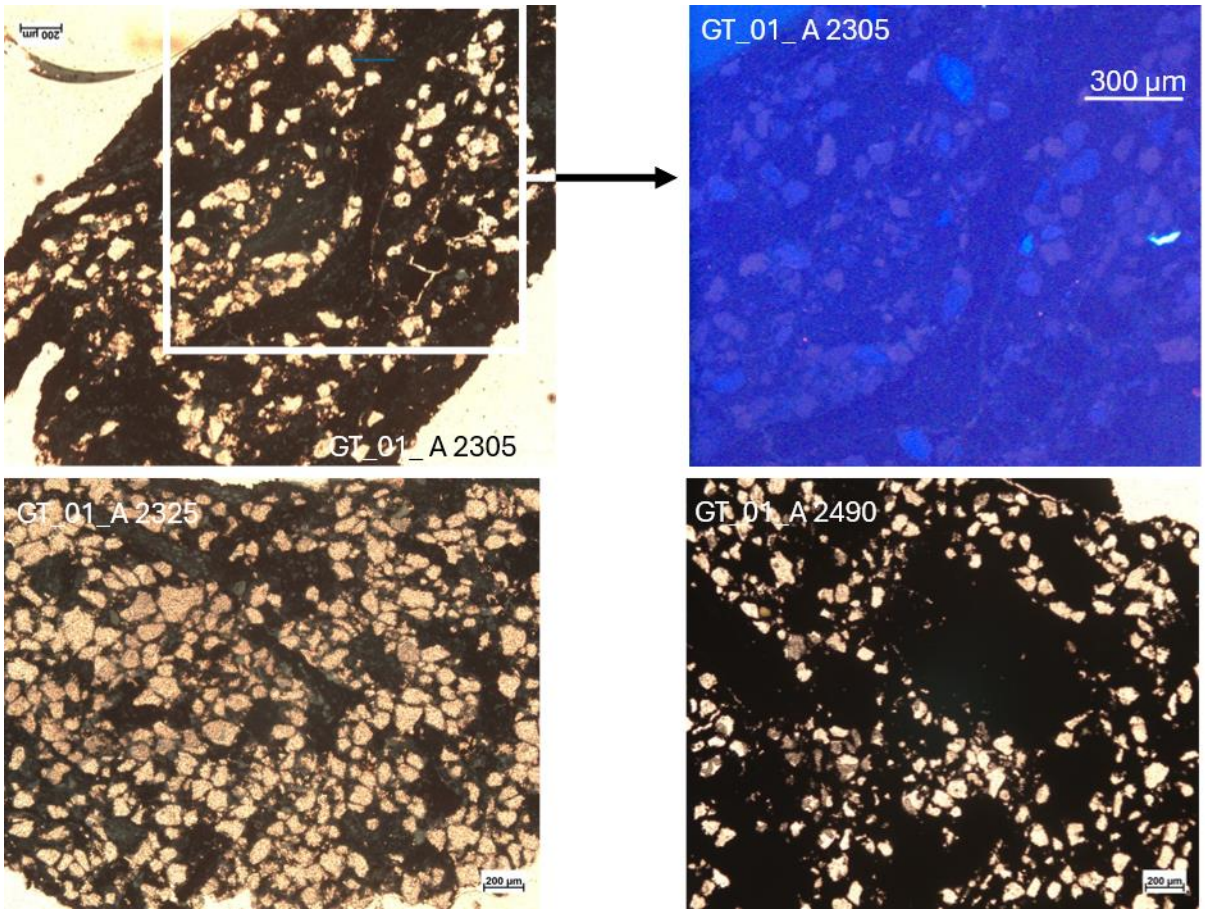

Figure 22: Thin section microphotographs of organic-rich phases often forming streaks or discrete components enclosing quartz grains. The blue colored picture corresponds to a cathodoluminescence microphotograph.

In transmitted light microscopy the organic-rich shales resemble the ones already described above. Therefore, the focus is on the bitumen cuttings. In most of the samples, they are fine grained with bitumen glueing the grains together (Figure 22). Some fragments display some fibrous to laminated texture (Figure 21A), likely corresponding to coal fragments. In contrast, others are shiny and possess some curved outlines. The latter correspond to solid bitumen (Figure 21C & D). In some cases, rather well sorted sandstone impregnated by bitumen was recognized. Here the organic-rich phases often form streaks or discrete components within the sandstones (Figure 22). The quartz grains have the same luminescence as the quartz grains encountered in the Namurian strata, namely they are blue or red purple (brown) luminescent (Figure 17B), but this does not necessarily mean that they are also of Namurian age. Bitumen has also been encountered within intercrystalline pores in some hypiodiotopic dolomite cuttings, and in some seldom cases it also occurs along stylolites (e.g. Swennen, 2023: S23 – 2120m – Plate 5).

In Table 4 results of the organic geochemical analysis are provided.

Table 4: Summary table of Rock-Eval parameters of organic rich samples from the interval 2285m – 2575m. Notice that the last sample has been measured twice (REP = replicate). Abbreviations: S1 = Hydrocarbons (HC) (mg/g Rock); S2 = Hydrocarbons (mg/g Rock); T_{max} = Temperature of maximum pyrolysis yield; PI = Production Index (S1/(S1+S2); HI = Hydrogen Index (mg HC/g TOC); OI = Oxygen Index (mg CO2/g TOC); TOC = % Total Organic Carbon.

Sample	S1	S2	T_{max}	PI	HI	OI	TOC
depth	**(mg/g)**	**(mg/g)**	**(°C)**				**%**
2285m	0,06	4,86	432	0,01	32	11	15,08
2290m	0,07	5,72	431	0,01	42	12	13,51
2295m	0,12	7,56	432	0,02	53	6	14,19
2350m	0,17	2,61	430	0,06	20	23	12,83
2390m	0,09	2,15	433	0,04	19	20	11,52
2430m	0,25	6,66	430	0,04	23	24	29,15
2445m	0,16	11,51	437	0,01	48	16	23,91
2575m REP	0,27	7,25	430	0,04	25	23	29,28
2575m REP	0,22	8,56	429	0,03	27	23	31,49

The high TOC values (varying between 11,52 and 31,49 wt%) as well as the rather low T_{max} values (varying around 433°C) in Table 4 could fit to Westphalian C & D coal with a vitrinite reflectance below 1.0 %. However, such Westphalian C & D strata do not occur in the Beerse area. The low vitrinite samples clearly differ from Namurian A black shales studied in the interval 1800 – 1840/1845m in this Beerse well and from the Namurian Chokier Formation in the Turnhout borehole, where TOC values varied around 3,6 wt% and vitrinite values varied around 3,5%. Of interest are two additional observations, namely: (i) an additional sample 2450 m containing large well preserved coaly fragments with all kinds of vitrinite, inertinite and liptinite macerals. It has a vitrinite reflectance of about 1.0 %; (ii) a few samples also contained a limited amount of organic-rich phases with high maturity, falling in the range of the studied Namurian black shales (see Table 3). Therefore, an alternative hypothesis is that the low vitrinite values originate from the weathering (oxidative alteration) of Namurian organic-rich layers, which is a likely process to affect organic-rich phases in a karst system. But apparently not all organic-rich cuttings were affected by this alteration. Notice that coal layers have been encountered in Namurian strata (Dusar, 2006), thus explaining the input of coaly particles. Why they possess such low vitrinite values while being well preserved (and thus not altered) remains an open question.

For comparison purposes Wei and Swennen (2022) report S1 values in the Turnhout borehole (n = 3 samples) varying between 0,04 – 0,1 HC mg/g rock, S2 values between 0,17 – 0,21 HC mg/g rock, T_{max} between 363 – 420°C, HI between 3,98 – 11,93 mg HC/g TOC, PI between 0,16 – 0,37 and a bitumen index (BI) between 2,27 – 2,50 mg CO2/g TOC, values that clearly differ from those reported in Table 4.

4.5 AUTHIGENIC QUARTZ

As mentioned replacive authigenic quartz (AQ) locally can make up 30% of the rock volume. No individual euhedral quartz crystals have been encountered, also not in the “diagenesis reference samples” (as checked by HCl 2N etching and the study of the crystal habitus as well as CL petrography; see comment Figure 12). The origin of the AQ is, however, not easy to infer. They post-date the dull blocky calcite, interpreted to be meteoric in origin. Furthermore, yellow to yellow orange luminescent veinlet locally borders authigenic quartz, thus likely post-dating the latter.

Muchez (personal communication) stressed the fact that the authigenic quartz phases often occur in rather pure limestone, thus there seems to be a lithological control. As silica source there are two options often mentioned in literature, namely remobilization of biogenic silica, for example derived from sponge spicules, or silica derived from clay mineral reactions, such as the conversion of smectite to illite. Since on the one hand no sponge relicts have been noticed, and on the other hand, smectite is a minor component while illite (= muscovite) was a common mineral reported in the mineralogical investigations carried out by Q-minerals, a burial origin seems the most likely option. This interpretation is in line with Dusar and Lagrou (2008), who state that the authigenic quartz phases they studied post-date stylolitisation. Indeed, for an effective smectite to illite transformation higher temperatures are needed. In this case one must consider that the shallow marine limestones are bordered along their slope by siliciclastics (especially shales), a situation also reported by Muchez (1990). The intercalations of siliciclastics below 2400m supports such a setting.

Some authigenic quartz crystals have been replaced by calcite (Figure 10). As quartz more easily dissolves in alkaline than acidic solutions, and within carbonates the fluids are host rock buffered and thus alkaline, interaction of these fluids along preferential fluid flow paths could be invoked to explain this replacement.

4.6 SEARCH FOR EVAPORITES

The presence of anhydrite was reported in the logging results from the Beerse GT 01 A well at following depth intervals (Along Hole Depth - AHD) :

- 1970 - 2010m: Rarely anhydrite (gray to blackish gray, crypto- to microcrystalline, calcite/dolomite inclusions)
- 2020 – 2070m: Packstone to wackestone when mixed with anhydrite (also indicated in the lithological composition)
- 2090 – 2110m: Accessory anhydrite
- 2130 – 2150m: Claystone aggregates of pyrite and anhydrite.

It is, however, unclear based on what criteria anhydrite was observed. Furthermore, tentative evaporite occurrences were reported from the “diagenesis reference samples” 1950m, 2070m, 2140m, 2325m, 2345m and 2410m (Figure 9). However, during the detailed microscopic inspection of the dried cuttings no evidence of the presence of anhydrite was found. This was also the case for the “diagenesis reference samples” where apart from the petrographic inspection also a short etching test with HCl 2N indicated only the presence of calcite. Furthermore, in the Beerse GT.01 well no anhydrite was reported.

In a mineralogy report of Q-Mineral (internal report accomplished for the Department of Environment; comprising FTIR and XRD analyses of the cuttings, focusing on Namurian shales and infills within the carbonate succession with higher gamma-ray signatures) no anhydrite was reported. The existence of very minor amounts of gypsum (<0,4%) was reported within samples 2080m, 2115m, 2160m, 2180m and 2475m. Of importance here is that the presence of mineral phases <1% is not easily detectable by XRD. Furthermore, the gypsum could be of secondary origin, i.e. it could relate to the weathering of pyrite of which its reaction product reacted with carbonate components, which evaporated during drying of the cuttings. Anyhow, gypsum, if present occurs at very low concentrations.

Since the optical microscopy did not give fully conclusive results, we evaluated the presence of sulphate minerals based on a chemical approach on 7 samples from the interval 2020 – 2070m from well GT 01 A. We took the finest powder from the dried cuttings. Since sulphate minerals dissolve in ammonium solutions, we mixed each of these fine powders with ammonium chlorite (1N). Subsequently, after filtering, we added Ba^{2+}. In the case sulphates were dissolved in the NH4Cl solution, the reaction with barium would lead to the precipitation of barite, resulting in a white colored solution. However, in none of the samples the solution colored white, thus indicating that no sulphates were present in the studied samples.

Thus, no evaporites were encountered. This is in contrast with the findings in the MOL-GT 01 well where indeed anhydrite as well as calcite pseudomorphs after gypsum (selenite) were found as well as inclusions of gypsum and anhydrite in calcite (Broothaers et al., 2020).

4.7 COMPUTERIZED TOMOGRAPHY OF CUTTINGS

In an attempt to distinguish the different lithologies (sandstone, dolomite, limestone, shale) in vacuum plastic bags that contain cuttings dispersed in water containing powdered rock constituents, we applied computerized tomography as a non-destructive technique. To calibrate the system, we made an artificial sample containing the four above-mentioned lithologies. This reference layered sample was scanned in four sections. Below you can find in figure 23 a representative slice for each section, with sandstone (section 1), dolomite (section 2), limestone (section 3), and slate (section 4).

Due to the high density of the vacuum sealed plastic bags containing the cuttings of the Beerse well, high voltages and power had to be applied (the scanning parameters were: Voltage: 150 kV; Power: 37.5 W; Voxel size: 37.5 µm; Shutter speed: 380 ms; Averaging: 3; Magnification: 4x).

The combined histogram of the four images is shown in Figure 24A, and the breakdown by data from the four sections is shown in Figure 24B.

The first and second peaks in each color spectrum represent the tomodensity of the environment and fluid. The third, rightmost peak of each color spectrum represents the actual lithology of the respective cuttings. We can use the following grayscale thresholds to select the different phases (Figure 24):

- Sandstone: 23,000 – 28,000
- Dolomite: 30,000 – 32,800
- Limestone: 31,500 – 35,000
- Slate: 13,000 – 16,750

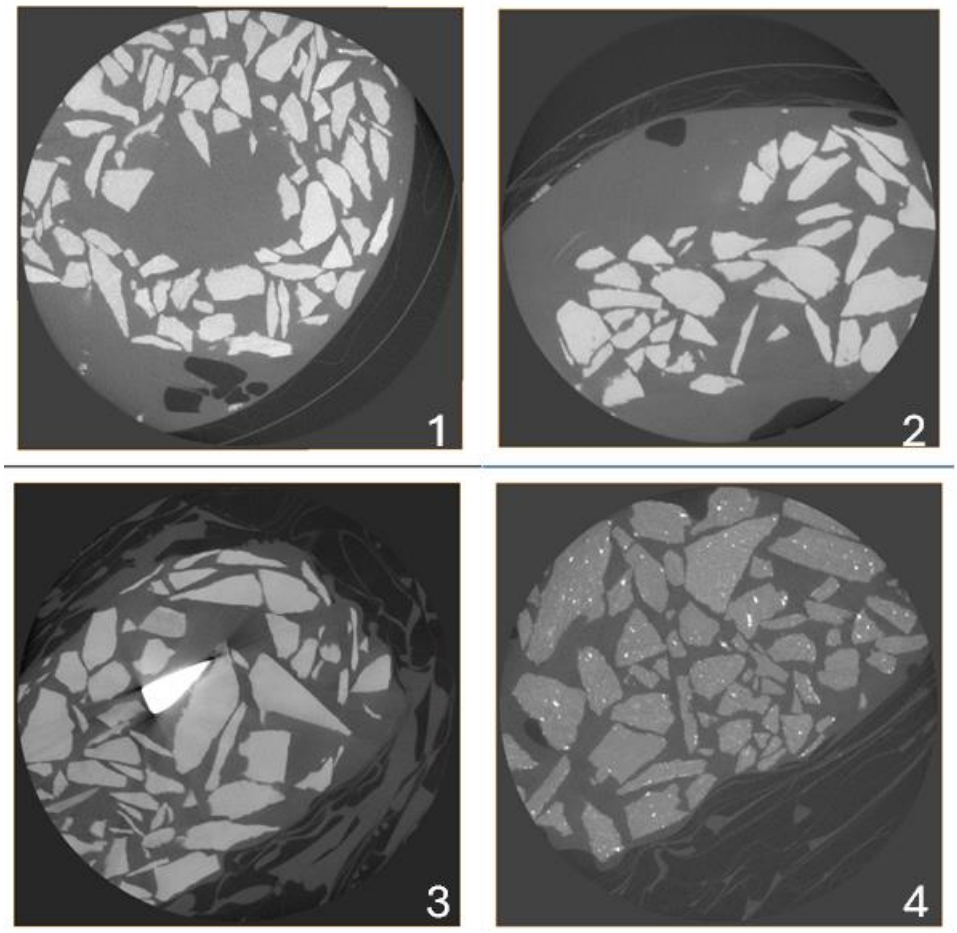

Figure 23: Representative slices for four sections through the reference sample (sandstone (section 1), dolomite (section 2), limestone with high density rock piece in the middle of the picture (section 3), and slate (section 4)).

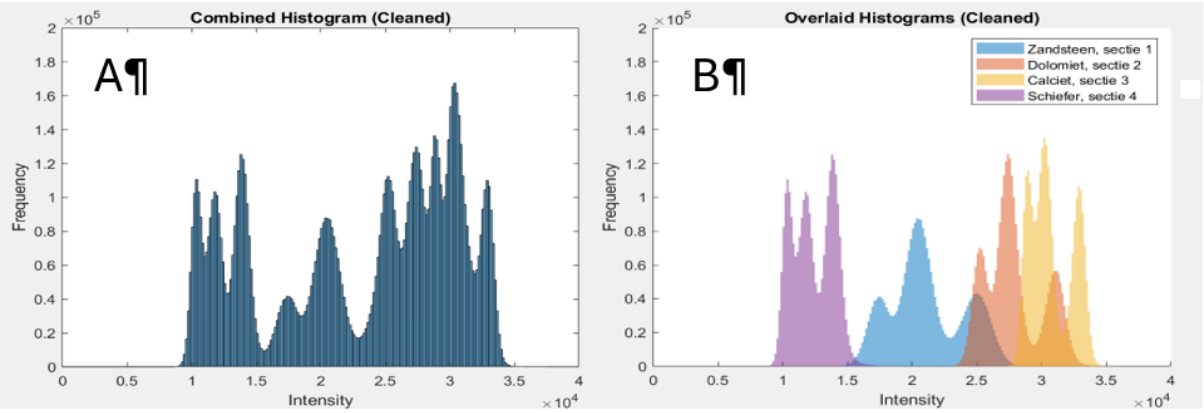

Figure 24: Combined histogram of the four images (A), and the breakdown by data from the four sections (B)

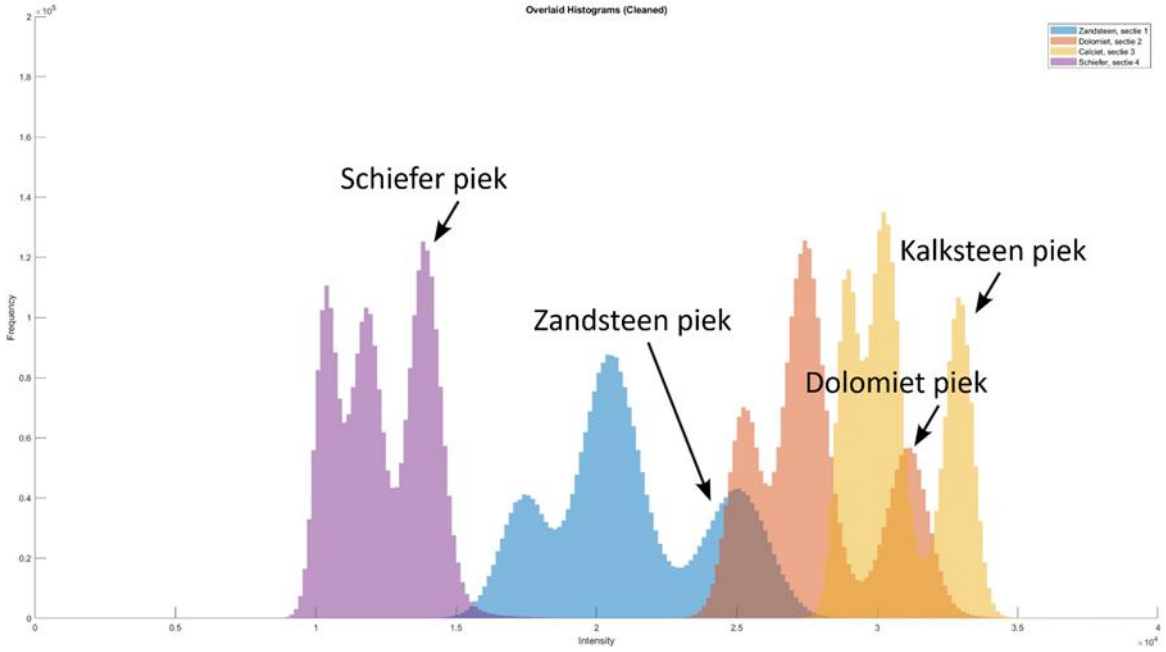

Figure 25: Grayscale thresholds of the different cuttings.

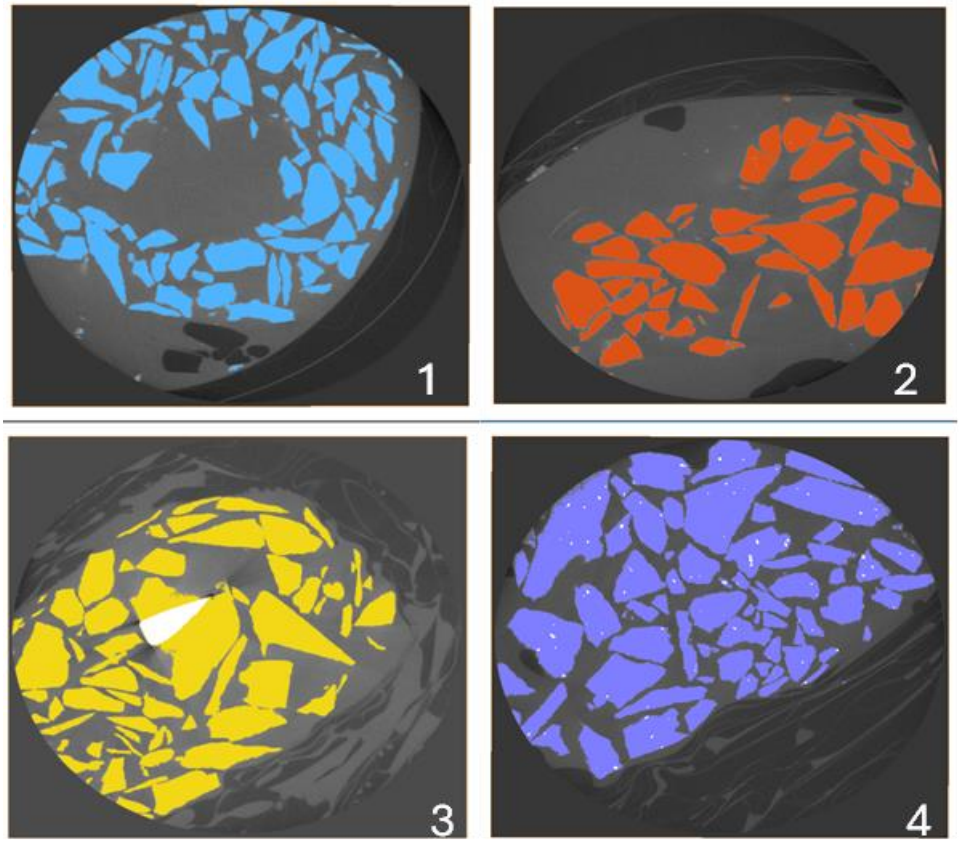

Figure 26: Result of the segmentation of the reference sample (sandstone (section 1), dolomite (section 2), limestone (section 3), and slate (section 4).

This shows that we have difficulty distinguishing between dolomite and limestone since their peaks are overlapping, but that we can distinguish sandstone and slate from carbonates. The result of the segmentation is shown in Figure 26.

The grayscale values of the different cutting types are relatively far apart, so we can reasonably be confident that distinguishing them in a single scan should be possible. However, the four scans have been taken separately, and this is not the same as capturing all four materials in one scan. For example, one can see that the peaks representing the environment (air) and fluid (water) shift for the different sections, where we would normally expect them to have approximately the same grayscale value. The histogram range shifts relative to the lightest and heaviest material found in each scan, and this varies from section to section. The way to avoid this, is by adding reference materials to each section, allowing to calibrate the histogram range. Normally, the materials added are lighter and heavier, respectively, than the materials we want to image, so we can properly normalize the histogram. An attempt to perform a normalization here was carried out by using ambient pixels (air) and fluid pixels for the different histograms of the four sections, which yields the summary histogram shown in Figure 27.

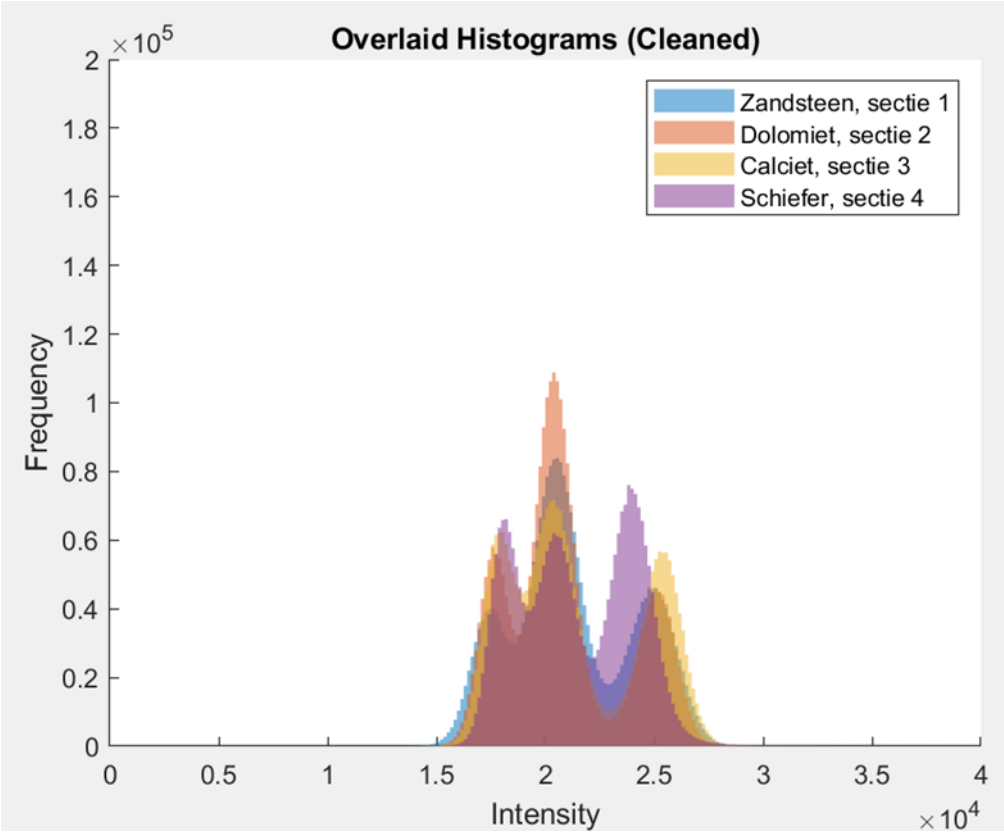

Figure 27: Normalized histogram based on the use of ambient pixels (air) and fluid pixels for the different histograms of the four sections.

The first two peaks (air and liquid) of each material in the reference mix now align better (as expected), but we see more overlap between sandstone and carbonates, which means that we will have difficulties to distinguish them in mixed samples. Again, the normalization performed here is not ideal.

Finally, two Beerse GT 01 A samples (2030m and 2140m) were scanned using the same parameters (Figure 28). These contain larger fragments that could potentially be segmented from the rest of the matrix, but this matrix is so fine and dense due to the presence of fine powered rock material that at the current resolution one cannot properly distinguish the different lithologies. Distinguishing different phases purely based on tomodensity for samples of this size is therefore very challenging and the result likely does not allow to screen in a fast way the existing vacuum plastic bags. Making the samples smaller would have advantages compared to scanning at lower energy, or dual energy (current and lower energy), and would also allow to see more detail in the finer fraction of the sample. But this was not an option at this research stage.

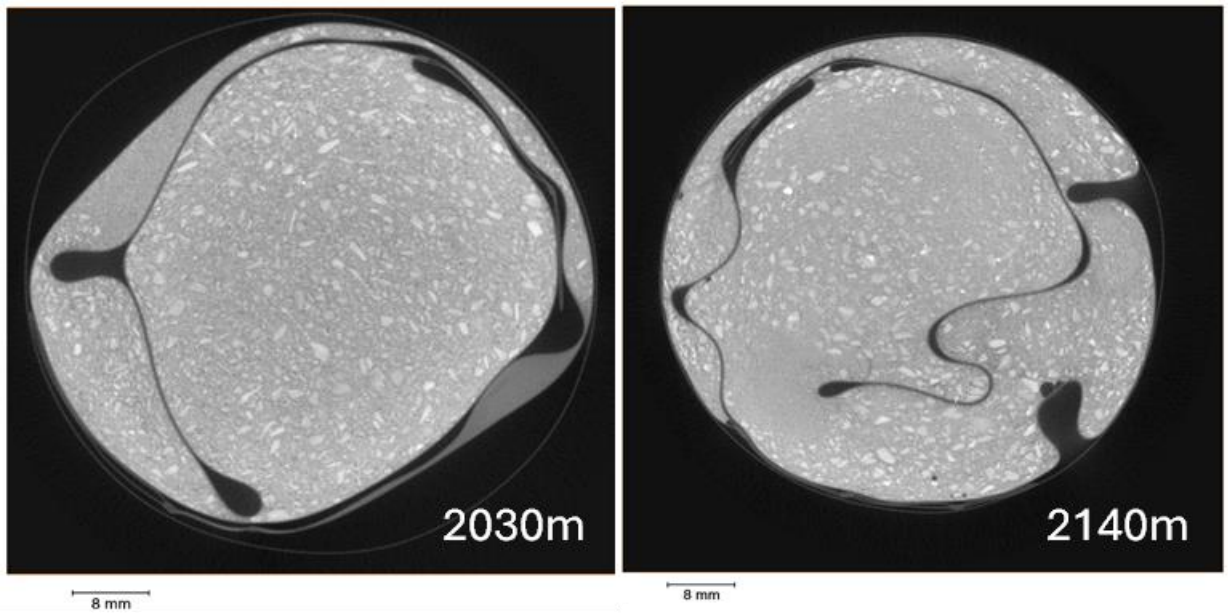

Figure 28: CT scans of samples Beerse GT 01 A 2030m and 2140 m.

4.8 DEDOLOMITE

Dedolomite was encountered only in few samples. It is characteristically marked by a bright yellow luminescent calcite bordering a dull core that often corresponds to relict dolomite phases. Regarding their origin, Nader et al. (2008) noticed that dedolomitization either is frequently associated with some emergence of dolomite host rock (and thus is very early diagenetic, but post-dolomitization) or is burial in origin. In the study case no indication for emergence phenomena, such as paleosols, have been encountered near the samples where the cuttings with dedolomite have been collected. Therefore, a burial origin is the most likely origin of the encountered dedolomites.

5 DISCUSSION AND CONCLUSION

5.1 OVERALL PALEOSETTING

The dominance of bioclastic wacke-/packstone points towards sedimentation in a shallow marine shelf setting, which according to Muchez et al. (1991) were deposited above wave base. The siliciclastic intercalations within the limestone succession below 2400m likely reflect a transition towards shelf slope facies.

Noteworthy is the absence of cryptalgal textures and/or microbial boundstones, as reported from the Heibaart and Poederlee well (Muchez et al., 1987, 1990). In addition, no paleosoil features (textures or stable isotope signatures) were encountered, supporting deposition away from the shallowest parts of the shallow carbonate shoal. This is also in line with the absence of karst collapse breccias, however, the latter are not so easy to infer in cuttings. Noteworthy is also that classical meteoric cements and dissolution vugs are rather rare in the carbonate sequence.

According to Dusar M. (personal communication) at the end of the Visean an important sea level fall and regression exposed the recently deposited Visean limestones on which a soil cover locally developed, likely on epikarst, at least on what is now the Brabant Massif and the western Campine. The Beerse area, as well as the eastern Campine and Geverik area likely remained marginally marine. The Namurian 'transgression' stepwise drowned a landscape which had formed during millions of years. Recent analogs could be Ha Long Bay in Vietnam and similar drowned karstic landscapes elsewhere in SE Asia (although the hiatus is much longer and the degree of consolidation of the limestones much higher). Drowning a landscape with karst topography was, however, not marked by a transgressive surface covered by basal gravels. On the contrary, only fine-grained sediments could be deposited that were eroded from the soils, hence fine-grained, acidic and organic-rich sediments, became probably deposited in a stratified water column with anoxic bottom conditions (resulting in black shales of the Chokier Formation).

In the Campine around the Heibaart dome flooding was punctuated by periods of sea-level stabilisation. During these periods a phreatic karst water table could develop inside the still emerged limestone hills at equilibrium levels with the sea-level. Around Heibaart fractured highly permeable levels are encountered in boreholes traversing the Dinantian reservoir at about 60 m intervals (also in the Merksplas-Beerse borehole, which was a lower lying part of the same karst topography). This likely also occurred in the Beerse area, where an extensively karstic zone was encountered (Janssen Pharmaceutica, 2023). Similar disturbed karst collapse was not recognized everywhere, however, it cannot be ruled out that karst pockets continued subhorizontally in that area. According to Vandenberghe et al. (1986) and Dreesen et al. (1987) the karstification occurred stepwise at different depth intervals, reaching 250m on the shoals and 120m on the intervening depressions. However, as stated above based on the sedimentology of the Beerse cuttings and the limited marine as well as classical meteoric phreatic diagenesis, the influence of the Visean – Early Namurian Sudetic emergence is considered to be limited in the Beerse area.

Notice that the black shales from the fault zone within the interval between the 2275m till 2310m interval, had low maturity and thus can be compared with Westphalian C & D strata, which however, do not occur in the Beerse area. Therefore, they could correspond to weathered (oxidative altered) Namurian black shales, a process that is known to affect negatively the vitrinite reflectance.

Whatever is the case, the presence of these organic-rich phases in the fault zone and its presence in underlying strata, which is interpreted in terms of karst infill, rather point to the importance of the Cretaceous – Lower Paleogene karstification event.

The effect of acidic fluids expulsed during coalification of the Westphalian deposits deeper in the Campine basin may have created additional pathways along border faults around the structural highs as well as paleokarst cavities. The latter could explain the infiltration of organic-rich strata into the Dinantian carbonate succession, however not of Westphalian C & D considering the huge distances involved.

The other possibility, namely contamination from the Westphalian or Namurian section occurring above the Dinantian carbonates, seems less likely. Indeed, the Westphalian - Namurian interval was already cemented by a casing, at the moment the Dinantian interval was drilled

5.2 DIAGENETIC EVOLUTION

In Figure 29 a summary paragenetic sequence is given, which summarizes the petrographic observations that are supplemented by additional geochemical data.

One of the first diagenetic features that developed shortly after sedimentation of the organic-rich Namurian sediments was the development of framboidal pyrite phases due to the interaction with sulphate reducing bacteria. The characteristics of these minute pyrite crystals reflect an euxinic to anoxic setting for the Namurian shales. The first diagenetic overprint in the shallow marine Dinantian shelf limestones is the limited development of non-luminescent syntaxial rim cements especially around crinoid ossicles. Whether some early diagenetic dolomitization occurred also could not be confirmed, but seems possible but it then was of limited importance. A more dominant intergranular cement type is made up of dull red purple (brown) luminescent sparite which is likely shallow burial in origin of possible meteoric origin with redox buffering. Indeed, the classical non-bright-dull meteoric cements that reflect an evolving groundwater influx varying from oxidizing to suboxic to reducing conditions, was not really encountered. Possibly the few bright yellow (sector) zoned calcite cements testify of such a meteoric influx. This influx also can explain the development of the few oversized dissolution cavities cemented by dull blocky calcite. However, the presence of the latter features occurs at rather few discrete depth intervals. Whether the interaction with the meteoric waters also caused some recrystallisation of the host limestones is unclear, since the depleted oxygen isotopes clearly testify of a burial recrystallisation at higher temperatures that might have overprinted a meteoric recrystallisation event. The absence of any intense marine as well as meteoric diagenesis and the few dolomite intervals likely relate to the somewhat deeper marine depositional setting where these Beerse limestones developed, and where they were less affected by shallow marine as well as subsequent Visean – Early Namurian Sudetic emergence related diagenesis. If this interpretation is correct also the karstification at the end Visean was likely of limited influence.

During subsequent burial diagenesis a large number of fractures and vein infills occurred. Within the samples only few crosscutting relationships have been encountered and the relationship of veining and stylolite development also could not very well be constrained. We therefore have to rely on previous studies carried out on core material from the Campine Basin where these diagenetic relationships are better developed. The frequently encountered monocrystalline calcite cuttings have a wide CL spectrum, ranging from (dull) orange till yellow. The (dull) orange cements could be

equivalent to the volumetrically most important cement encountered in fractures reported by Muchez et al. (1991) in the Campine Basin. Whether they also formed during the early Westphalian from marine-derived waters at around 60°C is difficult to infer due to the lack of microthermometric data from primary fluid inclusions and the rather wide spread in stable oxygen isotopes in which no individual populations could be recognized. For $\delta^{18}O$ the values range between -9,0 to -15,3 ‰. If these calcite infills originated from the same burial fluid, thus reflecting a uniform $\delta^{18}O_{SMOW}$ value, then the spread of 6,3‰ corresponds to a temperature spectrum of about 26°C (as 1°C change in water temperatures equates 0,24‰; Andrews, 2006). The depleted nature of the $\delta^{18}O$ values of the mono-crystalline calcites supports the involvement of slightly hot basinal brines, that also can explain the resetting of the limestone signatures. Another option is based on Muchez et al. (1994b), i.e. based on the $\delta^{18}O$ calcite signatures that vary between -9,0 to -15,3 ‰ and inferred crystallisation temperatures of 45 to 93°C, $\delta^{18}O$ SMOW values of -3 to -3,5‰ were calculated (Figure 19). According to the former authors these values reflect involvement of marine derived fluids that mixed with meteoric water.

Another important issue relates to the existence of bright yellow luminescent coarse crystalline calcites. In literature they are often reported to relate to thermal sulphate reducing (TSR) processes. TSR is a set of redox reactions between organic matter and dissolved sulphates at temperatures >120°C that occurs in varied environments including deeply buried sulphate bearing carbonates and siliciclastics. During TSR, sulphate is reduced to H_2S, and organic matter is sulphurized to sulphur-rich components, solid bitumen, and oxidized to carboxylic acids and finally to CO_2, with a final net reaction (Machel et al., 1995):

$$SO_4^{2-} + 1.33\ CH_2 + 0{,}66\ H_2O \rightarrow H_2S + 1{,}33\ CO_2 + 2OH^-$$

Notice that in such settings, H_2S often reacts with Fe^{2+} that is present since reducing conditions prevails forming pyrite. Identifying TSR in sedimentary basins is important since H_2S is a harmful and corrosive gas (which could harm the geothermal installations), and it degrades the quality of existing hydrocarbons. Since Fe is reacting to form pyrite, no or only very limited iron is incorporated into calcite, resulting in very bright yellow luminescing calcite. Thus, the existence of the latter may indicate TSR. To test whether the calcite relates to TSR, measuring its $\delta^{13}C$ signature is very powerful, since if TSR is involved the carbon of the calcite is derived from the altered hydrocarbons and is extremely negative. This is not the case in any of the coarse calcite cuttings analysed from the Beerse GT 01 A well and together with the fact that no evaporites have been encountered we can exclude the possible interference of TSR-related processes.

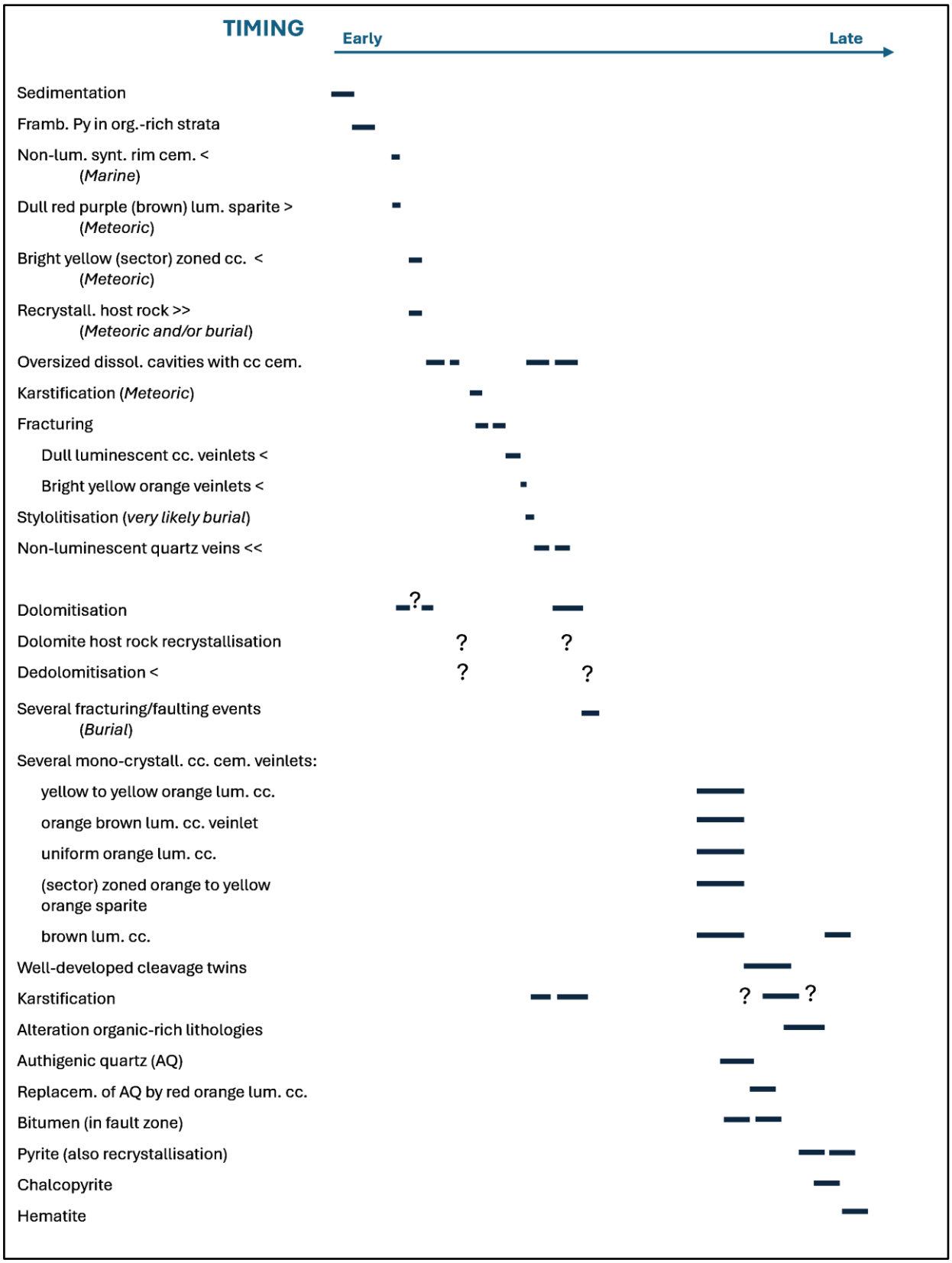

Figure 29: Paragenetic succession in the Beerse GT 01 A cuttings (<< very, < limited development; > common development; >> widespread development).

Of importance is the existence of a major fault zone occurring between about 2239m and 2300m. In this interval the just described coarse crystalline calcite cuttings are common, but also organic phases that occur together with limestone cuttings. The organic phases are clearly not Dinantian in origin, and several of them display some low maturity which is difficult to explain. Notice that also organic-rich cuttings reflecting a high maturity, similar to the Namurian organic-rich shales studied in the 1800 – 1840/1845m interval, were encountered next to the low maturity phases. The mixture of these organic-rich cuttings is interpreted in terms of severe karstification that developed in the fault zone and in the strata below, likely influenced by the high degree of fracturing of these limestones as reflected by the many coarse crystalline calcite cuttings. The low mature organic-rich cuttings resemble Westphalian organic strata, but their very low maturity would point to Westphalian C & D strata that do not occur in the Beerse area. Import from these components would mean transport over very far distances which seems not realistic. Another hypothesis is the influx in the karst system of weathered organic-rich shales. During weathering oxidation of the organic constituents took place. Such alteration has been documented in weathered top of Westphalian strata in the Campine Basin, and thus could explain the low maturity values if Namurian black shales were affected by weathering, which concurs with the inferred karstification. If this is the case, then it is unclear whether the organic-rich phases are indeed of Namurian or Westphalian in age. The mixture with high maturity organic phases would rather support a Namurian origin, which seems also more feasible from a regional geological point of view.

As mentioned above, no indications of evaporites were found in this study. Furthermore, no euhedral hydrocarbon bearing quartz or calcite phases have been detected by fluorescence microscopy. Within certain interval replacive authigenic quartz crystals were encountered that likely relate to clay mineral reactions that were linked to siliciclastic intervals occurring along slope settings that occurred adjacent to the carbonates. Locally the authigenic quartz crystals are replaced by a blocky calcite, likely due to the alkaline nature of the host rock buffered fluids in which quartz more easily dissolves. In addition, very locally some dedolomites have been recognized, also likely of burial origin.

5.3 CONCLUSION FOR RESERVOIR DEVELOPMENT

With regard to reservoir characterization, one can conclude that it turned out to be very difficult to infer reservoir properties from studying cuttings. A likely explanation is that rocks will break and become crushed during drilling along weak zones, such as porous intervals and or fractured/faulted intervals. Also karstified intervals would be severely affected. Based on the studied cuttings one can state that the Namurian shale from the studied interval 1800 – 1840/1845m were rather intact. The limestones above 2250m, i.e. above the fault zone dominantly testified of some well cemented limestones. In general, the limestones are rather compact and cemented, however, as stated above marine phreatic and classical meteoric phreatic cements are no so common, and also would indicate that the Late Visean – Early Namurian Sudetic karstification phase likely had a limited impact on reservoir properties.

Once within the fractured interval in the Dinantian carbonates, the coarse crystalline calcite cuttings below 2250m also testify of dominance of closed fractures and indeed only seldomly some euhedral (skalenohedral) calcite cuttings, testifying of some open fractures, were identified. However, the presence of many organic-rich cuttings below 2250m likely testifies of some severe karstification, that likely was positively influenced by the severe faulting and fracturing of the limestones. The

latter explains the good production rates of the Beerse GT 01 A well. The karst system, however, became infilled by organic-rich strata, reducing the open space.

Other diagenetic processes also seem to have had only a limited influence on reservoir properties. Only very few bitumen impregnated idiotopic dolomite cuttings were encountered, while most dolomite cuttings were tight. Very locally some stylolite seams were impregnated by bitumen. The authigenic quartz phases, which are replacive, neither their calcite pseudomorphs enhanced the porosity. This also accounts for the dedolomites. Finally, the maturation of organic phases, such as the encountered bitumen, also had no clear effect on reservoir properties, as was also supported by the absence of any TSR related processes.

5.4 RECOMMENDATIONS

In contrast with studying cores, which allow to work out a detailed paragenesis and to reconstruct the fluid-rock interaction through time, the study of cuttings is far more complicated. Nevertheless, they help to unravel part of the geological history of the drill location.

To refine the diagenetic history of the Beerse well additional clumped isotope analysis of specific calcite as well as dolomite cuttings is recommended, since it will allow to constrain the formation or recrystallisation temperatures of specific diagenetic phases. Also to constrain the marine signatures of some features, and/or the interaction with fluids that testify of clay mineral transformations (e.g. smectite to illite transformation), Sr-isotope analysis of specific calcite cuttings is recommended. In addition to refine the paragenesis, U/Pb dating of calcite and dolomite cuttings is highly recommended. Based on the latter datings, it should be possible to reconstruct the timing of the emplacement of specific calcite cements, being relatively early in the burial history or rather late as the cements dated by Swennen et al. (2021).

In fact, the above given recommendations are certainly also valid for the study of other existing boreholes with core material in the Campine basin.

Additional research about the possible infiltration of Westphalian or Namurian organic-rich fragments (especially the coaly cuttings), likely by lateral input via large karst cavities is also recommended, since the latter could provide valuable information of the geothermal potential of the Beerse region, as well as on the subsurface connectivity of the karst system in the Poederlee – Beerse – Turnhout area. In this respect, it could be useful to carry out U/Pb analysis of recrystallized limestone cuttings, potentially allowing to constrain the timing of karstification. A more advanced sampling and study of the bitumen cuttings would also highlight the origin of these hydrocarbons.

With regard to the organic-rich cuttings it is recommended to analyze their organic $\delta^{13}C$ signature, constraining their origin and potential alteration processes.

A thorough analysis of the geophysical logs should be envisaged with a focus on characterizing and quantifying karst related features.

BIBLIOGRAPHY

Andrews, J.E., 2006, Palaeoclimatic records from stable isotopes in riverine tufas: synthesis and review. Earth Science Reviews, 75, 85 – 104.

Behar, F., Beaumont, V., and Penteado, H. (2001). Rock–Eval 6 technology: Performances and developments. Oil & Gas Science and Technology, 56(2):111–134.

Broothaers, M., Bas, S., Lagrou, D., Ferket, H., Harcouët-Menou, V and Laenen, B., 2020, Insights into a complex geothermal reservoir in the Lower Carboniferous carbonates in northern Belgium. Proceedings World Geothermal Congress, Reykjavik.

Burkhard, M. (1993). Calcite twins, their geometry, appearance and significance as stress-strain markers and indicators of tectonic regime: a review. Journal of Structural Geology, 15.

Dreesen, R., Bouckaert, J., Dusar, M., Soille, P and Vandenberghe, N., 1987, Subsurface structural analysis of the late-Dinantian carbonate shelf at the northern flank of the Brabant Massif (Campine Basin, N-Belgium). Mémoires Explicatives des Cartes Géologiques et Minières de Belgique, V. 21, 1-37.

Dusar, M., 2006, Namurian. Geol. Belgica, 9, 163 – 175.

Dusar, M. and Lagrou, D., 2008, Paleokarst-Enhanced Reservoir for Geothermics and Gas Storage in Carboniferous Limestone (Campine Basin, NW European Carboniferous Basin). In: Sasowsky, I.D., Feazel, C.T., Mylroie, J.E., Palmer, A.N. & Palmer, M.V., Karst from Recent to Reservoirs, June 7-11, Rapid City, South Dakota. Karst Waters Institute Special Publication, 14, 43-51.

Götte, Th. and Richter, D.K., 2006, Cathodoluminescence characterization of quartz particles in mature arenites. Sedimentology, 53, 1347 – 1359.

Hance, L., 2023, Biostratigraphic review of the Campine Basin. Unpublished study accomplished for the Flemish Department of Environment.

Janssen Pharmaceutica nv, 2023. Eindrapport betreffende de waarborg voor het opsporen en winnen van aardwarmte in de diepe ondergrond in de regio Beerse. Administrative document available via Databank Ondergrond Vlaanderen.

Machel, H.G., Krouse, H.R. and Sassen, R., 1995, Products and distinguishing criteria of bacterial and thermochemical sulfate reduction. Appl. Geochem., 10, 373 – 389.

Matthews, A. and Katz, A., 1977, Oxygen isotope fractionation during the dolomitization of calcium carbonate. Geochim. et Cosmochim. Acta, 41, 1431 – 1438.

Meyers, W.J. and Lohmann, K.C., 1985, Isotope geochemistry of regionally extensive calcite cement zones and marine components in Mississippian limestones, New Mexico, in “Carbonate cements”, Schneidermann, N., and Harris, P.M., eds. Soc. Econ. Paleontol. Mineral. Spec., 36, 223 – 239.

Muchez, Ph., 1988, Sedimentologische, Diagenetische en Geochemische Studie van de Dinantiaan Strata ten Noorden van het Brabant Massief (Bekken van de Kempen). Unpublished Ph. D. thesis KU Leuven, 311 pp.

Muchez, Ph., Conil, R., Viaene, W., Bouckaert, J. & Poty, E., 1987, Sedimentology and biostratigraphy of the Visean carbonates of the Heibaart (DzH1) borehole (northern Belgium). Ann. Soc. Géol. Belg., 110, 199 – 208.

Muchez, Ph., Viaene, W., Bouckaert, J., Conil, R., Dusar, M., Poty, E., Soille, P. & Vandenberghe, N., 1990, The occurrence of a microbial buildup at Poederlee (Campine Basin, Belgium): Biostratigraphy, sedimentology, early diagenesis and significance for Early Warnantian paleogeography. Ann. Soc. Géol. Belg., 113, 329 – 339.

Muchez, Ph., Viaene, W., Keppens, E., Marshall, J.D. & Vandenberghe, N., 1991, Vein cements and the geochemical evolution of subsurface fluids in the Visean of the Campine basin (Poederlee borehole, Belgium). J. Geol. Soc. London, 148, 1005 – 1117.

Muchez, Ph., Marshall, J.D., Touret, J.L.R. & Viaene, W., 1994a, Origin and migration of paleofluids in the Upper Visean of the Campine Basin, northern Belgium. Sedimentology, 41, 133 – 145.

Muchez, Ph., Hein, U. F., Van Den Broeck, K., Vandecasteele, C., 1994b, Lithological influence on the composition of vein cements in the Carboniferous of the Campine Basin (northern Belgium). Eur. J. Mineral.6, 985 – 994.

Nader, F., Swennen, R. and Keppens, E., 2008, Calcitization/dedolomitization of Jurassic dolostones (Lebanon): Results from petrographic and sequential geochemical analyses. Sedimentology, 55, 1467-1486, doi: 10.1111/j.1365-3091.2008.00953.x.

Poty, E., 2016, The Dinantian (Mississippian) succession of southern Belgium and surrounding areas: stratigraphy improvement and inferred climate reconstruction. Geol. Belgica, 19, 177-200.

Rombaut, B., Deckers, J., Dirix, K. and Van Baelen, K., 2024. Nieuwe inzichten en geologische 3D modellen van het Dinantiaan in het Bekken van de Kempen. Studie uitgevoerd in opdracht van: VLAKO / VLAANDEREN. Referentie: 2021/RMA/R/2477. https://dov.vlaanderen.be/page/geologisch-3d-model-dinantiaan

Swennen, R., 2023, Summary report of the petrographic analysis of cutting samples of the Beerse borehole. Study carried out on request of VPO. ”Enclosure 8.6 TS description Beerse. In: Vinci, F., Pascarella, A. and Amory, J., 2023. Sedimentological reconstruction of the Campine Basin during the Dinantian. Study accomplished for the Flemish Planning Bureau for the Environment and Spatial Development. https://researchportal.be/en/publication/enclosure-86-ts-description-beerse"

Swennen, R., & Muchez, P. (2016). Sedimentologie und Diagenese in Karbonatgesteinen des Unterkarbons in Ostbelgien und im Raum Aachen. Jahresberichte Und Mitteilungen Des Oberrheinischen Geologischen Vereins, 98, 55–80. https://doi.org/10.1127/jmogv/98/0005

Swennen, R., Van der Voet, E., Wei, W., Muchez, Ph., 2021, Lower Carboniferous fractured carbonates of the Campine Basin (NE-Belgium) as potential geothermal reservoir: Age and origin of open carbonate veins. Geothermics, 96, 102147.

Vandenberghe, N., Poggiagliolmi, E and Watts, G., 1986, Offset-dependent seismic amplitudes from karst limestone in northern Belgium. First Break, EAGE Conference Issue, 4, no-5, 9-27.

Vandenberghe, N., 1990, The occurrence of a microbial buildup at Poederlee (Campine Basin, Belgium): Biostratigraphy, sedimentology, early diagenesis and significance for Early Warnantian paleogeography. Ann. Soc. Géol. Belg., 113, 329 – 339.

Vinci, F., Pascarella, A. and Amory, J., 2023. Sedimentological reconstruction of the Campine Basin during the Dinantian. Study accomplished for the Flemish Planning Bureau for the Environment and Spatial Development. https://www.friscris.be/en/publications/sedimentological-reconstruction-of-the-campine-basin-during-the-dinantian(ff261c07-f675-40f6-906e-194146f30191).html

Walkden, G.M. and Williams, D.O., 1991, The diagenesis of the late Dinantian Derbyshire carbonate platform, Central England. Sedimentology, 38, 643 – 670.

Wei W., 2023, Sedimentology, geochemistry, and pore characterization of Namurian mudstones in Belgium and the southern Netherlands. Unpublished Ph. D thesis KU Leuven. 220pp.

Wei W. and Swennen, R., 2022. Sedimentology and lithofacies of organic-rich Namurian Shale, Namur Synclinorium and Campine Basin (Belgium and S-Netherlands). Marine and Petroleum Geology, 105553

Wilkin, R. T., Barnes, H. L., and Brantley, S. L. (1996). The size distribution of framboidal pyrite in modern sediments: An indicator of redox conditions. Geochimica et Cosmochimica Acta, 60(20), 3897– 3912.

ANNEX I

Photo plates of the microscopic study of the Beerse samples of well GT 01 A are provided in a separate pdf file “Microphotographs of cuttings Beerse GT 01 A”. Below, a brief description of the cuttings is given. Depth position relates to Along Hole Depth (AHD).

It is important to mention that the described cuttings do not necessarily be representative for the entire assemblage of the cuttings taken from a certain depth, since sometimes the sampling was selective (for example sampling only calcite cuttings or organic rich phases). Sometimes lithology is not easily discernible due to drilling powder that covers the cuttings.

The scale bar = 0,5 cm.

Abbreviations used: Sst = Sandstone ; Py = Pyrite; cc = calcite; XX = crystalline; Lst = Limestone; D = Dolomite; LG = Light Grey; DG = Dark Grey; reXX = recrystallised; SI = Siltstone; BS : Black Shale; Bit = Bitumen; Q = Quartz;

1800 : Quartzite, Sst, py
1805 : Sst, cc
1810 : Sst, possibly coarse XX Lst, cc
1830 : Coarse Sst
1845 : LG reXX Lst, py
1855 : Quartzite, SI
1860 1 : LG reXX Lst
1860 2 : DG fine XX Lst (large fragments)
1870 : Fine XX Lst, grey
1870 (Beerse GT 01) : Sst, BS, py
1875 : Sst
1880 : Sst with one Lst
1885 : DG Lst
1900 : DG fine XX Lst + LG Lst
1910 : DG fine XX Lst + LG Lst
1920 : LG Lst + DG fine XX Lst
1930 (Beerse GT 01): Sst, BS
1935 (Beerse GT 01): Sst, BS
1945 : DG fine XX Lst + LG Lst reXX
1950 : DG fine XX Lst + LG Lst
1965 : DG fine XX Lst + LG Lst + possibly Bit
1970 : Brown Sst with Fe-oxides
1975 : Brown Sst with Fe-oxides, Q, cc
1980 : LG Lst reXX + DG fine XX Lst
1995 : LG Lst + DG Lst reXX
2005 : cc (one piece)
2010 : LG Lst + DG Lst partially reXX
2020 : LG Lst reXX, one with cc piece
2030 : LG Lst reXX
2035 : LG Lst reXX + cc
2040 : polyXX cc, <py

2045 : LG Lst + DG Lst
2065 : LG Lst + DG Lst reXX
2070 : Coarse XX cc
2075 : cc
2095 : cc & D, crosscutting veins
2105 : LG Lst + DG Lst + cc
2110 : cc
2125 : DG Lst reXX + cc
2130 : LG & DG Lst + cc
2140 : cc & py<
2145 : polyXX cc
2150 : DG Lst, cc, py, possibly chalcopy
2165 : LG & DG Lst, reXX
2185 : cc (coarse XX and skalenoeder)
2200 : LG & DG Lst, cc
2220 : DG Lst, cc
2190: LG & DG Lst
2215: LG & DG Lst + cc, possibly D
2230: LG & DG Lst + cc, possibly D
2245: DG Lst + cc + D
2250: DG Lst reXX + cc
2275 : Bit
2280 : Bit
2285 : Bit
2285 2 : detail Bit
2290 : Bit & Lst
2295 : Bit & Lst
2305: LG Lst & Bit
2310 : Bit
2330 : Lst & cc
2335 : LG & DG Lst
2335 2: cc & <py
2340 : cc
2345: LG Lst & cc>>
2350: DG Lst
2350 Bit : Bit
2350 2 : Lst & cc>>
2380: DG Lst & Bit
2385: DG Lst reXX & Bit
2390 Bit : Bit
2390 Bit 2 : detail Bit
2395: cc & Bit
2400: DG Lst, D reXX
2405: DG & LG Lst, Bit <, D <
2420: DG Lst, cc, Bit<<, D<
2425: DG Lst, LG Lst<, cc, D?
2430: cc
2430 Bit : Bit
2430 Bit2 : Detail Bit

2435: Coarse cc, sometimes grey
2435 Bit : Bit
2435 Bit2 : Detail Bit
2440: DG Lst, cc, Bit, D<
2445: cc, Bit
2445 Bit : Bit
2445 Bit2 : Detail Bit
2455: DG & LG Lst, D<
2465 dol : D
2465 cc: cc
2465 dol 2 : detail D with vein
2465 cc 2 : detail cc
2470: cc with stylolite (arrow), solid Bit, D<<
2470 2: detail cc with stylolite (arrow), solid Bit
2485: cc, solid Bit, fibrous Bit
2485 2: detail cc, solid Bit, fibrous Bit
2490 cc: cc
2490 Bit : Bit
2490 Bit 2 : Detail Bit
2500 cc: cc
2500 Bit 1 : Bit
2500 Bit 2 : Detail Bit
2505: cc, Bit
2520: cc, Bit
2520 2 : detail cc, Bit
2525: cc, Bit
2535: cc, coarse XX & skalenoeder, Bit
2545: cc, coarse XX
2550 Bit : Bit
2550 Bit 2 : Detail Bit
2575 Bit : Bit
2575 Bit 2 : Detail Bit

ANNEX II

More detailed description of the Beerse cuttings

The micro photo plates are provided in a separate file "Microphotographs of thin sections Beerse GT 01 A". The sample number as well as the picture number (e.g. 1920-1 & 2) are given. Sometimes reference is made to pictures reported in our former report (e.g. S23-15-Plate 5 in Swennen 2023 also referred as S23). Depth position relates to Along Hole Depth (AHD).

In this section some additional information is provided on the lithology as well as kind of diagenetic products of the thin sections studied under transmitted light and under cathodoluminescence. in which In the text below, specific features are described which are often indicated by an arrow in the microphotographs.

First limestone cuttings (yellow orange to dull red purple luminescent bioclastic wackestones which often show indications of recrystallisation) were encountered in sample 1855m, however, in this sample sandstone cuttings still are dominant.

Subsequently the limestone cuttings become more dominant and consist of yellow orange or dull red purple luminescent bioclastic wacke-/packstone. Some of these limestones show recrystallisation features (such as spotted CL textures), but most of the bioclasts are non-luminescent. Several of the crinoids are overgrown by faintly zoned dominantly non-luminescent calcite, possibly of marine phreatic origin (S23-15-Plate 5 in Swennen 2023, 1920-1 & 2). They occur next to non- to dull orange luminescent blocky calcite which may reflect a marine origin.

However, apart from some recrystallisation features, diagenetic products reflecting meteoric diagenesis are scarce. Only in 1920 (3 & 4) an oversized pore is filled by a dull brown luminescent blocky calcite. The latter, however, is not a typical meteoric cement based on its uniform luminescence color. The succession also seems not much been affected by fracturing and veining till 2030m, only locally some yellow luminescent and thin dull luminescent calcite veinlets have been encountered. Only in sample 1920m a coarse crystalline non-luminescent calcite vein occurs while from this sample downwards as for example in 1935m & 1940m some yellow luminescent veinlets occur, which also locally seem to affect the limestone matrix (e.g. 1945-3 & 4). In sample 1965 (1 & 2) the dull luminescent veinlet is clearly cut a bright yellow orange veinlet and in sample 2020m two generations of dull luminescent calcite were recognized.

A curious feature is the existence at 1970m of sandstone and siltstone cuttings. Furthermore, in this study the first authigenic quartz crystals were encountered in sample 1980 (3 & 4), while in the previous study they were sporadically encountered already in sample 1965m (S23 -17- plate 2). But from 1980m they are common till 2140m. The latter post-date the blocky calcite.

Also, in samples 2020m & 2030m & 2035m dull blue luminescent quartz grains in sandstones (some with authigenic quartz overgrowths) occur, of which their abundance decreases from 2040m. One of the sandstones is cut by a non-luminescent quartz vein and is cut by a stylolite (2035-7 & 8). Several of the sandstones are cemented by yellow to yellow orange luminescent (sometimes zoned) calcite, which postdates the quartz vein since it fills some open space (2035 - 7 & 8). The latter calcite also seems to occur as coarse crystalline orange to yellow orange luminescent mono-crystalline calcite cuttings, which frequently occur below 2035m. They clearly testify from some

intense fracturing. These cuttings occur in sample 2035 next to rare red luminescent bioclastic packstone still containing many non-luminescent authigenic quartz crystals. In samples 2030 (5 & 6) & 2045 (5 & 6) a yellow to yellow orange luminescent veinlet locally borders an authigenic quartz crystal, and thus seem to post-date the latter.

In sample 2060m, some yellow luminescent calcite veinlets occur, of which one is crosscut by an orange brown luminescent calcite veinlet. Both veinlet types occur also in lower samples studied (e.g. 2070 - 2 (1 & 2)). In 2060 (1 & 2) also a seldom dull purple luminescent calcite vein was identified.

In the thick sections (2070m, 2075m, 2090m), orange luminescent monocrystalline calcite cuttings or calcite cuttings containing many impurities as well as fluid inclusions, also possessing an orange luminescence, occur. Sometimes a faint sector zonation is present, as well as some cleavage twinning.

In sample 2105m, mono- to polycrystalline calcite cuttings still are common. In sample 2105 - 1 & 2, a succession can be seen evolving from a uniform orange luminescent calcite, surrounded by (sector) zoned orange to yellow orange sparite (see also 2105 - 5 & 6) which might be meteoric in origin. The latter is covered by a brown luminescent calcite. In this sample also red orange luminescent calcite is replacing authigenic quartz (2105 - 7 & 8). This calcite also occurs as polycrystalline calcite (2105 - 9 & 10) and possibly is crosscut by a stylolite. In sample 2105m the host rock consists of purple to red orange luminescent recrystallised bioclastic packstone to microsparite. The CL colors are clearly more intense than in the samples higher upwards. Notice that silt- and sandstone cuttings still sporadically occur (S23-21-plate 1).

Sample 2120m, which was studied in S23 is an interesting one, since the red to red purple luminescent recrystallised bioclastic packstone first is crosscut by a dull luminescent calcite veinlet, that on its turn is crosscut by a bright yellow orange calcite veinlet (which is the reverse order then before). Furthermore, the uniform orange luminescent sparite is followed by yellow luminescent calcite, which also occurs as blotchy large sparite phases.

In sample 2125m & 2130m & 2140m the dull brown luminescent (sometimes recrystallised) bioclastic packstone, is often crosscut or bordered by dull, orange or the characteristic yellow luminescent calcite (e.g. 2130 - 5 & 6; 2140 - S23-23-plate 7 & 8). Here locally authigenic quartz crystals, sometimes replaced by calcite, occur. In sample 2140m again some quartz phases occur, cemented by bright yellow calcite. In 2140m (S23 - 23-plate 9) a red luminescent hypiodiotopic dolomite cutting was encountered being in contact with bitumen.

In sample 2145m & 2150m, authigenic quartz occurs adjacent to orange or yellow luminescent monocrystalline calcite. In the latter sample also (dull) blue to non-luminescent zoned quartz cement was observed (2150 - 5 & 6). Authigenic quartz still sporadically occurs in sample 2165m, floating into dominantly red orange luminescent recrystallised bioclastic packstone. In the latter sample, siltstone cuttings were still encountered as well as in underlying samples (e.g. S23 - 24 & 25 & 26 - plate 1).

In sample 2185m the bioclastic to peloidal wacke/packstones are still dull orange luminescent with yellow luminescent spots, possibly reflecting some recrystallisation. In sample 2185 - 3 & 4, one can see a former dissolution cavity (oversized pore) likely originating from meteoric phreatic dissolution that is cemented by dull luminescent blocky calcite and that is bordered by zoned bright yellow to

orange calcite crystals. While the latter are likely meteoric in origin, the pre-dating dull luminescent calcites testify from uniform precipitation conditions.

In sample 2190m some yellow orange luminescent calcite phases surrounding dull luminescent phases, likely corresponding to dedolomite phases were encountered. Also, in this sample some zoned bright yellow orange calcite crystals border dull luminescent bioclastic wackestone (also recognized in S23 – 25 – plate 8). Of interest here is that they are followed by blotchy dull purple luminescent coarse crystalline dolomite, whereby the blotchy nature testifies of recrystallisation.

In sample 2200m the limestone luminescence testifies of less recrystallisation. Orange luminescent monocrystalline calcite cuttings (also in sample 2215m) are still present as well as few cuttings with bright orange luminescent calcite pseudomorphs after authigenic quartz crystals. In sample 2215-9 & 10 again dull luminescent blocky calcite occurring in a dull luminescent bioclastic wackestone is followed by a bright yellow (in this case not zoned) sparite.

From 2220m onwards the limestones are again often non- to dull luminescent and often display recrystallisation features as manifested by orange luminescent spots. In sample 2250 (11 & 12) a stylolite borders an orange luminescent recrystallised limestone from a non-recrystallised dull luminescent limestone area. The latter contains orange luminescent calcite pseudomorphs after authigenic quartz, similar in luminescence as the recrystallised limestone part. This leads to the following paragenesis: limestone development, stylolitisation, authigenic quartz development, recrystallisation and replacement of the quartz crystals. Some limestones contain non-luminescent authigenic quartz crystals. Orange as well as yellow luminescent (zoned) monocrystalline calcite cuttings or veins still occur and testify of some fracturing. In some samples tiny dull luminescent veinlets occur (e.g. 2230 - 3 & 4), that pre-date some dull uniform orange luminescent calcite veining (2250 - 1 & 2).

From 2275 – 2310m black shales dominate, but organic-rich shale cuttings (mentioned in organic geochemistry section) were already encountered in sample 2250m (S23 – 26 – plate 1 & 5) from which downwards sandstone impregnated by bitumen regularly occurs. In sample 2305m some dull to orange red luminescent bioclastic wacke-/packstone are more common, which continue to be present from below the shales. In the former sample they occur next to well sorted sandstones containing well-rounded dull blue or dull purple luminescent quartz grains, sometimes floating into bitumen (e.g. 2305 – 1 & 2; S23 – 27 – plate 1). One sandstone cutting was also encountered in sample 2330m, while organic-rich cuttings still are common in sample 2325m (S23 – 28 - plate 1 & 3), however, here the wacke-/packstones dominate again next to orange to dull orange luminescent monocrystalline calcite cuttings.

Samples 2335m, 2340m, 2345m & 2350m contain dominantly coarse crystalline calcite cuttings, with colors varying from yellow orange to dull orange, and sometimes some zoning occurs (e.g. 2335 – 5 & 6). Also red orange luminescent zoned calcite was encountered (e.g. 2345 – 7 & 8). These calcites are sometimes inclusion rich.

In sample 2390m apart from the orange to red orange luminescent bioclastic wackestone, the presence of zoned dull to red luminescent dolomite rhombs is noteworthy which crosscut the typical bright yellow luminescent calcite veins. It is not unlikely that these dolomites already occur from 2345m as it was encountered in S23 – 29 – plate 7 as well as sample 2420m (S23 – 31 – plate 2 & 5). Also in sample 2380m, 2400m, 2405m, 2415m, 2420m, 2440m & 2465m (and 2420m: S23 – 32 – plate 3 as well as 2445m: S23 – 33 – plate 8 & 9) zoned hypiodiotopic dolomite occur (possessing

some limited intracrystalline porosity (e.g. 2465 – 7 & 8 and 2470 – 1 & 2 with bitumen filling the pores) or dolomite rhombs are floating into intraclastic to bioclastic packstones. Below 2470m, dolomite cuttings are less common where they make up only 5 – 10% of the cuttings (based on a binocular description of the cuttings). In some dolomite cuttings (2405 – 5 & 6; 2440m) some oolite ghost textures occur. Noteworthy is also that bright yellow luminescent calcite veins or cements are also common in this dolomite rich interval. Sometimes these calcite cements are zoned and/or form skalenoeders bordering the fragment (2445m: S23 – 33 – plate 9) (and thus testifying from some former open pore space). In sample 2400 – 5 & 6 and 2420 – 3 & 4 the red luminescent dolomite seems to replace the yellow luminescent calcite or is filling up some space between the calcite. It thus post-dates the yellow luminescent calcite. In samples 2415 (1 & 2 and 7 & 8) light and dark blue and purple luminescent quartz grains make up a sandstone piece as well as some siltstone.

Coarse mono-crystalline cuttings regularly occur (e.g. 2465-2 and thick sections 2480m & 2485 & 2500m, notice the impurities as well as the twinned cleavage planes). Crosscutting relationships, however, are scarce, except in sample 2440 - 7 & 8 and 2520 – 9 & 10. In the former a non-luminescent coarse crystalline calcite vein is crosscut by a thin bright red orange calcite veinlet. In the latter sample, a thin non luminescent veinlet is crosscut by a monocrystalline bright yellow luminescent calcite vein. The latter vein type is rather common in sample 2505m. However, in samples 2525m & 2535m & 2545m, the mono-crystalline calcite cuttings display a broad spectrum of luminescence, again without crosscutting relationships.

In sample 2520 – 1 & 2, a rare former oversized dissolution cavity is filled by a dull luminescent sparite. Next to it some recrystallisation features occur. Both features support a shallow meteoric dissolution stage, however, a dull luminescent cement infill does not so commonly develop in a meteoric phreatic realm, it therefore more likely reflects some shallow burial cementation.

ANNEX III

Cathodoluminescence study of the Beerse GT 01 A samples

The photo plates are provided in a separate file “Microphotographs of thin sections Beerse GT 01 A”. Depth position relates to Along Hole Depth (AHD).

Below, first a more general description of the thin section is given, sometimes also mentioning cuttings from which no microphotographs were taken. This is often followed by the description of specific microphotographs. The description given in italic originates from the former report by Swennen (2023). The ones given in bold are from thick sections. “CCC” stand for “classical calcite cuttings”.

1800 (general description): Sandstone cuttings, in which sometimes the grains still can be identified but sometimes they are well cemented and thus less clear. The grains are dominantly dull blue (different shades) luminescent. Locally some purple red zoned dolomite phases occur.
1800 (1 & 2): Intensively cemented sandstone with dull to dull blue luminescence.
1800 (3 & 4): Sandstone in which dull to dull blue purple (brown) luminescent quartz grains still can be identified. The dull purple red zoned phases likely correspond to dolomite cement.
1800 (5 & 6): Intensively cemented sandstone with dull luminescent quartz grains crosscut by a dull purple red fine crystalline dolomite vein (central part).

1805 (general description): Sandstone cuttings, in which sometimes the grains still can be identified but sometimes they are well cemented. The grains are dominantly dull blue (different shades) luminescent.
1805 (1 & 2): Intensively cemented sandstone with dull blue luminescence.
1805 (3 & 4): Sandstone in which individual dominantly dull blue (different shades) luminescent quartz grains can be identified occurring in a non-luminescent matrix. Notice the dull blue luminescent faintly recognizable crack and seal veinlets (see especially right arrows).
1805 (5 & 6): Sandstone with blue luminescent (cemented) quartz grains with non-luminescent dolomite vein on the left (see arrows).

1810 (general description): Sandstone cuttings, with dominantly dull blue (different shades) color, sometimes with non-luminescent dolomite cement. Also, one cutting of a zoned dull blue purple luminescent coarse crystalline quartz vein occurs.
1810 (1 & 2): Zoned dull blue purple luminescent coarse crystalline quartz vein.
1810 (3 & 4): Sandstone with blue luminescent cemented quartz grains with non-luminescent dolomite vein in the middle.
1810 (5 & 6): Floating blue luminescent quartz grains in non- to dull purple luminescent dolomite cement.

1830 (general description): Sandstone cuttings, with well cemented dull blue luminescent quartz grains. Also laminated non luminescent siltstone occur.
1830 (1 & 2): Dull blue purple luminescent coarse crystalline well-cemented sandstone.
1830 (3 & 4): Dull luminescent coarse crystalline dull brown purple luminescent quartz grains bordered by an organic-rich laminated mud-/siltstone

1845 (general description): Sandstone cuttings, with dominantly dull blue (different shades) color. One piece is bordered by a non-luminescent dolomite vein.
1845 (1 & 2): Sandstone in which individual dominantly dull blue and dull blue purple (brown) luminescent quartz grains can be identified occurring in a non-luminescent matrix. Some of the quartz grains display some cracks.
1845 (3 & 4): Sandstone in which individual dominantly dull blue and dull blue purple luminescent quartz grains can be identified as well as some authigenic quartz overgrowth.
1845 (5 & 6): Sandstone in which individual dominantly dull blue and dull blue purple (brown) luminescent quartz grains are bordered to the right by a non-luminescent dolomite vein.

1855 (general description): Mainly sandstone cuttings, with dominantly dull blue (different shades) color. One organic-rich cutting with many parallel oriented shells and one dull luminescent bioclastic wackestone was identified.
1855 (1 & 2): Sandstone in which individual dominantly dull blue and dull blue purple (brown) luminescent quartz grains can be identified. Some fine-grained opaque phases occur between the quartz grains.
1855 (3 & 4): Organic-rich cutting with many dull brown to orange luminescent parallel oriented shells.
1855 (5 & 6): Dull luminescent bioclastic wackestone with large non-luminescent crinoid ossicle in the upper right corner.
1855 (7 & 8): Sandstone with intensively cemented dominantly dull blue and dull blue purple luminescent quartz grains cemented in its central part by a red purple dolomite vein.

1860-1 (general description): Yellow orange to dull red purple (brown) luminescent bioclastic wackestone next to sandstone with dull purple and blue luminescent quartz grains with bitumen in intergranular pores.
1860-1 (1 & 2): Sandstone with dull purple and blue luminescent quartz grains. Some bitumen (black) occurs between the grains.
1860-1 (3 & 4): Right, yellow orange luminescent bioclastic recrystallised wackestone. Left, dull red purple luminescent bioclastic wackestone. In both cuttings the bioclasts are non-luminescent. Some bitumen (black) occurs between the grains. The white arrows indicate an artefact related to the thin section preparation.
1860-1 (5 & 6): Dull red purple luminescent bioclastic wackestone. Some bitumen (black) occurs in intergranular pores.

1860-2 (general description): Siltstone.
1860-2 (1 & 2): Very fine black siltstone with dull purple, blue and red luminescent quartz grains.

1865 (general description): Dull luminescent bioclastic wacke- to packstone (with several bioclasts that are non-luminescent).
1865 (1 & 2): Dull luminescent bioclastic wacke- to packstone (with several bioclasts that are non-luminescent), crosscut by a dull luminescent (white arrow) and yellow luminescent (yellow arrow) veinlet.
1865 (3 & 4): Dull luminescent bioclastic packstone (with several bioclasts that are non-luminescent).

1870 (general description): Laminated black mudstone next to siltstone with dull purple and blue luminescent quartz grains and dull red purple (brown) luminescent recrystallised bioclastic wackestone.

1870 (1): Fine laminated black mudstone with stylolite perpendicular to the layering.
1870 (2 & 3): Siltstone with dull purple and blue luminescent quartz grains.
1870 (4 & 5): Dull red purple luminescent recrystallised bioclastic wackestone.

1880 (general description; 1 & 2): Dull to purple blue luminescent bioclastic wackestone with in central part a non-luminescent crinoid partially covered by a faintly zoned orange yellow syntaxial cement.

1885 (general description and 1 & 2): Laminated black mudstone.

1900 (general description): Dull luminescent bioclastic wacke- to packstone. Also, many organic-rich mudstone and siltstone cuttings occur.
1900 (1 & 2): Dull luminescent bioclastic packstone.
1900 (3 & 4): Dull luminescent recrystallised bioclastic packstone.

1910 (general description): Dull to red orange luminescent bioclastic wacke- to packstone (with several bioclasts that are non-luminescent).
1910 (1 & 2): Dull luminescent bioclastic packstone (with several bioclasts that are non-luminescent) crosscut by red orange luminescent veinlets.
1910 (3 & 4): Dull luminescent (right) to red orange luminescent (left) bioclastic wacke- to packstone (with several bioclasts that are non-luminescent).

1920 (general description): Dull to yellow orange spotted (sometimes) recrystallised luminescent bioclastic wacke- to packstone sometimes crosscut by yellow luminescent veinlets or coarse crystalline non-luminescent calcite vein. One siltstone piece was also encountered (not shown in the figures).
1920 (1 & 2): Dull luminescent bioclastic packstone with in the middle a non-luminescent crinoid that displays a zoned syntaxial overgrowth that is dominantly also non-luminescent. The sample is crosscut by yellow luminescent veinlets.
1920 (3 & 4): Dull luminescent bioclastic packstone. In the middle an oversized pore is filled by a dull brown luminescent blocky calcite.
1920 (5 & 6): Dull luminescent bioclastic packstone, bordered by a coarse crystalline non-luminescent calcite vein. Some zoned dominantly non-luminescent syntaxial overgrowth occur.
1920 (7 & 8): Dull to yellow orange spotted recrystallised luminescent bioclastic packstone.

1935-1 (general description): Dull to dull red orange luminescent bioclastic wacke- to packstone.
1935-1 (1 & 2): Dull luminescent bioclastic wackestone with dull luminescent calcite veinlet (see arrows).
1935-1 (3 & 4): Dull to red orange luminescent recrystallised bioclastic wackestone with yellow luminescent veinlet (see arrows).
1935-1 (5 & 6): Dull to red orange luminescent (recrystallised) bioclastic wackestone with yellow luminescent veinlet (see arrows).

1935-2 (general description): Dull to red orange luminescent bioclastic wacke- to packstone (with several bioclasts that are non-luminescent) with non-luminescent siltstone.
1935-2 (1 & 2): Non-luminescent siltstone locally containing blue luminescent quartz grains.
1935-2 (3 & 4): Dull to red orange luminescent bioclastic wacke- to packstone (with several bioclasts that are non-luminescent).

1940 (general description): Dull luminescent bioclastic wackestone next to siltstone cuttings.
1940 (1 & 2): Dull luminescent bioclastic wackestone.
1940 (3 & 4): Dull luminescent bioclastic wackestone.
1940 (5 & 6): Dull luminescent bioclastic wackestone crosscut by yellow luminescent vein.

1945 (general description): (Dull) red luminescent sometimes recrystallised bioclastic wackestone with non-luminescent bioclasts next to siltstone with dull purple and blue luminescent quartz grains.
1945 (1 & 2): Dull red luminescent recrystallised bioclastic wackestone with non-luminescent bioclasts.
1945 (3 & 4): Red luminescent bioclastic wackestone with non-luminescent bioclasts. Locally some irregular yellow luminescent spots testify of some recrystallisation.
1945 (5 & 6): Siltstone with dull purple and blue luminescent quartz grains. Locally some reddish luminescent quartz grains also occur.

1950 (general description): Dull red luminescent recrystallised bioclastic wackestone with some non-luminescent bioclasts.
1950 (1 & 2): Dull red luminescent recrystallised bioclastic wackestone with some non-luminescent bioclasts.
1950 (3 & 4): Dull red luminescent recrystallised bioclastic wackestone with some non-luminescent bioclasts.
1950 (5 & 6): Dull red luminescent recrystallised bioclastic wackestone with some non-luminescent bioclasts. Notice the dull luminescent zoned syntaxial overgrowth around a crinoid (arrow), as well as the existence of cleavage twins.

1965 (general description and 1 & 2): Dull red luminescent recrystallised bioclastic wackestone crosscut by a dull luminescent veinlet that on its turn is crosscut by a bright yellow orange veinlet.

1970 (general description): Bitumen as well as sand- as well as siltstone cuttings.
1970 (1 & 2): Thin section of bad quality with individual rather well-rounded dull blue (different shades) quartz grains floating in a black fine-grained matrix.
1970 (3 & 4): Siltstones with dull luminescent detrital grains.

1980 (general description): Dull red luminescent recrystallised bioclastic packstone with sometimes many authigenic quartz crystals.
1980 (1 & 2): Dull red luminescent recrystallised bioclastic packstone with authigenic quartz crystals (arrows).
1980 (3 & 4): Red luminescent recrystallised bioclastic packstone with some non-luminescent bioclasts and few authigenic quartz crystals (arrow).

1995 (general description): Dull red luminescent recrystallised bioclastic packstone sometimes containing authigenic quartz crystals.
1995 (1 & 2): Dull red luminescent recrystallised bioclastic packstone with some authigenic quartz crystals (arrows).
1995 (3 & 4): Dull red luminescent bioclastic packstone with some non-luminescent bioclasts. Locally some irregular yellow luminescent spots occur.
1995 (5 & 6): Dull red luminescent bioclastic packstone with some non-luminescent bioclasts.

2010 (general description): Dull brown purple to red orange luminescent bioclastic to intraclastic packstone/wackestone often with several non-luminescent authigenic quartz crystals.

2010 (1 & 2): Dull brown purple luminescent bioclastic to intraclastic packstone crosscut containing several non-luminescent authigenic quartz crystals (AQ), crosscut by a yellow luminescent calcite veinlet.
2010 (3 & 4): Red orange luminescent intraclastic wackestone containing several non-luminescent authigenic quartz crystals (AQ). The latter seem to post-date the sparite cementation (see arrow).
2010 (5 & 6): Red orange luminescent possibly recrystallised, bioclastic wackestone. The bioclasts are often non luminescent as are the several non-luminescent authigenic quartz crystals (AQ). A small orange luminescent thin veinlet crosscuts the wackestone. The blue spot either is a small K-feldspar grain or an artefact (polishing powder).
2010 (7 & 8): Dull red brown luminescent bioclastic wackestone. Several of the crinoids with their syntaxial calcite overgrowth are non-luminescent. The wackestone is crosscut by a yellow luminescent calcite veinlet.

2020 (general description): Dull red brown luminescent bioclastic wackestone with sandstone cemented by a yellow luminescent calcite cement.
2020 (1 & 2): Dull red brown luminescent bioclastic wackestone with sandstone cemented by a yellow luminescent calcite cement. The quartz grains are non-luminescent.
2020 (3 & 4): Sandstone with non-luminescent quartz grains with authigenic overgrowth cemented by a yellow luminescent calcite cement.
2020 (5 & 6): Dull red brown luminescent wackestone with many small non-luminescent authigenic quartz crystals and a dull orange luminescent veinlet (see arrow).
2020 (5 & 6): Dull red brown luminescent mudstone with many small non-luminescent authigenic quartz crystals as well as at least two crosscutting dull luminescent veinlet generations.

2030 (general description): Sandstone with yellow or red luminescent calcite cement. The quartz grains are dull or non-luminescent. Furthermore, some red luminescent bioclastic packstone containing many non-luminescent authigenic quartz crystals occur. The packstone samples are crosscut by yellow luminescent veinlets
2030 (1 & 2): Sandstone with yellow luminescent calcite cement. The quartz grains are dull luminescent.
2030 (3 & 4): Red luminescent bioclastic packstone containing many non-luminescent authigenic quartz crystals.
2030 (5 & 6): Red luminescent bioclastic packstone containing many non-luminescent authigenic quartz crystals. The sample is crosscut by yellow luminescent veinlets that locally border the authigenic quartz crystals (see arrows).
2030 (7 & 8): Red luminescent bioclastic packstone containing some small non-luminescent authigenic quartz crystals. The sample is bordered by a yellow luminescent vein.
2030 (9 & 10): Upper, red luminescent bioclastic packstone containing some small non-luminescent authigenic quartz crystals (see arrows). A very tiny yellow luminescent veinlet crosscuts the samples. Lower, sandstone with non-luminescent quartz grains with authigenic non-luminescent overgrowths, and locally some red luminescent calcite cement.

2035 (general description): Sandstone with non-luminescent transparent quartz vein, or cemented by orange calcite cement, together with red orange luminescent bioclastic packstone containing some small non-luminescent zoned authigenic quartz crystals.
2035 (1 & 2): Sandstone with dull blue luminescent quartz grains and yellow luminescent calcite cement. Possibly some bitumen (black) occurs between the grains.

2035 (3 & 4): Right, red orange luminescent bioclastic packstone containing some small non-luminescent zoned authigenic quartz crystals (see arrows). Left, orange luminescent mono-crystalline calcite.
2035 (5 & 6): Sandstone with non-luminescent to faint red purple quartz grains, locally cemented by orange yellow luminescent calcite. The feature indicated by white arrows likely correspond to an artifact created during thin section preparation (= scratch)
2035 (7 & 8): Sandstone with non- to blue luminescent quartz grains, crosscut by a stylolite (white arrows) and a transparent dark blue luminescent quartz vein, containing some orange calcite cement. The latter post-date the quartz veining.
2035 (9 & 10): Lower, sandstone with non-luminescent quartz grains, cemented by a yellow orange zones calcite cement, possessing cleavage twins. Upper, dull red orange luminescent bioclastic packstone containing some small non-luminescent zoned authigenic quartz crystals (arrows).

2040 (general description): Several monocrystalline and polycrystalline calcite cuttings next to dull orange luminescent bioclastic wackestone with non-luminescent authigenic quartz crystals.
2040 (1 & 2): Dull orange luminescent monocrystalline calcite cuttings next to a irregularly distributed yellow orange to brown calcite surrounding an opaque (black) pyrite.
2040 (3 & 4): Dull orange to orange luminescent bioclastic wacke- (left) to mudstone (right). In the latter many non-luminescent authigenic quartz crystals occur while the left cutting is crosscut by a yellow luminescent veinlet.
2040 (5): In the top, dull luminescent bioclastic wackestone crosscut by a yellow luminescent veinlet. To the left a monocrystalline blotchy yellow orange luminescent calcite occurs. Similar luminescence occurs locally in the right cutting as calcite cement in a non- to blue luminescent sandstone.
2040 (6 & 7): Three pieces of monocrystalline yellow orange luminescent calcite cuttings.

2045 (general description): Several rather dull luminescent wacke- to packstones often containing non-luminescent authigenic quartz crystals (some of which are crosscut by calcite veins), next to calcite cemented sandstone.
2045 (1 & 2): Dull orange to orange luminescent bioclastic packstone with many authigenic quartz crystals (white arrows) and crosscutted by an orange luminescent calcite veinlet (yellow arrow).
2045 (3 & 4): Non-luminescent sandstone cemented by yellow orange luminescent calcite cement. In the upper right part, a dull orange to orange luminescent bioclastic packstone occurs.
2045 (5 & 6): Dull red orange luminescent bioclastic wackestone with many non-luminescent authigenic quartz crystals crosscut by a yellow orange luminescent calcite vein. One of the authigenic quartz crystals seems to partially crosscut the calcite vein (white arrow) and thus post-dates it.
2045 (7 & 8): Dull red luminescent bioclastic wackestone, possibly partially recrystallised explaining the yellow luminescent spots.

2060 (general description): Red to orange luminescent sometimes recrystallised bioclastic packstone, sometimes crosscut by purple as well as orange brown and yellow orange luminescent veins.
2060 (1 & 2): Red luminescent bioclastic packstone, crosscut by a dull purple luminescent calcite vein.
2060 (3 & 4): Red luminescent bioclastic packstone, crosscut by yellow luminescent calcite veinlets, of which one is crosscut by an orange brown luminescent calcite veinlet (arrow in CL figure). Locally some small authigenic quartz crystals occur (arrows in transmitted light figure). They latter locally crosscut the yellow luminescent calcite vein (yellow arrow).

2060 (5 & 6): Red (lower & right) to orange (left upper) luminescent bioclastic packstone. The upper one testifies of recrystallisation (with cleavage twins) and is crosscut by a yellow orange calcite vein.
2060 (7 & 8): Red to orange luminescent bioclastic packstone crosscut by yellow orange luminescent calcite veins. The two dark blue spots in the upper part of the figure are artefacts (resin).

2070 (general description, thick section): Either orange luminescent monocrystalline calcite cutting or calcite cutting containing many impurities as well as fluid inclusions and also possessing an orange luminescence.
2070 (1 & 2): Orange luminescent monocrystalline calcite cutting with cleavage twins and faint sector zonation.
2070 (3 & 4): Orange luminescent monocrystalline calcite cutting containing many impurities as well as fluid inclusions.
2070 (5 & 6): Upper, orange luminescent monocrystalline transparent calcite cutting with in lower part orange luminescent monocrystalline calcite cutting containing many impurities as well as fluid inclusions.
2070 (7 & 8): Orange luminescent monocrystalline calcite cuttings with cleavage twins.
2070 (9 & 10): Orange luminescent monocrystalline calcite cutting containing many impurities as well as fluid inclusions. The irregular upper border likely is an artefact (A)(resin) before the glass plate of the thick section appears.
2070 (11 & 12): Orange luminescent monocrystalline calcite cutting containing many impurities.

2070 (general description and 1 & 2): Red orange luminescent bioclastic wackestones, crosscut by a bright yellow orange calcite vein which is on its turn crosscut by a dull brown luminescent calcite vein, that is bordered by an orange red luminescent calcite veinlet.

2075 (general description, thick section): CCC

2095 (general description, thick section): CCC

2105 (general description): Purple to red orange luminescent recrystallised bioclastic packstone to microsparite. Locally some zoned orange luminescent monocrystalline calcite of sparite infill occurs. In one piece the former authigenic quartz crystals are now replaced by orange luminescent calcite.
2105 (1 & 2): Piece of calcite vein, with (sector) zoned orange to yellow orange sparite, surrounding a uniform orange luminescent calcite (white arrows) and surrounded by a brown luminescent calcite (yellow arrows).
2105 (3 & 4): Dull to purple luminescent bioclastic packstone with red to red orange spots. In this piece four air bubbles with dark outline occur, which are artefacts.
2105 (5 & 6): Lower, red orange luminescent recrystallised bioclastic packstone, with several bioclasts being non-luminescent. The packstone is bordered by some zoned red orange luminescent calcite. The latter also crosscuts the packstone (see arrow). Upper, non-luminescent organic siltstone.
2105 (7 & 8): Red orange luminescent recrystallised bioclastic packstone, with some bioclasts being non-luminescent. The right piece is crosscut by an orange luminescent calcite vein, while in the left piece several former authigenic quartz crystals are now replaced by orange luminescent calcite.
2105 (9 & 10): Red orange luminescent recrystallised microsparite bordered in its lower part by an orange red luminescent sparite vein. The microsparite is also crosscut by a stylolite along which orange red luminescent sparite occurs.
2105 (11 & 12): Lower, red orange luminescent recrystallised bioclastic packstone, with bioclasts being non-luminescent. Upper, virtually non-luminescent bioclastic packstone.

2105 (13 & 14): Orange luminescent recrystallised microsparite or cataclastic vein fragment. Some of the larger crystals contain cleavage twins. The black spots likely are bitumen.
2105 (15 & 16): Lower, dull red orange luminescent recrystallised microsparite. Upper, zoned orange luminescent monocrystalline calcite.

2120 (general description): Red to red purple luminescent recrystallised bioclastic packstone first is crosscut by a dull luminescent calcite veinlet, that on its turn is crosscut by a bright yellow orange calcite veinlet. Furthermore, a uniform orange luminescent sparite is followed by yellow luminescent calcite, which also occurs as blotchy large sparite phases.
2120 (1 & 2): Red purple luminescent recrystallised bioclastic packstone with non-luminescent authigenic quartz (arrows) crosscut by a dull luminescent calcite veinlet, that on its turn is crosscut by a bright yellow orange calcite veinlet.
2120 (3 & 4): Red luminescent recrystallised bioclastic packstone in contact with uniform orange luminescent sparite, displaying yellow luminescent streaks that developed along cleavage planes, and which also occurs in a small veinlet (arrows).
2120 (5 & 6): Red luminescent recrystallised bioclastic limestone in contact with bright yellow luminescent blotchy calcite.

2125 (general description): Dull brown luminescent (sometimes recrystallised) bioclastic packstone, crosscut or bordered by orange luminescent calcite. Locally some bright orange luminescent monocrystalline calcite occurs. In some samples authigenic quartz crystals occur, that sometimes are replaced by orange luminescent calcite.
2125 (1 & 2): Left, dull brown luminescent (recrystallised) bioclastic packstone, crosscut by a dark brown luminescent calcite vein that is bordered by an orange luminescent calcite, that also fills another vein. The latter seems also to occur along a stylolite (see arrows). Right, orange luminescent monocrystalline calcite.
2125 (3 & 4): Dull brown luminescent bioclastic packstone, surrounded by zoned yellow orange calcite cements.
2125 (5 & 6): Dull brown luminescent recrystallised bioclastic packstone, bordered in its lower part by zoned bright yellow to orange yellow calcite crystals. Notice some authigenic quartz crystals (see arrows).
2125 (7 & 8): Dull brown luminescent recrystallised bioclastic packstone, bordered in its lower part by an orange luminescent calcite vein, with its crystals developing perpendicular to the vein wall. Notice the many replaced authigenic quartz crystals that consist now of an orange luminescent calcite, that also fill a minute veinlet.
2125 (9 & 10): Brown to orange brown luminescent bioclastic packstone, crosscut by orange luminescent calcite veinlets.
2125 (11 & 12): Upper, brown to orange brown luminescent bioclastic packstone. Lower, bright orange luminescent monocrystalline calcite.

2130 (general description): Most cuttings consist of dull (red) brown to red orange spotted luminescent bioclastic (with sometimes intraclastic) packstone (sometimes crosscutted by thin veinlets). Locally some polycrystalline orange luminescent calcite with cleavage twins, as well as yellow luminescent monocrystalline calcite cutting, also with cleavage twins occurs.
2130 (1 & 2): Polycrystalline orange luminescent calcite with cleavage twins.
2130 (3 & 4): Lower cutting, dull red brown luminescent bioclastic (with foraminifera) to intraclastic packstone. Several bioclasts are non-luminescent. The packstone is crosscut by several orange luminescent thin calcite veinlets. Upper cutting, recrystallised orange luminescent microsparite.

2130 (5 & 6): Upper cutting, dull brown luminescent bioclastic packstone with most bioclasts being weakly luminescent. Left cutting, red orange spotted luminescent recrystallised bioclastic packstone crosscutted by a dull luminescent calcite vein (see arrow). Lower right, yellow luminescent monocrystalline calcite cutting, with cleavage twins.
2130 (7 & 8): Dull brown orange luminescent bioclastic wackestone crosscut by yellow luminescent calcite veinlets. In the wackestone one authigenic quartz crystal (AQ) occurs. The arrow indicates some impurity (artefact).
2130 (9 & 10): Dull brown orange luminescent bioclastic packstone crosscut by brown luminescent calcite veinlet (see arrow). Several non-luminescent authigenic quartz crystals (AQ) also occur.

2140 (general description, thick section): CCC
2140 (1 & 2): Zoned orange luminescent calcite crystals surrounded by a more dull orange sector zoned calcite.
2140 (3 & 4): Purple blue luminescent quartz crystals with an impurity rich (dark) core cemented by a bright yellow calcite.
2140 (5 & 6): Bright yellow calcite crystals bordered by non to dark blue luminescent quartz crystals.
2140 (7 & 8): Uniform orange luminescent calcite with cleavage twins. The color change to brighter colors is an artefact due to thick-section preparation.

2145 (general description, thick section): Dull luminescent monocrystalline as well as orange luminescent monocrystalline calcite cutting often containing non-luminescent authigenic quartz crystals (AQ).
2145 (1 & 2): Dull luminescent monocrystalline calcite cutting.
2145 (3 & 4): Orange luminescent monocrystalline calcite cutting.
2145 (5 & 6): Orange luminescent monocrystalline calcite cutting containing non-luminescent authigenic quartz crystals (AQ).
2145 (7 & 8): Orange luminescent monocrystalline calcite cutting containing non-luminescent brecciated quartz grains.
2145 (9 & 10): Orange luminescent monocrystalline calcite cutting containing many non-luminescent authigenic quartz crystals (AQ).

2150 (general description, thick section): Orange luminescent monocrystalline calcite cutting containing non-luminescent authigenic quartz crystals (AQ) next to blue luminescent to non-luminescent (sometimes zoned) quartz cement.
2150 (1 & 2): Orange luminescent monocrystalline calcite cutting containing large non-luminescent authigenic quartz crystals (AQ).
2150 (3 & 4): Dull orange luminescent monocrystalline calcite cutting.
2150 (5 & 6): Dull blue to non-luminescent zoned quartz cement in contact with yellow luminescent calcite (right lower corner).

2165 (general description): Orange to dull brown to non-luminescent recrystallised bioclastic packstone sometimes with non-luminescent authigenic quartz crystals, next to fine siltstone with dominantly non-luminescent to dull blue luminescent quartz grains.
2165 (1 & 2): Lower, dull to non-luminescent bioclastic packstone, with some minor orange luminescent sparite. The upper very fine siltstone is non-luminescent.
2165 (3 & 4): Red orange luminescent recrystallised bioclastic packstone, sometimes with a spotted character. Notice the few non-luminescent authigenic quartz crystals (see arrows).
2165 (5 & 6): Red orange luminescent recrystallised bioclastic packstone, with some bioclast being non-luminescent as are the authigenic quartz crystals (see arrows).

2165 (7 & 8): Upper, orange to red orange luminescent recrystallised bioclastic packstone, with some bioclast being non-luminescent. Lower, siltstone with some blue luminescent quartz detritals.

2185 (general description): Several dull orange monocrystalline calcite cuttings next to dull orange luminescent partially recrystallised bioclastic wackestone.
2185 (1 & 2): Dull orange luminescent monocrystalline calcite cutting.
2185 (3 & 4): Dull orange luminescent peloidal wackestone with yellow luminescent spots, possibly reflecting some recrystallisation that could relate to the interaction with fluids that gave rise to the zoned bright yellow to orange calcite vein present in the lower part. Notice also the dull luminescent blocky calcite that is filling a large dissolution vug (= oversized pore; see arrows) and that is cut by a yellow orange thin calcite veinlet.
2185 (5 & 6): In the upper part yellow luminescent monocrystalline calcite cutting with artefacts due to thin section preparation). In the lower part, dull orange to orange yellow luminescent bioclastic wackestone. The spotted fabric might relate to recrystallisation in relation to interaction with fluids that gave rise to the yellow orange luminescent thin veinlet (see arrow).

2190 (general description): Dull luminescent bioclastic wackestone next to dedolomite. Prominent diagenetic phase is bright yellow calcite cement which precedes blotchy dull purple luminescent coarse crystalline dolomite.
2190 (1 & 2): (Right) Dull luminescent host rock bordered by a sector zoned bright yellow calcite cement that is on its turn in contact with blotchy dull purple luminescent coarse crystalline dolomite. The blotchy nature testifies of recrystallisation.
2190 (3 & 4): Yellow orange luminescent calcite phases surrounding dull luminescent crystals. This likely corresponds to a dedolomite.
2190 (5 & 6): Dull luminescent bioclastic wackestone crosscut by a bright yellow luminescent calcite veinlet that on its turn is cut by an orange luminescent thin veinlet (see arrow).
2190 (7 & 8): Yellow orange luminescent calcite phases surrounding dull luminescent phases. This likely corresponds to a dedolomite.

2200 (general description): Orange luminescent monocrystalline calcite cuttings next to dull red and dull orange luminescent bioclastic wackestone. Also, one siltstone cutting is present.
2200 (1 & 2): Orange luminescent monocrystalline calcite cuttings.
2200 (3 & 4): Dull luminescent bioclastic wackestone.
2200 (5 & 6): Dull red and dull orange luminescent bioclastic wackestone.
2200 (7 & 8): Dull orange luminescent bioclastic wackestone with bright orange luminescent calcite pseudomorphs after authigenic quartz crystals. In upper right corner, orange luminescent bioclastic wackestone.

2215 (general description): Orange luminescent monocrystalline calcite cuttings or blocky calcite cements, next to dull luminescent bioclastic wackestone cemented by non-luminescent blocky calcite. Also, one siltstone cutting is present.
2215 (1 & 2): Orange luminescent monocrystalline calcite cutting.
2215 (3 & 4): Central part, dull luminescent bioclastic wackestone. Upper part, orange luminescent monocrystalline calcite cutting.
2215 (5 & 6): Central part, orange luminescent monocrystalline calcite cutting. Left, dull luminescent bioclastic wackestone.
2215 (7 & 8): Orange luminescent monocrystalline calcite cuttings. The upper one displays some cleavage twins.

2215 (9 & 10): Dull luminescent bioclastic wackestone affected by two calcite cement phases, i.e. first a dull luminescent blocky calcite, followed by an orange luminescent blocky calcite, enclosing some opaque pyrite phases (arrows).

2220 (general description): Non- to dull, to orange luminescent bioclastic wacke-/packstone next to orange or orange yellow luminescent zoned monocrystalline calcite cuttings.
2220 (1 & 2): Non- to dull luminescent bioclastic packstone.
2220 (3 & 4): Lower part, non- to dull luminescent bioclastic packstone. Upper part, orange luminescent zoned monocrystalline calcite cutting.
2220 (5 & 6): Orange luminescent bioclastic wackestone bordered by a zoned calcite cement with an orange core and purple rim.
2220 (7 & 8): Upper part, dull luminescent bioclastic wackestone, next to two orange yellow luminescent monocrystalline calcite cuttings.

2230-1 (general description): Dull to orange (red) luminescent bioclastic packstone, sometimes crosscut by an orange (yellow) luminescent calcite veinlet. Also, one siltstone cutting is present.
2230-1 (1 & 2): Dull luminescent bioclastic packstone, possibly partially recrystallised explaining the yellow orange luminescent spots.
2230-1 (3 & 4): Dull to orange red luminescent bioclastic wacke/packstone. The upper one is cut by a dull luminescent calcite veinlet (see arrow).
2230-1 (5 & 6): Orange luminescent bioclastic wackestone, likely recrystallised explaining the yellow orange luminescent spots and crosscut by an orange luminescent calcite veinlet (see arrow).
2230-1 (7 & 8): Dull luminescent bioclastic wackestone, crosscut by a yellow orange luminescent calcite vein.

2230-2 (general description): Recrystallised dull luminescent peloidal to bioclastic wacke/packstone, sometimes very dull luminescent. Some cuttings contain opaque phases or are crosscut by first a dull luminescent coarse crystalline calcite vein, followed by a tiny orange red luminescent calcite vein. Some orange luminescent monocrystalline calcite cuttings also occur.
2230-2 (1 & 2): Dull luminescent peloidal packstone, partially recrystallised explaining the red orange luminescent spots. The cutting is crosscut by a dull luminescent calcite vein (se white arrows) which seems to be affected also by recrystallisation.
2230-2 (3 & 4): Recrystallised dull luminescent peloidal to bioclastic packstone, possibly with in central part an oversized pore filled by sometimes bright yellow luminescent microspar. Some opaque phases are indicated by a white arrow.
2230-2 (5 & 6): Dull luminescent peloidal to bioclastic wackestone containing few authigenic quartz crystals. The cutting is bordered by a dull luminescent coarse crystalline calcite vein, which on its turn is crosscut by a tiny orange red luminescent calcite vein. Some artifacts are indicated by white arrows.
2230-2 (7 & 8): Upper part, orange luminescent monocrystalline calcite cutting (with some sector zonation). Lower part, dull luminescent microspar with some ghost textures of former foraminifera.

2245 (general description): Several monocrystalline orange luminescent calcite cuttings devoid of cleavage twins, next to dull luminescent recrystallised limestone or bioclastic packstone which are sometimes crosscut by a thin orange luminescent calcite vein.
2245 (1 & 2): (Left) Dull luminescent recrystallised limestone, crosscut by orange luminescent calcite possibly a crack & seal type), of which a monocrystalline orange luminescent calcite equivalent occurs on the right side of the picture.

2245 (3 & 4): Three monocrystalline orange luminescent calcite cuttings. Notice the absence of cleavage twins.
2245 (5 & 6): Dull luminescent bioclastic packstone crosscut by a thin orange luminescent calcite veinlet.

2250 (general description): Mainly dull to sometimes bright orange to brown orange luminescent recrystallised limestones, with peculiar features such as fossil cement stratigraphy and the effect of stylolitisation on recrystallisation.
2250 (1 & 2): Dull luminescent bioclastic wackestone crosscut first by a zoned dull-orange calcite vein (white arrows) and subsequently by a dull uniform orange luminescent calcite vein (yellow arrow).
2250 (3 & 4): Dull to orange luminescent bioclastic wacke/packstone which likely was affected by recrystallisation. Notice in the lowermost left corner the presence of a monocrystalline orange luminescent calcite cutting.
2250 (5 & 6): Upper and lower cutting consisting of dull to orange luminescent bioclastic wacke/packstone of which the upper clearly shows signs of recrystallisation manifested by the orange luminescent spots. The cuttings in the right middle is a yellow orange luminescent monocrystalline calcite cutting.
2250 (7 & 8): (Upper) Dull luminescent bioclastic wackestone, crosscut by a thin dull orange luminescent calcite vein. (Lower) Intensely recrystallised limestone with bright orange to brown orange luminescent microspar.
2250 (9 & 10): Dull luminescent bioclastic wackestone with shell relict that first is cemented by some bright orange luminescent dogtooth cements, followed by orange luminescent blocky cements and finally some non-luminescent blocky cements. The bright – dull variation might reflect some changes in redox potential during cementation.
2250 (11 & 12): Contact along a stylolite (white arrows) between an orange luminescent recrystallised limestone (lower part) and a dull luminescent limestone containing orange luminescent calcite pseudomorphs after authigenic quartz, indicating that the orange luminescent developed as latest diagenetic phases.

Black shales present from 2275 – 2310m, some of which were studied in RWTH-Aachen.

2305 (general description): Quartz bearing bitumen, sandstone and dull to orange red luminescent bioclastic wacke/packstone.
2305 (1 & 2): Detrital quartz bearing bitumen. The grains either display a dull blue or dull purple luminescence. They are rather well sorted but not well-rounded.
2305 (3 & 4): Central part, dull blue or dull purple luminescent quartz grains in sandstone, next to dull to orange red luminescent bioclastic wacke/packstone.

2330 (general description): Dull to orange luminescent bioclastic packstone next to dominantly orange to dull orange luminescent monocrystalline calcite cuttings and one sandstone cutting.
2330 (1 & 2): Orange to dull orange luminescent monocrystalline calcite cuttings.
2330 (3 & 4): Dull to orange luminescent bioclastic packstone. Many of the fossils are non-luminescent.
2330 (5 & 6): Orange luminescent monocrystalline calcite cutting in contact with thinly zoned orange luminescent blocky calcite.
2330 (7 & 8): Dull blue or dull purple luminescent quartz grains in sandstone.

2335 (general description, thick section): CCC

2335 (1 & 2): Yellow orange luminescent calcite next to dull blue luminescent quartz (central part).
2335 (3 & 4): Dull orange luminescent calcite, sometimes impurity rich.
2335 (5 & 6): Zoned yellow orange luminescent calcite together with CCC.

2340 (general description, thick section): CCC
2340 (5 & 6): A = artefact due to thick section preparation.

2345 (general description, thick section): CCC
2345 (7 & 8): upper = zoned based on fluid inclusions.

2350 (general description): Mainly dull orange luminescent monocrystalline calcite cuttings, sometimes bright orange. The polycrystalline calcite displays different orange luminescence shades.
2350 (1 & 2): Dull orange luminescent monocrystalline calcite spar with very faint cleavage twins.
2350 (3 & 4): Different dull orange luminescent monocrystalline calcite spar with very faint cleavage twins.
2350 (5 & 6): Different dull orange luminescent monocrystalline calcite spar with very faint cleavage twins. Notice that the middle cutting is polycrystalline and displays different shades from dull orange to orange luminescence.
2350 (7 & 8): Two polycrystalline with different shades, i.e. bright orange (lower) and dull orange (upper). The latter is in contact with dull luminescent bioclastic wackestone.

2380 (general description): Hypidiotopic dolomite with dull red luminescence with minor porosity and sometimes crosscut by a dull orange luminescent calcite vein. Furthermore, a dull to dull orange luminescent bioclastic packstone cuttings occurs that is crosscut by a thin dull luminescent calcite vein which is similar in luminescence as the blocky sparite.
2380 (1 & 2): Hypidiotopic dolomite with dull red luminescence. Some porosity is visible as black intracrystalline spots.
2380 (3 & 4): Dull to dull orange luminescent bioclastic packstone crosscut by a thin dull luminescent calcite vein (white arrows) which is similar in luminescence as the blocky sparite (Sp).
2380 (5 & 6): (Right) Hypiodiotopic red luminescent dolomite with minor intracrystalline porosity (black spots). (Left) dull brown orange luminescent mudstone with luminescent red to brown zoned dolomite crystals.
2380 (7 & 8): Hypiodiotopic red luminescent dolomite. In the upper cuttings the dolomite crystals possess a dirty core.
2380 (9 & 10): Hypiodiotopic red brown luminescent impure dolomite which is crosscut by a dull orange luminescent calcite vein.

2390 (general description): Bioclastic wackestone to packstone with zoned dolomite rhombs and authigenic quartz. The matrix in the wacke- and packstone is orange luminescent with dull spots. Locally some bitumen with detrital quartz grains occurs.
2390 (1 & 2): Yellow orange luminescent micrite, partially dolomitized by zoned dull to red luminescent dolomite rhombs (D) and locally some non-luminescent authigenic quartz (AQ). Notice also the orange luminescent thin calcite vein (see arrows) which seems to precede the dolomite formation.
2390 (3 & 4): Blue and brown purple luminescent quartz grains surrounded by black bitumen.
2390 (5 & 6): Bioclastic wackestone with orange luminescent with dull spots. Notice the existence of a thin orange luminescent veinlet (see arrows).

2390 (7 & 8): Bioclastic wackestone with non- to dull luminescent fossil relicts and orange luminescent matrix, crosscut by spotted bright yellow luminescent calcite veins which on their turn are crosscut (see arrows) by red luminescent dolomite (D).
2390 (9 & 10): Bioclastic wackestone with orange to red orange luminescence with dull spots, which is crosscut by a bright yellow luminescent calcite vein

2400 (general description): Some hypiodiotopic zoned dolomite (red luminescent core with brown to yellow rim) occur next to intraclastic to bioclastic packstones (see details below). The limestone cuttings sometimes contain authigenic quartz crystals and are sometimes affected by replacive dolomitization. They are crosscut first by red luminescent dolomite veins, and subsequently by bright yellow luminescent calcite.
2400 (1 & 2): Hypiodiotopic dolomite, with limited intercrystalline porosity (see arrows). The dolomite crystals are zoned with a red luminescent core and a brown to yellow rim. The center of the dolomite crystals often displays a dark core with irregular outline, testifying from some recrystallisation.
2400 (3 & 4): Partially recrystallised mudstones with non-luminescent small fossils, explaining the yellow brown spotted luminescence, partially dolomitized (red luminescent phases D) and crosscut by a yellow brown luminescent calcite vein (arrow).
2400 (5 & 6): Two fragments of intraclastic to bioclastic packstones, of which the allochems possess a spotted rather dark brown luminescence with small yellow spots, floating in a non-luminescent calcite spar. One of the fragments is bordered by a red luminescent dolomite vein (D) containing dull red to non-luminescent spots as well as bright yellow spots that likely is of similar origin as the very thin veinlet crossing the packstone (arrow).
2400 (7 & 8): On the left intraclastic to bioclastic packstone, of which the allochems possess a dark brown to orange luminescence, floating in a non-luminescent calcite spar. Locally some authigenic quartz crystals occur (AQ). On the right, bioclastic packstone with calcispheres with orange luminescence, crosscut by a bright yellow luminescent calcite vein. The packstone itself also contains bright yellow spots that likely relate to interaction with the fluids giving rise to the calcite vein.

2405 (general description): Fine laminated organic rich shale, hypidiotopic dolomite with zoned rhombs, as well as xenotopic dolomite with large crystals, with ghost oolite textures (red luminescent). Bioclastic packstone with non-luminescent fossils and red purple luminescent matrix. However, other bioclastic packstone display red luminescent allochems and non-luminescent sparite cement. Furthermore, monocrystalline calcite, with cleavage twins occur which display a yellow reddish spotted luminescence.
2405 (1 & 2): Hypidiotopic dolomite with red to dull red luminescence (zoned). Locally between the rhombs some porosity occurs (see arrows).
2405 (3 & 4): Bioclastic packstone with ghost fossil relicts, which are non-luminescent, while the likely recrystallised matrix is red luminescent.
2405 (5 & 6): Xenotopic non-porous dolomite with large red luminescent crystals, with ghost oolite textures (see arrows).
2405 (7 & 8): Orange luminescent monocrystalline calcite with dense cleavage twins, in which red luminescent dolomite crystals are floating (see arrows)

2415 (general description): Bioclastic (non-luminescent) packstone rich in foraminifera, of which the sparite has a dull brown to non-luminescent, with locally blue luminescent quartz grains. Dull luminescent bioclastic wackestone. Other bioclastic wackestone possess dull luminescent fossils while their micrite is dull red luminescent. Non-luminescent mudstone with blue luminescent

detritals. Coarse crystalline sparite with uniform yellow orange luminescence. Dolomite, siltstone and sandstone.
2415 (1 & 2): Detail of a sandstone with light and dark blue and purple luminescent quartz grains.
2415 (3 & 4): Siltstone with purple luminescent quartz grains and blue luminescent K-feldspar grains. Some porosity exists (dark spots).
2415 (5 & 6): Red (zoned) luminescent dolomite with dull luminescent micrite with small orange luminescent micrite between the crystals (see arrows). Notice the yellow orange thin veinlet that borders the dolomites (see yellow arrow).
2415 (7 & 8): Disturbed contact between fine grained sandstone with dull purple luminescent quartz grains and blue luminescent grains next to red zoned dolomite rhombs (D) occurring next to a bright yellow luminescent calcite spar (CC).

2420 (general description): Different dolomite pieces, next to bioclastic wackestone of which the micrite is orange red luminescent while the sparite is dull luminescent. Many bright yellow luminescent monocrystalline calcite spars, often with cleavage twins.
2420 (1 & 2): Left piece is an orange luminescent likely recrystallised packstone with dull spots as well as (red (zoned) luminescent dolomite rhombs (see arrows). Right piece is a red luminescent xenotopic dolomite.
2420 (3 & 4): Yellow orange luminescent sparite in which red zoned dolomite rhombs occur. If the dolomites developed first then they were floating in the open space, thus the dolomite is filling open space between the calcite crystals.
2420 (5 & 6): Top left and bottom left pieces are red to dull red luminescent dolomite pieces. The right bright yellow piece is a coarse crystalline sparite.
2420 (7 & 8): Top left is a red luminescent xenotopic dolomite piece, with next the right a bright yellow piece is a coarse crystalline sparite with clear cleavage twins.
2420 (9 & 10): Zoned yellow luminescent coarse crystalline calcite, followed by zoned red to brown calcite. Furthermore, zoned dolomite rhombs (D) occur which are less ideally developed at the contact with the latter calcite cement, and thus seem to post-date them.

2440 (general description): Different bright orange luminescent monocrystalline calcite spars with faint cleavage twins. Non-luminescent micrite. Dolomite with relict oolites. Siltstone, with blue luminescent quartz detritals, with dull veins.
2440 (1 & 2): Different bright orange luminescent monocrystalline calcite spars with faint cleavage twins.
2440 (3 & 4): Left, dull luminescent siltstone. Right red luminescent xenotopic dolomite.
2440 (5 & 6): Contact (likely by the development of a stylolite) between red to red orange luminescent calcite (bottom) with bioclastic packstone with most fossils being non-luminescent and the micrite locally containing red luminescent spots.
2440 (7 & 8): Packstone with dull luminescent matrix locally containing red luminescent spots. This lithology is first crosscut by a non-luminescent coarse crystalline calcite vein (with some crystals with cleavage twins) which on its turn is crosscut by a thin bright red orange calcite veinlet (see arrow).

2465 (general description): Dominantly dull luminescent bioclastic wackestone, often with faint orange or yellow luminescent spots. Red luminescent dolomite, if composed of rhombs then some porosity is present.
2465 (1 & 2): Dull luminescent bioclastic wackestone crosscut by coarse crystalline bright yellow luminescent calcite. Some thin red luminescent veinlets crosscut the wackestone.
2465 (3 & 4): Dull luminescent recrystallised limestone or dolomite, with dispersed red luminescent dolomite phases.

2465 (5 & 6): Recrystallised wackestone with dull and faint orange luminescent spots.
2465 (7 & 8): Red luminescent hypiodiotopic dolomite. Locally some porosity occurs between the sub-rhombic crystals.

2465-2 (general description, thick section): CCC

2470 (general description): Bright yellow luminescent monocrystalline calcite cement, with cleavage twins. Red to dull red luminescent xenotopic dolomite with micrite spots. Red luminescent zoned porous dolomite, with bitumen between the crystals containing detritals.
2470 (1 & 2): Thinly red luminescent zoned porous dolomite, with bitumen between the crystals (black colored in the right picture) and a blue luminescent K-feldspars or quartz detritals (white arrows). Also some dull purple quartz crystals occur (yellow arrows).
2470 (3 & 4): Dull luminescent wackestone with dispersed yellow luminescent spots.
2470 (5 & 6): Red to dull red luminescent xenotopic dolomite.
2470 (7): Bioclastic to peloidal packstone with red-orange luminescent rock components and non-luminescent calcite cement.
2470 (8 & 9): Bright yellow luminescent monocrystalline calcite cement, with cleavage twins.
2470 (10 & 11): Red to dull red luminescent xenotopic non-porous dolomite with to the right a bright yellow luminescent monocrystalline calcite cement.
2470 (12 & 13): Bright yellow luminescent monocrystalline calcite cement, with fluid inclusions.

2480 (general description, thick section): CCC
2480 (7 & 8): CCC with blue purple colored artefacts (A)

2485 (general description, thick section): CCC
2485 (5 & 6): A = artefact due to thick section preparation.
2485 (7 & 8): A = artefact due to thick section preparation.

2500 (general description, thick section): CCC (variation in color is often due to artefacts that developed along cleavage planes or that relate to residual polishing products).

2505 (general description): Monocrystalline calcite cuttings (orange, yellow orange or spotted red orange luminescent (without or with cleavage twins). Sometimes weakly luminescent bioclastic wackestone.
2505 (1 & 2): Several orange to yellow orange luminescent monocrystalline calcite cuttings, some of which possess cleavage twins.
2505 (3 & 4): Upper and lower left, yellow orange luminescent monocrystalline calcite cuttings, of which the upper possessing well developed cleavage twins. The bioclastic wackestone to the right is weakly luminescent and is crosscut by brown luminescent thin veinlets.
2505 (5 & 6): Lower left, yellow orange luminescent monocrystalline calcite cutting. Upper left spotted red orange luminescent monocrystalline calcite cutting. The bioclastic wackestone to the right is weakly luminescent.
2505 (7 & 8): Two yellow orange luminescent monocrystalline calcite cuttings, of which the right one possesses faint cleavage twins. Within these calcite cuttings some fluid inclusions are apparent (see arrows)

2520 (general description): Dull brown orange (recrystallised) bioclastic wackestone as well as red luminescent mudstone, with locally some siltstone containing non-luminescent and dull blue luminescent quartz grains. Within some of the limestone cuttings some zoned red luminescent

replacive dolomite rhombs occur that pre-date an orange calcite vein. Furthermore, bright yellow luminescent calcite veins are common which crosscut dull luminescent thin calcite veinlets.
2520 (1 & 2): Dull brown orange recrystallised bioclastic wackestone, cemented and partially replaced or recrystallised by dull luminescent sparite, yielding cleavage twins. The cemented area resembles a dissolution cavity. Some borders of the sparite crystals are outlined by yellow orange luminescent calcite rims.
2520 (3 & 4): Orange spotted red luminescent bioclastic mudstone, containing zoned red luminescent replacive dolomite rhombs, next to an orange calcite vein (arrow). Whether they crosscut the dolomite rhombs is not obvious.
2520 (5 & 6): Lower part, siltstone containing non-luminescent and dull blue luminescent quartz grains. Upper part, monocrystalline bright yellow luminescent calcite.
2520 (7 & 8): Orange spotted red luminescent bioclastic mudstone, containing one irregular zoned red luminescent replacive dolomite rhomb (D). The mudstone is crosscut by an orange yellow luminescent calcite vein that seem to contain the dolomite rhomb. This calcite vein postdates non-luminescent very thin calcite veins (white arrow).
2520 (9 & 10): Orange spotted red luminescent bioclastic to intraclastic packstone, crosscut by a dull luminescent calcite vein (containing cleavage twins), and bordered by a monocrystalline bright yellow luminescent calcite vein, that seems to crosscut the former vein (see arrow). Notice that near the arrow also a thin non luminescent veinlet is displaced by the other vein. In the upper part of the picture appears a bright yellow luminescent calcite piece of vein, displaying clear cleavage twins.

2525 (general description, thick section): CCC with bitumen
2525 (7 & 8): Sandstone with dull and blue luminescent quartz grains and opaque (possibly altered feldspar) grains.

2535 (general description, thick section): CCC
2535 (7 & 8): A = artefact due to thick section preparation.

2545 (general description): Many large monocrystalline transparent crystals, with as well as without cleavage twins.
2545 (1 & 2): Bright yellow orange luminescent monocrystalline calcite cement, without cleavage twins.
2545 (3 & 4): Several bright yellow orange to brown orange luminescent monocrystalline calcite cement, sometimes with cleavage twins. The areas indicated by an arrow correspond to artefacts related to the fabrication of the thin section.

ANNEX IV

Incident light and fluorescence microscopy study of the Beerse samples

The photo plates are provided in a separate file "Incident light and fluorescence microphotographs of the Beerse GT 01 A well". Depth position relates to Along Hole Depth (AHD).

Incident light microscopy

- Plate 1: 1810-1: view on chalcopyrite in mono-crystalline calcite.
- Plate 2: 1810-2, 1860-2-1, 1870-1 & 1870-2: A. Minute chalcopyrite crystals in poly-crystalline calcite. B. Rectangular shaped hematite crystal in fine grained organic-rich siltstone. C. Minute framboidal pyrite crystals that developed along bioturbations. D. Lensoid hematite phases occurring in fine grained organic-rich siltstone.
- Plate 3: 1870-3, 2010-1, 2030-1 & 2030-2: A. Fine grained organic-rich siltstone with stylolite that developed perpendicular to layering infilled by hematite. B. Minute framboidal pyrite crystals that developed in fine grained organic-rich siltstone. C. Minute chalcopyrite crystals aligned a crack next to authigenic quartz crystals (see arrows). There also exists one 100µm large chalcopyrite crystal. D. Several pyrite crystals in fine grained organic-rich siltstone.
- Plate 4: 2035-1 & 2105-1: A & B. Polycrystalline calcite with in A the presence of pyrite (Py) and chalocopyrite (Cpy), while in B only chalcopyrite occurs. Notice in B the cleavage twins in the calcite crystals.
- Plate 5: 2065-1: Layered fine grained organic-rich siltstone with light grey reflecting calcite phases and bright yellow white reflecting pyrite.
- Plate 6: 2145-2 & 2145-4: A & B. View on chalcopyrite in the same sandstone. Notice that the spectrum of colours is an artefact of oil that still occurred on the thin section.
- Plate 7: 2150-1, 2165-1, 2200-1 & 2505-1: A. View on pyrite crystals in polycrystalline calcite. B. View on minute framboidal pyrite crystals in fine grained organic-rich siltstone. C. Fine grained organic-rich siltstone with bioturbation accentuated by the presence of a large amount of minute framboidal pyrite crystals. D. Exceptional view on pyrite crystals in monocrystalline calcite which is rather seldom.
- Plate 8: 2230-1: Honeycomb type of network of pyrite.
- Plate 9: 2230-2: Siltstone containing framboidal pyrite of which the larger ones are likely the product of recrystallisation.
- Plate 10: 2245-1: Large cluster of pyrite crystals with minor amounts of hematite (arrows).

Fluorescent light microscopy

- Plate 11: 2020-1: Bioclastic limestone with several non-fluorescent authigenic quartz crystals (of which three are indicated with an arrow).
- Plate 12: 2070-1: Photomicrographs of fluorescent and transmitted light of two monocrystalline calcite cuttings, of which the lower contains many inclusions, while the upper one is transparent displaying some cleavage features.
- Plate 13: 2095-1: Monocrystalline calcite cuttings which contains many inclusions, explaining the refraction of the fluorescent light.
- Plate 14: 2130-1: Monocrystalline calcite cuttings with disturbed crystals, explaining the refraction of the fluorescent light.

- Plate 15: 2140-1: Polycrystalline calcite with in the upper part well developed transparent crystals. The refraction of the fluorescent light explains the different color shades.
- Plate 16: 2140-2: Photomicrographs of fluorescent and transmitted light of calcite crystal with inclusion-rich center and transparent outer border, explaining the refraction of the fluorescent light.
- Plate 17: 2140-4: Photomicrographs of fluorescent and incident light of sparite cemented sandstone with cubic and pentagon dodekaeder shaped pyrite.
- Plate 18: 2240-1 & 2240-2: Photomicrographs of fluorescent and transmitted light of bioclastic wacke/mudstone crosscutted by a calcite vein (see arrow).
- Plate 19: 2335-1 & 2335-2: Photomicrographs of fluorescent and transmitted light of transparent mono-crystalline calcite with cleavage features.
- Plate 20: 2340-1 & 2340-2: Photomicrographs of fluorescent and transmitted light of transparent mono-crystalline calcite with plain of secondary inclusions.
- Plate 21: 2345-1 & 2345-2: Right photomicrograph of transparent mono-crystalline calcite with many inclusions and cleavage features. Left view of a non-transparent calcite cutting.
- Plate 22: 2465-1 & 2465-2: Right photomicrograph of transparent mono-crystalline calcite with few inclusions and cleavage features. Left view of a non-transparent calcite cutting.
- Plate 23: 2480-1 & 2480-2: Photomicrographs of fluorescent and transmitted light of monocrystalline calcite with clear cleavage twins.
- Plate 24: 2480-3 & 2480-4: Photomicrographs of fluorescent and transmitted light of monocrystalline calcite with clear cleavage twins containing some solid inclusions.
- Plate 25: 2485-1 & 2485-2: Photomicrographs of monocrystalline calcite with clear cleavage twins (left) and steaks of inclusions (right), explaining the refraction of the fluorescent light.
- Plate 26: 2500-1: Photomicrographs of monocrystalline calcite with two sets of cleavage twins, explaining the refraction of the fluorescent light.
- Plate 27: 2500-2 & 2500-3: Photomicrographs of fluorescent and transmitted light of monocrystalline calcite with cleavage twins and many inclusions, explaining the refraction of the fluorescent light.
- Plate 28: 2535-1 & 2535-2: Photomicrographs of fluorescent and transmitted light of monocrystalline calcite with faint cleavage features and many inclusions, explaining the refraction of the fluorescent light.

ANNEX V

Analytical protocol of $\delta^{18}O$ and $\delta^{13}C$ on micro milled and bulk carbonate samples

Samples for carbonate $\delta^{18}O$- and $\delta^{13}C$-analyses are transferred into exetainer vials. The vials are flushed with He (>99.9996%). After flushing samples are allowed to react with phosphoric acid (103%) for 24h at constant temperature (typically, 25°C).

The CO_2 gas formed in this reaction is analysed using a GasBench II coupled to an IRMS system (Thermo Delta Plus XP).

The raw data are calibrated using four standards:

Standard	$\delta^{13}C$ (‰)	$\delta^{18}O$ (‰)
LSVEC	-46.60	-26.70
NBS19	1.95	-2.2
Merck*	-9.65	-18.42
Fluka*	2.36	-4.04

The standard deviation on the measured $\delta^{13}C$- and $\delta^{18}O$-values of these standards is typically lower than 0.08 ‰.

The final delta values are expressed relative to international standards VPDB (Vienna PeeDee Belemnite) for ^{13}C and VSMOW2 for ^{18}O.

* Merck an Fluka are in-house standards calibrated against LSVEC and NBS19 (the latter two are certified reference materials).

ANNEX VI

Results of the stable C- & O-isotope analysis.

The sample depth corresponds to the sample identification number used in the petrography part. Notice that in the micro milled samples R1 to R21 sometimes different phases were micro-sampled originating from one and the same sample/thin section (e.g. calcite and dolomite).

Abbreviations: CC = calcite; XX = crystals; cem = cement; mono XX = mono-crystalline; Dolo = dolomite; ? = not 100% pure; rexx = recrystallised; rexx ? = possibly recrystallised (features not always straightforward); Lst = limestone DG = dark grey. All values are in PDB ‰. Depth position relates to Along Hole Depth (AHD).

Sample codes: MM: Micro Milling ; MCC: Micro-crystalline calcite ; D: Dolomite ; Lst or L: Limestone ; TS : Thin section ; BC : Bulk sample.

Sample reference	borehole	Depth (m AHD)	Sample description	$\delta^{18}O$	$\delta^{13}C$
Samples collected by micro milling in calcite cements					
R1	Beerse GT 01 A	2465m	cc line 4	-13,3	1,8
R2	Beerse GT 01 A	2465m	cc	-15,4	1,4
R3	Beerse GT 01 A	2465m	turbid cc	-15,1	0,1
R4	Beerse GT 01 A	2465m	transparent cc	-15,0	0,7
R5	Beerse GT 01 A	2500m	cc1	-13,9	1,7
R6	Beerse GT 01 A	2500m	cc2	-15,5	2,0
R7	Beerse GT 01 A	2500m	cc with cleavage twins	-13,7	1,7
R8	Beerse GT 01 A	2500m	rectangular XX	-13,8	1,9
R9	Beerse GT 01 A	2345m	zoned XX (but deep sampling till 200µm)	-9,2	-4,1
R10	Beerse GT 01 A	2345m	transparent cc	-16,9	1,2
R11	Beerse GT 01 A	2345m	transparent cc	-8,8	-3,3
R12 : 68A	Beerse GT 01 A	2470m	cc cem mono XX	-15,0	1,9
R13 : 68B	Beerse GT 01 A	2470m	cc cem mono XX	-15,6	1,7
R14 : 69	Beerse GT 01 A	2490m	cc cem mono XX	-13,3	1,9
R15 : 70	Beerse GT 01 A	2485m	cc cem mono XX	-13,6	2,0
R16 : 71	Beerse GT 01 A	2500m	cc cem mono XX	-13,7	2,0
R17 : 72A	Beerse GT 01 A	2505m	cc cem transparent mono XX	-13,8	2,1
R18 : 73A	Beerse GT 01 A	2520m	milky cc cem mono XX	-14,2	1,8
R19 : 74	Beerse GT 01 A	2535m	cc cem XX terminations ΔΔ	-13,8	2,1
R20 : 76	Beerse GT 01 A	2545m	cc cem	-8,9	1,7
R21 : 76	Beerse GT 01 A	2545m	cc cem	-8,2	1,0
Monocrystalline calcite samples					
26	Beerse GT 01 A	2040m	cc cem bulk	-12,3	1,5
29	Beerse GT 01 A	2070m	cc cem mono XX	-9,7	1,8
30	Beerse GT 01 A	2075m	cc cem bulk	-10,5	2,0
31	Beerse GT 01 A	2095m	cc cem	-11,5	0,9
36	Beerse GT 01 A	2140m	cc cem bulk	-13,2	1,4
37	Beerse GT 01 A	2145m	cc cem bulk	-11,4	1,1
43A	Beerse GT 01 A	2215m	cc cem monoXX	-12,4	1,4
45A	Beerse GT 01 A	2230m	cc cem bulk	-13,4	0,3
50	Beerse GT 01 A	2335m	cc cem bulk	-12,9	0,9

52	Beerse GT 01 A	2345m	cc cem monoXX	-9,5	-3,1
53A	Beerse GT 01 A	2350m	cc cem (White turbid, monoXX)	-12,0	0,2
53C	Beerse GT 01 A	2350m	cc cem transparent	-14,1	1,8
56	Beerse GT 01 A	2395m	cc cem monoXX	-13,1	1,6
59A	Beerse GT 01 A	2420m	cc cem monoXX	-9,0	0,4
60A	Beerse GT 01 A	2425m	cc cem monoXX	-14,5	2,0
62	Beerse GT 01 A	2435m	cc cem monoXX	-13,0	1,8
67	Beerse GT 01 A	2465m	cc cem monoXX	-15,3	1,7
Dolostone samples					
45B	Beerse GT 01 A	2230m	Dolo (?)	-13,5	3,1
44	Beerse GT 01 A	2220m	Dolo (?)	-11,9	2,9
63	Beerse GT 01 A	2440m	Dolo	-6,5	3,6
66	Beerse GT 01 A	2465m	Dolo?	-8,3	3,9
R13 : 68C		2470m	dolo	-3,5	3,5
Bulk limestone samples (sometimes recrystallized)					
5	Beerse GT 01 A	1845m	Lst rexx	-12,6	1,0
6	Beerse GT 01 A	1855m	Lst rexx	-10,5	0,8
7	Beerse GT 01 A	1860m	Lst (LG) rexx	-9,4	0,7
9	Beerse GT 01 A	1870m	Lst (LG) rexx	-9,2	0,9
10	Beerse GT 01 A	1900m	Lst (DG) rexx	-13,7	0,3
11	Beerse GT 01 A	1910m	Lst (LG) rexx	-13,7	1,0
12	Beerse GT 01 A	1920m	Lst (LG) rexx	-13,4	1,8
13B	Beerse GT 01 A	1935m	Lst rexx	-12,2	0,7
14	Beerse GT 01 A	1945m	Lst rexx	-13,3	2,4
19	Beerse GT 01 A	1980m	LG Lst rexx ?	-14,0	1,4
20	Beerse GT 01 A	1995m	LG Lst rexx ?	-14,2	3,3
22	Beerse GT 01 A	2010m	LG Lst rexx ?	-14,5	3,3
24	Beerse GT 01 A	2030m	LG Lst rexx ?	-14,1	3,3
28	Beerse GT 01 A	2065m	Lst rexx ?	-14,4	2,9
32	Beerse GT 01 A	2105m	Lst rexx ?	-13,4	1,8
34	Beerse GT 01 A	2125m	Lst rexx	-13,8	2,3
39	Beerse GT 01 A	2165m	Lst rexx ?	-12,3	2,3
41	Beerse GT 01 A	2125m	Lst rexx? + org-rich Lst	-12,8	2,5
43B	Beerse GT 01 A	2215m	Lst & Dolo (?)	-11,2	3,1
47	Beerse GT 01 A	2250m	Lst rexx?	-13,8	3,2
53B	Beerse GT 01 A	2350m	Lst	-13,2	1,7
54	Beerse GT 01 A	2380m	DG Lst	-12,4	4,0
57	Beerse GT 01 A	2400m	DG Lst	-9,4	4,1
58	Beerse GT 01 A	2405m	DG Lst	-12,7	4,3
59B	Beerse GT 01 A	2420m	Lst	-9,4	4,2
60B	Beerse GT 01 A	2425m	Lst	-8,5	3,8
R17 : 72B	Beerse GT 01 A	2470m	Lst	-10,2	5,7
R18 : 73B	Beerse GT 01 A	2520m	DG Lst	-10,7	5,2